

Western University

Scholarship@Western

---

Chemical and Biochemical Engineering  
Publications

Chemical and Biochemical Engineering  
Department

---

5-25-2021

## Harnessing the physicochemical properties of DNA as a multifunctional biomaterial for biomedical and other applications

Aishik Chakraborty

*Western University*, achakr26@uwo.ca

Shruthi Polla Ravi

*Western University*

Yasmeen Shamiya

*Western University*, yshamiya@uwo.ca

Caroline Cui

*Western University*

Arghya Paul

*Western University*, arghya.paul@uwo.ca

Follow this and additional works at: <https://ir.lib.uwo.ca/chemengpub>



Part of the [Biomedical Engineering and Bioengineering Commons](#), and the [Chemical Engineering Commons](#)

---

### Citation of this paper:

Chakraborty, Aishik; Ravi, Shruthi Polla; Shamiya, Yasmeen; Cui, Caroline; and Paul, Arghya, "Harnessing the physicochemical properties of DNA as a multifunctional biomaterial for biomedical and other applications" (2021). *Chemical and Biochemical Engineering Publications*. 5.

<https://ir.lib.uwo.ca/chemengpub/5>

# Harnessing the Physicochemical Properties of DNA as a Multifunctional Biomaterial for Biomedical Applications and Other Applications

Received 00th January 20xx,  
Accepted 00th January 20xx

DOI: 10.1039/x0xx00000x

Aishik Chakraborty<sup>a</sup>, Shruthi Polla Ravi<sup>b</sup>, Yasmeen Shamiya<sup>c</sup>, Caroline Cui<sup>c</sup>, Arghya Paul<sup>a, b, c\*</sup>

The biological purpose of DNA is to store, replicate, and convey genetic information in cells. Progress in molecular genetics have led to its widespread applications in gene editing, gene therapy, and forensic science. However, in addition to its role as a genetic material, DNA has also emerged as a nongenetic, generic material for diverse biomedical applications. DNA is essentially a natural biopolymer that can be precisely programmed by simple chemical modifications to construct materials with desired mechanical, biological, and structural properties. This review critically deciphers the chemical tools and strategies that are currently being employed to harness the nongenetic functions of DNA. Here, the primary product of interest has been crosslinked, hydrated polymers, or hydrogels. State-of-the-art applications of macroscopic, DNA-based hydrogels in the fields of environment, electrochemistry, biologics delivery, and regenerative therapy have been extensively reviewed. Additionally, the review encompasses the status of DNA as a clinically and commercially viable material and provides insight into future possibilities.

## 1. Introduction

Interest in DNA as a natural biopolymer dates back to as far as the 1960s<sup>1</sup>. Since then, the role of DNA has been evolving continuously in the biomedical field<sup>2</sup>. In addition to being a genetic material, DNA is also considered as a nongenetic, generic biopolymer. Many new functions of this biopolymer has been developed, including biomedical, electrochemical, and environmental applications<sup>2–5</sup>. The exceptional reputation of DNA arises from its ability to (i) program the nucleotide sequences, (ii) control the chain length, (iii) predict the self-assembling structure, and (iv) bind specifically to other molecules. Well-established chemical synthesis techniques and straightforward modification methods, which will be discussed in the following sections, have added to the programmability of this material remarkably<sup>6–8</sup>. This programmable, self-assembling nature of DNA also allows for the construction of exquisite two-dimensional<sup>9,10</sup> and three-dimensional materials<sup>11,12</sup>, including DNA hydrogels<sup>13–18</sup>.

DNA-based hydrogels are a group of three-dimensional materials comprising of complex networks and pores that can store water. Being a highly polar molecule, DNA readily dissolves in water<sup>19</sup>. However, the complex network prevents the dissolution of these hydrogels. Instead, in the presence of water, hydrogels increase in volume. The hydrophilic nature and large surface area allow hydrogels to interact with a vast number of small<sup>20</sup> and large biomolecules<sup>21</sup>. The network making up the DNA-based hydrogels is

formed either by physical or chemical crosslinking where the entire hydrogel can be made of DNA, or DNA can be a part of the hydrogel. Comprising of DNA and a substantial volume of water, DNA-based hydrogels tend to be biocompatible and biodegradable, both of which are important for formulating clinically relevant materials<sup>22</sup>. Moreover, the physical and chemical nature of these hydrogels can be easily manipulated. Besides having DNA as a constituent, these hydrogels have the same advantages as that of DNA polymers. The biocompatibility, degradability, high programmability, and specificity of such materials help in implementing them in different areas of research, including environmental and biomedical fields (**Fig. 1**). In addition, DNA-based hydrogels can also incorporate nanomaterials inside their networks<sup>23–27</sup>. These nanocomposite hydrogels offer features that are quite different from their pure DNA counterpart. Introducing nanomaterials into these hydrogels can provide unique properties, like electro-conductivity<sup>28</sup> or light responsiveness<sup>29</sup>. With limitless possibilities, DNA-based hydrogels have emerged as a fascinating new material in the polymer world.

In the past 15 years, much progress has been made in synthesizing DNA polymers with desired chain lengths, compositions, and conjugated functional groups<sup>5</sup>. This progress, in turn, has advanced our understanding of how the polymer backbones can control material properties ranging from chemical stability, mechanical strength, structural integrity, biodegradability, and processability. Reviews on various applications of DNA-conjugated materials have been extensively published in the areas of biomedical engineering<sup>2,30–39</sup>, bioanalytical chemistry<sup>40–46</sup>, molecular machines<sup>47–49</sup>, and electronics<sup>50–52</sup>. But here, we primarily focus on the conjugation chemistry. In the first part, we aimed to illustrate the fundamental chemical reactions that DNA nucleotides go through when interacting with different macromolecules, chemical groups/handles, and two-dimensional nanomaterials.

Specifically, we have reviewed how DNA polymers can be hydrolyzed and hybridized in the presence of enzymes. These enzymatic reactions are frequently used to synthesize DNA-based materials.

<sup>a</sup> Department of Chemical and Biochemical Engineering, The University of Western Ontario, London, ON N6A 5B9, Canada

<sup>b</sup> School of Biomedical Engineering, The University of Western Ontario, London, ON N6A 5B9, Canada

<sup>c</sup> Department of Chemistry, The University of Western Ontario, London, ON N6A 5B9, Canada

Electronic Supplementary Information (ESI) available: [details of any supplementary information available should be included here]. See DOI: 10.1039/x0xx00000x

Following this, we have detailed the various non-covalent and covalent interactions by which different types of materials (e.g., transition metals, alkaline earth metals, metal-organic-frameworks) can bind to DNA, and how these interactions influence the structural (e.g., shape, size) and functional (e.g., mechanical, biological, electrochemical) properties of the resulting composite materials. Additionally, we have introduced different synthetic techniques by which functional groups can be attached to DNA nucleotides. These functionalized DNA nucleotides can eventually bind to desired drugs, proteins, dyes, or other nucleotides, broadening their applicability. We have also discussed the conjugation principles driving the self-assembly of DNA nanodevices that can be applied in biomedicine. In addition, we have highlighted the synthesis of DNA nanocomposite hydrogels, where nanoparticles in tandem with DNA-based hydrogels yield fascinating biomaterials.

In the second part, we have presented a comprehensive overview of the various emerging applications of DNA as a generic material and evaluated their potential in translational medicine, taking research from the “bench-to-bedside.” We review how DNA-based hydrogels can act as sensors for detecting heavy metals in wastewater, and as synthetic mimics of enzymes. We also discuss how these hydrogels can be used to prepare electrical conductors and actuators. Furthermore, we highlight the use of DNA-based hydrogels as vehicles for drug delivery, as scaffolds for tissue engineering, and as highly specific biosensors. In addition, we mention novel applications where DNA-based hydrogels act as tools for biomolecule production. With such fascinating applications, we predict a promising future for DNA as a versatile biopolymeric material.

## 2. What is the Chemical Nature of DNA?

Before we discuss the possible routes of chemically manipulating the DNA, we must first understand how they are built. The structure and chemical makeup of DNA has been shown in **Fig. 2A**. DNA is a complex, biological, anionic polymer consisting of multiple subunit<sup>53</sup>. Each subunit, called a nucleotide, consists of a deoxyribose sugar with five carbons, a phosphoric acid molecule, and either of the four possible nitrogenous bases (**Fig. 2B**): adenine, thymine, guanine, or cytosine. A single, polynucleotide chain of DNA consists of repeating units, covalently connected through phosphodiester bonds. These phosphodiester bonds make up the backbone of the linear DNA chain, or strand. Each strand has a chemical polarity, i.e., directionality, to it. One end (5') of the strand consists of the phosphate molecule, whereas the other end (3') consists of the hydroxyl molecule. However, the 3D structure of the DNA is far more complicated than the single strand just described. In three dimensions, two of the strands combine antiparallely to form a twisted ladder. This is known as the double helix. The bases of the double helix are linked together with hydrogen bonds, that hold the overall structure together. The bulkier, double-ringed (purine: adenine and guanine) nitrogenous base of one strand binds to the lighter, single-ringed (pyrimidine: thymine and cytosine) nitrogenous base of the other. Adenine always binds to thymine, and guanine always binds to cytosine. This phenomenon of binding is also called Watson-Crick complementary base pairing and holds the two strands at a uniform distance throughout the length of the DNA<sup>54</sup>. The two strands also twist around themselves at every tenth pair, giving rise to the double helical shape of the native DNA. Although the steps of this winding ladder are held together by hydrogen bonds, the outer edges of the steps are open to other molecules. A protein's ability to specifically bind to a DNA site depends on its accessibility to the outer edges of the DNA base pairs<sup>55</sup>.

Electrostatic interactions also drive DNA to bind to cationic molecules<sup>56</sup>. DNA has an overall negative charge arising from the

phosphate group of the nucleotide backbone. However, the negative charge is distributed unevenly among the four oxygen atoms in the phosphate molecule. Hence, instead of having localized point charges, an electronegative cloud surrounds the DNA. The base pairs, on the other hand, consist of electron pair donor and acceptor regions that help with specific binding. Moreover, the double-helix is twisted in such a way that each groove in the backbone is not equidistant. There are major and minor grooves along the length of the DNA. Major grooves are in locations where the consecutive strands are spaced far apart, while minor grooves are in locations where the strands are nearer to each other. The electronegativity of the DNA is dependent on these grooves and the corresponding base pairs. Cations take advantage of these properties and can target regions that contain minor grooves that are abundant with adenine-thymine steps or major grooves that are rich in guanine-cytosine steps. Therefore, like many complex compounds, the stereochemical properties play a crucial part in chemically manipulating the fate of DNA. Over the past 20 years, such chemical manipulation has led to an increase in the use of DNA-based materials in a wide range of applications (**Fig. 2C and 2D**).

## 3. How do we Chemically Manipulate DNA?

Understanding the basic chemical nature of the different constituents of DNA is the first step towards manipulating this biopolymer into favorable structures. A vast array of reactions is at the disposal of a chemist to modify DNA into usable materials. Four different methods have been highlighted in **Fig. 3**. In this section, we will discuss some of the simple chemical modifications that have been used to formulate novel products. The tools presented here will be valuable to any young scholar interested in oligonucleotide research.

### 3.1. Enzyme-Mediated Hydrolysis

Without any chemical or biological intervention, DNA is an extremely stable molecule<sup>57</sup>. However, simple chemical tweaks can drastically change their physicochemical behavior. For example, even though the phosphodiester bond of DNA is exceptionally stable for about 30 million years at physiological conditions, they are vulnerable to certain compounds<sup>57</sup>. The phosphodiester bond can be hydrolyzed with biocatalysts, called enzymes, to form either a 3' or a 5' phosphate. This enzyme-mediated hydrolysis of the DNA backbone is useful for processes that require parts of the DNA to be cleaved. For example, in the case of recombinant DNA technology, a part of DNA is sliced by hydrolysis. This sliced DNA is then attached to a complementary sequence by a process called DNA ligation<sup>58</sup>. Ligation also uses an enzyme to catalyze the binding of the two DNA strands. Although enzymatic hydrolysis has been used for years, only recently, Molina *et al.* visualized the process<sup>59</sup>. Here, each intermediate step of the reaction has been observed to show that metal ions facilitate the cleavage of the phosphodiester bond. Another interesting approach to determine the activity of an enzyme is by chemiluminescence (**Fig. 4A**)<sup>60</sup>. Light was emitted only when an enzyme cleaved the DNA to form a specific DNA structure, called G-quadruplex. G-quadruplex forms when four guanine molecules combine in a single plane through Hoogsteen hydrogen bonds<sup>61</sup> between the guanines. Many such planes stack on top of each other by  $\pi$ -stacking interactions. A ferrous molecule, hemin was then complexed with this structure, which oxidized luminol and emitted light. In short, enzymes are critical in modifying DNA structures.

### 3.2. Enzyme-Mediated Chain Elongation

Another critical role of enzymes in biological applications is the elongation of DNA by the polymerization chain reaction<sup>62</sup>. The polymerase chain reaction is a replication approach where parts of

DNA are amplified using the enzyme, DNA polymerase<sup>62</sup>. This enzyme connects different nucleotides to produce the desired elongated polymer. The primary chemistry involved in this reaction is the phosphoryl transfer reaction. Here, the phosphate group of the incoming nucleotide binds with the hydroxyl group of the nucleotide already present in the chain<sup>63</sup>. A divalent magnesium complex facilitates the polymerization process. Overall, the reaction uses a template DNA that carries the targeted sequence of nucleotides, primers that contain the complementary nucleotide sequence, and nucleotides that serve as the building blocks. The reaction is carried out in a thermal cycler. First, the template strand is denatured at a high temperature, where the steps of the double helix break to form two strands. Next, the temperature is reduced, and the primers bind to their complementary base pairs on the template strand. In the end, the temperature is increased again. The enzyme taq polymerase helps the building blocks attach to their complementary base pairs to elongate the desired chain.

Other than the polymerase chain reaction, the isothermal rolling circle amplification (RCA) process has also become an efficient tool for the elongation of nucleic acids<sup>64</sup>. This process is increasingly implemented for creating bioassays and diagnostic methods. A circular DNA template is usually used in this case. Polymerase enzymes (eg.,  $\phi 29$ ), derived from bacteria, are used to elongate the desired chain isothermally on a solid substrate. Because of its ability to work on cell surfaces, RCA finds use in unique applications like cell entrapment<sup>65</sup>. As shown in Fig. 4B, RCA generated repeating aptamers capable of binding to biomarkers, which are presented on cancer cells. These aptamers, which are single-stranded, short-chained oligonucleotides, then captured the target cells from the blood. RCA can also be coupled with a hyperbranched amplification process to form a DNA network. One such complex DNA network was used to encapsulate live cells<sup>66</sup>. Some simple chemical processes have also been observed or devised to modify DNA. We discuss such processes in the following subsections.

### 3.3. Non-Covalent Interaction

In some cases, metal complexes can bind to DNA through a non-covalent binding strategy, called intercalation<sup>67</sup>. The intercalating compounds can penetrate the DNA backbone, thereby altering the shape of the DNA, and form Van der Waals interactions with the base pairs. Fluorescent dyes (such as ethidium bromide<sup>68</sup>) can be added to DNA by intercalation (Fig. 5A)<sup>69</sup>. Another key non-covalent binding exists in the form of electrostatic interaction. The electronegative backbone of the DNA makes it possible for cations to bind to the DNA. Interactions of cationic surfactants with DNA has opened a broad avenue of applications ranging from electronics to medicine<sup>70</sup>. In the case of drug delivery, polymeric cations have taken advantage of this property to attach to DNA<sup>71</sup>. This process of charge neutralization is called DNA condensation, which changes the shape of the DNA from strings to folded loops<sup>72</sup>. The folded loops can enter the cells and carry out their therapeutic functions. DNA condensation, with the help of positively charged polymers, also prevents unwanted degradation by enzymes<sup>73</sup>.

Anionic charge of immune modulating DNA chains can also be used to design anion-cation complexes capable of delivering antigens<sup>74</sup>. Unmethylated cytosine-phosphate-guanine (CpG) motif-containing anionic DNA can be recognized by the protein, Toll-like receptor 9, which is expressed by B cells and plasmacytoid dendritic cells (pDC) in humans<sup>74</sup>. It triggers the host's immune response, resulting in the elimination of the infectious agent or pathogen<sup>75</sup>. Therefore, CpG motif containing anionic DNA can accompany vaccines as adjuvants and enhance the immune response against antigens. Fig. 5B shows one such vaccine formulation where antigens were trapped inside

cationic lipid-polymer complex loaded with anionic cytosine-phosphate-guanine motif-containing DNA sequences<sup>76</sup>.

Furthermore, anionic DNA can also form complexes with cationic metals, and serve as metal sensors for both environmental and biological applications<sup>77</sup>. Transition metal ions, like silver, can form complexes with DNA to work as antimicrobial agents<sup>78</sup>. Because of a growing population of antibiotic-resistant bacteria, researchers are now looking at such DNA-based solutions.

### 3.4. Covalent Interaction

A variety of functional groups can be covalently attached to DNA through either in-synthetic or post-synthetic methods<sup>79</sup>. In-synthetic methods refer to attaching a functional group to a phosphoramidite molecule and incorporating it during DNA synthesis. Post-synthetic methods refer to conjugating the desired functional group to a chemical group already attached to the DNA. Afterwards, molecular reporters, such as biotin and fluorescein, can be attached to the modified DNA with the help of the functional groups<sup>79</sup>. Here, we discuss some of the chemical tools and strategies that can be applied to incorporate various functional groups to synthetic DNA (also highlighted in Table 1).

Amines can be attached to DNA by chemically modifying deoxyribonucleosides, such as deoxycytidine<sup>80–82</sup>. Fig. 6A illustrates an example where an amine-modified DNA was covalently tethered to polydopamine by Michael addition<sup>83</sup>. This amine-modified DNA could hybridize with a probe DNA, which can act as biosensor for detecting mercury ions. Cytidine can be modified through a bisulfite-catalyzed transamination reaction. This reaction attaches an amine-terminating linker arm to the amino group on cytidine at the N-4 position<sup>84,85</sup>. Thymidine can be modified with a palladium-mediated olefination reaction. In this case, a linker arm containing a carbon-carbon double bond is attached to the thymidine. The carbon double bond is subsequently removed to achieve the desired compound<sup>86</sup>. Thiols can be attached by synthesizing a phosphite derivative containing a free thiol, which can be then incorporated into DNA using phosphoramidite synthesis<sup>87</sup>. Alternatively, a free thiol can be introduced to thymidine through the phosphorylation of 5'-dimethoxytritylthymidine and subsequent coupling of the nucleotide to 3,3'-dithiodipropyl. The modified thymidine is coupled to aminopropyl controlled pore glass for phosphoramidite synthesis<sup>88</sup>. Alkynes can be synthesized by adding an alkyne group through a  $S_N1$  substitution reaction to an iodide-containing deoxyuridine for subsequent phosphoramidite synthesis<sup>89</sup>. Aldehydes can be synthesized post-synthetically by the oxidation of an alkenyl containing oligonucleotide to a diol. The vicinal diols are cleaved to gain the aldehyde group<sup>90</sup>. Carboxylic acids can be attached through in-synthetic or post-synthetic methods. For the in-synthetic method, non-nucleosidic phosphoramidites made with levulinic acid are synthesized and incorporated during phosphoramidite synthesis<sup>91</sup>. For the post-synthetic, methyl ester phosphoramidites are synthesized and used in DNA synthesis. Then the methyl ester is hydrolyzed to a carboxylic acid<sup>92</sup>.

N-Hydroxysuccinimide (NHS) ester derivatives are commonly used to attach other compounds to amino-modified oligonucleotides through reactions with primary amines. For example, an amino-modified oligonucleotide can be conjugated with the NHS derivatized hydrazinonicotinamide moiety. A bond forms between the amine and the moiety, kicking out NHS<sup>93,94</sup>. Additionally, NHS esters, such as NHS-Carboxy-dT which is commercially available, can be directly incorporated into the oligonucleotide and subsequently conjugated to a label<sup>79</sup>. Maleimides can be added by Diels-Alder reaction. For this purpose, furan and maleic anhydride undergo a Diels-Alder addition reaction to form an adduct. An amine is then put into this adduct<sup>95</sup>.

The *exo* adduct of the maleimide product, N-(2-Hydroxyethyl)maleimide, is made into a phosphoramidite and coupled to oligonucleotides using phosphoramidite synthesis<sup>96</sup>.

Azides are attached post-synthetically. For example, an amino-modified DNA can be reacted with either a diazo transfer reagent to convert the amine (NH<sub>2</sub>) to the azide (N<sub>3</sub>)<sup>97</sup>, or it can be reacted with a NHS ester that contains an azide group<sup>98</sup>. Additionally, 5'-iodo-thymidine monomers can be assembled into an oligonucleotide. Afterwards, sodium azide transforms the iodine to an azide to create 5'-azido-thymidine<sup>99</sup>. All the above chemical modifications can be used for a variety of biomedical applications.

Targeted drug delivery is a lucrative area where DNA can be covalently bonded with drugs<sup>100</sup>. Aptamers can specifically bind with disease biomarkers. Therefore, aptamer-drug conjugates can decrease toxicity, especially in the case of cancer treatment by chemotherapy. "Click" chemistry is one critical covalent linking strategy that has grown popular in synthesizing DNA molecules<sup>101</sup>. The primary purpose of click chemistry is to join small units through heteroatom links (C-X-C). Under this classification, reactions need to strictly adhere to a set of guidelines<sup>102</sup>. These set guidelines dictate that the reactions must have high product yields. They must produce harmless byproducts that can easily be removed without using chromatographic methods. The reactions must also be stereospecific and must involve modular blocks as the reactants. The reaction conditions must be simple, without being sensitive to water and oxygen. The reagents must be readily available, solvents must either be avoided or be innocuous, and product isolation should be easy. Cycloaddition of two unsaturated compounds like azides and alkynes is one type of reaction that complies with this set of rules. Azide-modified DNA can be attached to an alkyl-modified reporter forming a triazole bond, as seen in **Fig. 6B**<sup>103</sup>. However, this reaction requires high temperatures. To avoid harsh temperature conditions, copper catalyzed azide-alkyne cycloaddition (CuAAC) has become a popular tool to chemically modify oligonucleotides for biological and nanotechnological research<sup>101</sup>. In this case, alkyl-modified DNA is interacted with an azide-modified reporter molecule. This reporter molecule can be another DNA as well. **Figure 6C** shows one example where copper was used as a catalyst to bind two DNA molecules by cycloaddition<sup>104</sup>.

### 3.5. Self-Assembled Constructs

Both covalent and non-covalent binding strategies have been used to advance DNA-based nanotechnology<sup>105</sup>. Such technological advances have given rise to self-assembled nanostructures that can work as drug delivery devices<sup>106</sup>. At acidic pH, cytosine-rich oligonucleotide sequences form a unique structure, called *i*-tetraplex or *i*-motif (**Fig. 7A**)<sup>107</sup>. Here, cytosines associate with each other forming a loop, which consists of two duplexes. One of the duplexes is parallel to the DNA chain, while the other is antiparallel. The cytosines present in the parallel duplex bind together. Similar bonds form between the cytosines of the antiparallel duplex. The cytosines then intercalate to give the final shape to the *i*-motif, which can be used as sensors<sup>106,108</sup>. These structures can detect changes in pH by changing their molecular shape. In biomedical diagnostics, the detection of pH is essential because any undesirable changes in the acid-base balance within the body is indicative of diseases<sup>109</sup>. Outside medicine, such pH-responsive sensors can be used in industrial and environmental applications. In the case of the pH sensor developed by Modi et. al., the strands were tagged with fluorophores in such a way that upon the formation of *i*-motifs, a fluorescence signal was observed<sup>110</sup>. A similar self-assembled pH-responsive structure has also been depicted in **Fig. 7B**<sup>111</sup>.

By manipulating the nongenetic, predictable and programmable nature of DNA, self-assembly has given rise to bottom-up, molecular approaches for synthesizing complex 1D, 2D, as well as 3D structures<sup>10,112–114</sup>. DNA tile is one such approach where various shapes and patterns can be fabricated by attaching DNA strands having 5 to 10 nucleotide-long sticky ends<sup>115</sup>. Because the complementary pairing of DNA is highly specific, the sticky end sequences can be programmed such that neighboring molecules self-assemble to form unique shapes. Here, shorter strands initially assemble into first order unit tiles or building blocks, which further continues to grow periodically, forming higher ordered structures. The abstract tile assembly model and the kinetic tile assembly model are the two modes of self-assembling strategies that are used for developing different nanostructures<sup>115–117</sup>. In the case of the abstract tile assembly model, rectangular tiles with up to four sticky ends are selected for binding the tiles together. Here, the binding depends on several parameters, including temperature, tile concentration, as well as the salt concentration of the solution. The tiles bind irreversibly to form the desired shape. On the contrary, the tiles bind reversibly in the case of the kinetic tile assembly model. Over the years, multiple tile-based design strategies have been developed, including double crossover tiles<sup>118</sup>, multi-arm junction tiles<sup>119</sup>, single stranded tiles<sup>120</sup>, among others<sup>121–123</sup>. **Figure 8A and 8B** shows nanostructures designed using double crossover tiles<sup>124,125</sup>. These tile-based nanostructures can be used to develop programmable, molecular machines that can find applications in electronics, optics, as well as biomedicine<sup>126–130</sup>.

Brick-based approach is another self-assembling method that can form complex 3D DNA structures. Here, the concept of 2D molecular canvas built using single stranded tiles, have been extended to 3D in the form of bricks<sup>131–133</sup>. Again, by complementary base pairing using four short sticky ends, a complex, large 3D structure can be made by a slow, single annealing step. Furthermore, in this process, hundreds of bricks can simply be mixed together forming the target shape in a modular manner, similar to building Lego® shapes. Mathematical models have shown the relevance of temperature while building such structures<sup>134</sup>. Currently, it has been shown that the introduction of a nucleating, long, seed strands into the mixture, results in increasing the accuracy of the process as well as the stability of the target structure<sup>135</sup> (**Fig. 9A**). **Fig 9B** shows another stable DNA brick assembly that can resist enzymatic degradation<sup>136</sup>. Moreover, the first generation of bricks were prepared with 32 nucleotide-long strands that had four 8 nucleotide-long stick ends<sup>131</sup>. It has now been demonstrated that even larger structures assembled with thousands of DNA bricks are possible<sup>137</sup>. Here, gigadalton-scaled shapes can be created by using longer binding domains. Building complex structures with DNA brick strategy, therefore, shows immense potential in DNA nanotechnology.

Another notable self-assembly technique is the building of DNA origami-based structures, where DNA is used as a scaffolding material<sup>138</sup>. DNA origami can be defined as the folding of DNA to create user-defined, self-assembled, two-dimensional or three-dimensional shapes in nanoscale sizes. DNA origami takes advantage of the specificity of Watson-Crick base pairing<sup>54</sup>, to generate unique

DNA-based nano-scaled scaffolding materials<sup>139,140</sup>. Here, the double-helical DNA is held together by a group of short-stranded, “staple” oligonucleotides, which ultimately combines with a long single-stranded “scaffold” chain<sup>141</sup>. Along the length of the DNA, there are antiparallel crossovers that are formed of immobilized Holliday junctions. These junctions form both at the staple and the scaffold part of the structure. The immobile Holliday junctions essentially depend on two factors<sup>142</sup>. First, the molecules must strictly adhere to the Watson-Crick base-pairing strategy, and second, the nucleic acid molecules should maximize the Watson-Crick base pairing while self-assembling. Once the design is conceptualized and formulated using software, the strands are synthesized, and the folding reactions are carried out in suitable solutions. **Fig. 10A** and **10B** displays some complex structures created by DNA origami<sup>143,144</sup>. **Fig. 11A** shows an approach where electrostatic interaction between anionic DNA origami-based nanostructures and cationic gold nanoparticles was exploited to assemble a 3D tetragonal superlattice<sup>145</sup>.

Among the different origami-based design strategies, meshes and wireframe origami has gained popularity recently<sup>146–149</sup>. Moving away from the traditional bottom-up design approach, wireframe designs are formulated by applying a top-down design approach. Here, the final shape is designed first and then, the rest of the steps are automated to fabricate the DNA structures. This automated approach aims at reducing human effort. Meshes of desired shapes and dimensions are built by hybridizing long scaffold DNA strand along with multiple short staple DNA strands. These wireframe structures are more stable than lattice-based origami designs in biological buffers and at low cation concentrations<sup>147</sup>. Therefore, wireframe assemblies are expected to find an array of biomedical applications. **Fig. 11B** depicts three different two-dimensional wireframe shapes, square, pentagon, and hexagon<sup>146</sup>. Other than the wireframes, fractal assembly is another new design approach for synthesizing DNA origami-based nanostructures, where complex shapes can be designed with relative ease<sup>150</sup>.

The addition of nanoparticle clusters to DNA origami-based designs is also useful for fabricating patterns. These **Fig. 11C** depicts an example where copper metallized DNA origami can be applied in nanophotonics<sup>151</sup>. Three-dimensional DNA frames have also been designed to hold nanomaterials within them<sup>152</sup>. Unique optical or catalytic properties come out of such nanomaterials. From nanoelectronics<sup>153</sup> to biomedicine<sup>154</sup>, DNA origami has found purpose in a substantial number of applications. The self-assembling nature, unique shape, and chemistry of DNA has also given rise to another unique class of DNA-based substances, known as DNA hydrogels<sup>2,3,155–159</sup>.

### 3.6. Nanocomposite Hydrogels

Hydrogels are hydrophilic, squishy materials that form complex networks in three dimensions<sup>160,161</sup>. These networks are insoluble in water because the chains are linked together by chemical or physical crosslinks. Because of their biocompatibility, biodegradability, and hydrophilicity, hydrogels are frequently used for biomedical applications<sup>162–165</sup>. However, there are certain drawbacks of using natural hydrogels<sup>166</sup>. (a) Without any modification, hydrogels have low tensile strength. Because of such weak mechanical property,

hydrogels can break under an applied force. In the case of applications related to drug delivery, there are more issues. (b) Drugs may not load homogeneously inside the hydrogel. (c) The natural hydrogel is not injectable. Therefore, surgeries are required to place the hydrogels inside the body, which can raise unnecessary complications. (d) The high-water content also rapidly releases the drug from the hydrogel, which is a drawback when a controlled release is preferred. (e) Also, it is difficult for the hydrogels to carry hydrophobic drugs. To overcome these obstacles, nanocomposite hydrogels, also called hybrid hydrogels, are prepared where nanomaterials are added to polymers<sup>167–169</sup>. Either non-covalent or covalent bindings are used to attach the nanomaterial to the polymers<sup>170</sup>. These nanomaterials enhance the properties of the polymers<sup>171–173</sup>. For example, carbon-based nanoparticles can make the polymer responsive to heat and electricity, polymeric nanoparticles can improve the drug loading efficiency, inorganic materials like silicate nanoparticles can make the polymer injectable, metallic nanoparticles like gold can make the polymer responsive to light, and the list goes on. DNA-based nanocomposites are particularly useful because they have the added advantage of the DNA polymer. **Fig. 12A**<sup>174</sup> and **12B**<sup>78</sup> show two schemes by which DNA polymers can interact with nanomaterials via covalent and coordination chemistry. Coordination chemistry can also be used to attach DNA to a promising nanomaterial called metal-organic framework<sup>175,176</sup>. Metal-organic frameworks are porous, crystalline nanomaterials that can store therapeutics for biomedical applications<sup>177</sup>. **Fig. 13** depicts the biomedical applications of DNA nanocomposite hydrogels. Micro-scale techniques and high throughput screening<sup>178</sup> are two emerging applications of DNA nanocomposite hydrogels. Table 2 summarizes the chemistry and applications of some nanocomposite DNA-based hydrogels. Over the past several years, our lab has innovated in this area of research, creating mechanically enhanced nanocomposite hydrogels for drug delivery and tissue engineering. The following section highlights a few emerging nanocomposite hydrogels in the field of biomedicine. Our lab has primarily used two-dimensional nanosilicate disks to enhance the mechanical properties of DNA-based hydrogels. Sayantani *et al.* synthesized injectable hydrogels for the purpose of drug delivery<sup>14</sup>. Two different double-stranded DNA were shown to crosslink by Watson-Crick complementary base pairing (**Fig. 14A**). Nanosilicates were attached to the anionic DNA by electrostatic interaction. The resulting hydrogel was injectable with the capability of controlled drug release. Some chemically crosslinked DNA-based hydrogels can inherently be injectable<sup>13</sup>. Shown in **Fig. 14B**, when DNA was chemically crosslinked to oxidized alginate by a Schiff base reaction, the resulting imine bond was observed to be reversible in nature. Such a bond formed by the covalent binding of the amine group of the DNA with the aldehyde group of the oxidized alginate and made the hydrogel “self-healing”. Self-healing hydrogels can deform under mechanical stress but return to original shape once the stress is removed. Silicate nanoparticles were added to the hydrogel by electrostatic forces. The nanomaterials helped with the sustained release of simvastatin, a drug that helps with bone regeneration. Nanosilicates were also used to strengthen mechanical properties for tissue engineering purposes<sup>15</sup>. **Fig. 14C** shows how nanosilicates made the DNA-based hydrogel elastic. In addition to improving the material properties, the nanosilicates also helped with the sustained release of the protein, stromal cell-derived factor-1 (SDF-1 $\alpha$ ). Electrochemical properties can be enhanced with carbon-based nanoparticles<sup>179–182</sup>. DNA was non-covalently wrapped around carbon nanotubes to prepare electrochemically active hydrogels<sup>180,183</sup>. Carbon dots have been used to make DNA hydrogels

fluorescent<sup>20</sup>. Here, amine-functionalized carbon dots were covalently attached to phosphorylated short-stranded DNA and used for controlled drug delivery. These studies demonstrate the value of carbon-based nanocomposites in biomedical applications.

Metallic nanoparticles like gold, can make DNA-based hydrogels light-responsive. Song *et al.* conjugated gold nanoparticles to DNA hydrogels via electrostatic interaction and used the resulting mixture to deliver the anticancer drug, Doxorubicin<sup>184</sup>. Thiolated-DNA can also be covalently conjugated to gold nanoparticles<sup>185</sup>. Such an interaction was used to prepare a nanocomposite hydrogel that can be used in biomedical applications<sup>23</sup>. Silver nanoparticles have also been used to formulate DNA nanocomposite hydrogels. Fig. 15 illustrates an example of a hydrogel where DNA was conjugated to silver nanoparticles<sup>186</sup>. Such hydrogels can be suitable for drug delivery applications. Thus, these examples establishes the growing popularity of DNA-based nanocomposite hydrogels.

As discussed here, DNA-based hydrogels have surfaced as the next generation of innovative materials capable of many uses. An overview of the applications of DNA-based hydrogels have been presented in Table 3. The following section covers some of their unique applications along with the traditional biomedical ones.

#### 4. What are the Multifaceted Applications of DNA and its Hydrogel Derivatives?

##### 4.1. DNA-Based Hydrogels as Sensors of Toxic Heavy Metals

The presence of toxic heavy metals and hazardous substances in natural water sources is a cause for concern owing to their severe impact on human health<sup>187</sup>. Many toxic metals are present in various water sources, and identifying specific metals by real-time, on-site can be challenging. Often, the detection of heavy metals requires expensive and extensively laborious analytical instrumentation<sup>188</sup>. To avoid such pitfalls, researchers are always looking for cheaper and quicker alternatives. Recently, DNA-based sensors have risen to the occasion<sup>189,190</sup>. DNA molecules with catalytic properties are emerging as a new class of material for detecting heavy metals in the environment. Catalytic DNA, called DNAzyme, can interact specifically with metal ions, and Li *et al.* designed the first DNAzyme capable of detecting lead ions<sup>191</sup>. Similar DNAzymes can also detect Zn<sup>2+</sup><sup>192</sup>, Cu<sup>2+</sup><sup>193</sup> and Hg<sup>2+</sup><sup>194</sup>.

After the inception of DNAzyme-based biosensors, DNA hydrogels are also being used to detect metal ions because of the hydrogel's intrinsic advantages<sup>192</sup>. DNA hydrogels are biocompatible, biodegradable, and have a high surface area. Moreover, these unique properties, combined with extreme specificity, give them a distinct edge over those hydrogels prepared from carbon-based materials, clay minerals, metallic materials, and those functionalized by acid groups<sup>192,194</sup>. Huang *et al.* manipulated the unique chemical property of DNAzymes to develop a simple colorimetric tool for the detection of lead ions in water<sup>195</sup>. As shown in Fig. 16A, DNAzyme coupled with a substrate sequence was used as the crosslinker, binding to two linear DNA-polyacrylamide strands by complementary base pairing. Also, because of their optical photophysical properties, gold nanoparticles were entrapped within the gel. In the presence of lead, the hydrogel broke apart, releasing the gold nanoparticles. This release of the nanoparticles turned the solution from colorless to red (Fig. 16B), which was further proven with UV-Vis absorbance (Fig. 16C). However, this colorimetric method falls short at quantifying the amount of lead in the sample. The same study presents an innovative solution to this quantitation problem. The gold nanoparticles were replaced with gold core/platinum nanoparticles capable of decomposing H<sub>2</sub>O<sub>2</sub> to O<sub>2</sub>. A device was designed that trapped H<sub>2</sub>O<sub>2</sub> gas. Upon the release of the

nanoparticles in the presence of lead, the gas was converted to O<sub>2</sub>, which pushed a dye inside the device. The distance traveled by this dye directly quantified the amount of lead present.

However, in the world of DNA, DNAzymes are not the only molecules capable of metal detection. Specific DNA sequences can bind to metals. For example, it was found that thymine-rich DNA sequences bind with mercury<sup>196</sup>. Dave *et al.* took advantage of this interaction to remove mercury ions from polluted water<sup>164</sup>. A polyacrylamide gel was functionalized with acrydite-modified DNA strands. In the presence of mercury, a stable thymine-Hg<sup>+</sup>-thymine bond formed. This bond essentially trapped the mercury into the gel, removing it from the water. Therefore, these studies indicate that DNA-based materials are uniquely suited for tackling heavy metal pollution in the environment.

##### 4.2. DNA-Based Hydrogels as Biocatalysts

Besides heavy metal pollution, DNA also finds use as biocatalysts<sup>197,198</sup>. Mimics of naturally occurring enzymes have been extensively studied<sup>199</sup>. These synthetic alternatives have excellent tolerance, lower molecular weights, and easier penetration into cells. Many studies have recently focused on finding a mimic for the enzyme, horseradish peroxidase (HRP)<sup>200,201</sup>. HRP is an enzyme that catalyzes the oxidation of various organic substrates by transferring electrons to hydrogen peroxide and finds use in biotechnological applications<sup>202</sup>. However, these mimics involved laborious and slow syntheses methods. This introduces the need for new HRP mimics that can address such limitations. DNAzymes provide a solution to this limitation and are relatively easy to synthesize and are resistant to higher temperatures than their natural counterpart<sup>203</sup>.

Using DNAzymes, DNA-based hydrogels are being prepared as mimics of natural enzymes<sup>204</sup>. As depicted in Fig. 17A, a DNAzyme crosslinked hydrogel was used to detect hydrogen peroxide, which is relevant in industrial<sup>205,206</sup>, and biomedical<sup>207,208</sup> applications. The components of the DNAzyme included a guanine-rich aptamer sequence embedded within a longer oligonucleotide chain. In the presence of cations, a guanine-rich sequence was used to form a unique structure, called G-quadruplex. This G-quadruplex was attached to an iron compound, called hemin. The resulting complex can mimic HRP. The hydrogel consisted of polyacrylamide bound to an acrydite-modified single-stranded DNA sequence that can attach to parts of the DNAzyme. Therefore, with the help of the bond between the acrydite-DNA and DNAzyme, the polyacrylamide was crosslinked, forming the hydrogel. Finally, this DNA-based hydrogel was used to catalytically oxidize the substrate, 3,30,5,50-tetramethylbenzidine (TMB) in the presence of hydrogen peroxide. The oxidation of the substrate caused the hydrogel to turn blue (Fig. 17B), indicating the presence of hydrogen peroxide. Huang *et al.* developed an even quicker and easier technique to synthesize enzyme mimics<sup>209</sup>. A one-step rolling circle amplification method was used to prepare a DNA hydrogel with HRP-like catalytic functions (Fig. 17C). The sequence was selected in such a way that it formed an interstrand G-quadruplex. Hemin was added to the DNA. The resulting structure was tested with the chromogenic substrate, 2,2'-Azino-bis (3-ethylbenzothiazoline-6-sulfonic acid) (ABTS). Fig. 17D demonstrates a change in color after the substrate's oxidation indicated the presence of hydrogen peroxide.

Although not many enzyme mimics have been studied using DNA hydrogels, the functions of HRP have been successfully mimicked. With such success, DNA hydrogels are sure to make their mark in catalytic applications. Stepping outside the realms of catalysis, we will discuss the unique features of DNA that makes it compatible with electroconductive materials.

### 4.3. DNA-Based Hydrogels as Electrochemical Conductors and Actuators

Electroconductive hydrogels combine the water-holding property of hydrogels with the constituent material's electroconductive property<sup>210</sup>. They are an emerging class of polymer-based material with biomedical and electrochemical applications<sup>211</sup>. DNA polymer's inherent programmability has propelled them to become the choice for electroconductive hydrogels<sup>28,212</sup>. **Fig. 18A** shows carbon nanotubes and silica nanoparticles were encapsulated within the elongated DNA chain and mixed to form the nanocomposite hydrogel. The chain elongation was carried out by rolling circle amplification. Therefore, the length and sequence of the DNA were easily programmable based on the amplification process. The resultant nanocomposite hydrogel was electroconductive because of the embedded carbon nanotubes and silica nanoparticles. This electroconductive nanocomposite hydrogel then served as a support to grow exoelectrogenic bacteria, as can be seen from the confocal images (**Fig. 18B**). Furthermore, the exoelectrogenic bacteria grew only in the presence of the electroconductive DNA-based hydrogel (**Fig. 18C**). Exoelectrogenic bacteria can transfer electrons outside their cells and such a unique property of these microorganisms has been used in electrochemical applications<sup>213</sup>. Therefore, DNA-based nanocomposite hydrogels can be implemented in electrochemical applications.

Another electronic use for DNA-based materials comes in the form of actuators<sup>214</sup>. An actuator is a part of an electronic control system that receives information in the form of energy. This energy is then transformed into a mechanical output<sup>215</sup>. Recently, the concept of using DNA-based material for actuators have gained popularity because of its cost and suitable chemical properties<sup>216</sup>. Lee *et al.* developed a nanocomposite hydrogel where DNA-wrapped carbon nanotubes were incorporated inside a polypyrrole hydrogel<sup>183</sup>. Here, a carbon nanotube was used as the conductor. The hydrogen bonds between DNA and polypyrrole improved the overall mechanical and electrochemical properties of the hydrogel. With the application of cyclical voltage differential, the nanocomposite hydrogel went through cycles of compressions and expansions. Such conversion of an electrical stimulus to mechanical output revealed the success of the material. Therefore, these examples showcase the possibility of using DNA hydrogels as electroconductive materials.

### 4.4. DNA-Based Hydrogels in Drug Delivery

The potential of various drugs used today is limited by their administration methods, predominantly the oral and intravenous administration<sup>165</sup>. The toxicity and side effects caused by the high dosage, the lesser retention time in the body leading to frequent administration, and the absence of targeting are majorly responsible for the decrease in the overall efficacy of the drugs<sup>165</sup>. Several systems are being investigated to improve the delivery of drugs into the body: beaded delivery systems, liposomal systems, nanoparticle systems, and hydrogels<sup>217</sup>. Hydrogels are emerging as an excellent drug delivery system to achieve a more targeted and controlled release of drugs<sup>35</sup>.

Hydrogels are often functionalized or cross-linked with a range of materials that enable sustained release, often in response to stimuli, and the encapsulation of a variety of drugs. DNA hydrogels show great promise as they are self-assembling and have a well-defined structure<sup>14</sup>. Moreover, both hydrophobic and hydrophilic molecules could be encapsulated in the hydrogel since the incorporation of these molecules depends upon their binding affinity to the nucleotide sequences in the hydrogel network<sup>218</sup>. Because of the ease of inclusion, different types of therapeutic molecules are

encapsulated or cross-linked into DNA hydrogels, namely small molecules, biomolecules, and antigens.

**4.4.1. Delivery of Small Molecules.** Small molecule drugs are widely used to treat diseases due to their well-characterized properties and the ability to enter cells easily<sup>218</sup>. Many research groups have encapsulated these small molecules in DNA hydrogels to increase their efficiency and targeting. Ma *et al.* developed DNA and RNA hydrogels with floxuridine, an anti-cancer drug, incorporated into the nucleic acid strands (**Fig. 19A**)<sup>219</sup>. Floxuridine, a pyrimidine analog, is hydrophilic and can be easily incorporated into a hydrogel. Single-stranded DNA and RNA, which were partially complementary to one another, containing floxuridine, were synthesized. Once annealed, they formed Y-shaped motifs that hybridized to form nanogels. These nanogels would enter cancer cells more effectively due to their spherical nucleic acid structures (**Fig. 19B**). Once inside the cells, they would be degraded by the DNases and RNases and release floxuridine. The study revealed a targeted release of floxuridine. As discussed earlier, hydrophobic drugs have also been encapsulated within DNA hydrogels<sup>218</sup>. As depicted in **Fig. 19C**, the synthetic polymer poly(lactic-co-glycolic acid), was used to incorporate the hydrophobic drug within the DNA hydrogel. The drug used in this study, Dexamethasone, can treat allergic conjunctivitis. It is an anti-inflammatory, hydrophobic drug and needs to be encapsulated in a polymer first due to its hydrophobicity. Firstly, Dexamethasone was encapsulated in the polymeric nanospheres. Single-stranded DNA monomers that were partially complementary to each other and crosslinker monomers were used to form the hydrogel network. When the drug-loaded nanospheres were incubated with the DNA monomers at appropriate ratios, they formed the hybrid hydrogels due to complementary binding, with the nanospheres encapsulated in them. Both *in vitro* and *in vivo* analysis showed that these gels were more efficient than the water-insoluble free drug (**Fig. 19D**). From these two examples, we learn how DNA can be used as a delivery vehicle to deliver both hydrophilic and hydrophobic small molecules.

In an exciting approach, stimuli-responsive DNA hydrogels have been prepared to control and regulate the release of the drug molecules<sup>184,220</sup>. Song *et al.* synthesized a DNA hydrogel into which positively charged gold nanoparticles were loaded via electrostatic interaction (**Fig. 20A**)<sup>184</sup>. Gold nanoparticles can heat up in the presence of light and melt the hydrogel to release any drug present inside. Here, Doxorubicin, an anti-cancer drug, was intercalated between the DNA molecules. Upon irradiation with a laser, the nanoparticles heated up and the DNA melted. As a result, the nanoparticles were disassembled, and the drug was released. When injected intratumorally and irradiated, heat generation and the thermal denaturation of DNA was observed along with the release of both the drug and the nanoparticles. As indicated in **Fig. 20B**, *in vivo* analysis revealed the efficacy of the doxorubicin-loaded nanocomposite hydrogel in reducing tumor over time. This study proved that the drug-loaded nanocomposite hydrogel could potentially be used as a combination of thermo and chemotherapy for cancer.

Similarly, the efficacy of pH and ligand-responsive (**Fig. 20C**) DNA hydrogel microcapsules loaded with Doxorubicin for cancer therapy has been studied<sup>220</sup>. Calcium carbonate microcapsules, which contained Doxorubicin-modified dextran, formed the core on the hydrogels. Polycationic and polyanionic polymers were coated onto the microcapsules to give them a surface charge. The outermost polymer layer was covalently linked to amine-modified nucleic acid strands that served as promoters to begin the enzyme-free polymerization reaction, called hybridization chain reaction<sup>221</sup>.

Acrylamide copolymer chains were functionalized with two aptamer sequences A and B, which formed hairpin structures. Without the promoter, the hairpins were stable. However, the addition of the promoter in the mixture, initiated the chain reaction. These chains formed the DNA matrix of the gel. For synthesizing the ligand-responsive gel, the acrylamide copolymer chains were functionalized with aptamer sequences bound to the ligands (ATP). As shown in **Fig. 20D**, the aptamer-functionalized hydrogel was able to specifically kill cancer cells. In the case of the pH responsive gel, pH-responsive i-motifs were functionalized onto the acrylamide chains. Cancer cells treated with these Dox DNA hydrogels exhibited a higher rate of cell death.

**4.4.2. Delivery of Biomolecules.** The term biomolecule is used to define molecules that are essential for biological processes to be carried out. It includes proteins, carbohydrates, lipids, nucleic acids, metabolites, and natural products. These molecules are therapeutically effective and are being increasingly used in the pharmaceutical industry as drugs<sup>222,223</sup>. Hydrogels are being investigated to deliver these biomolecules to the target site to achieve targeted delivery and sustained release<sup>2</sup>. Hydrogels are efficient drug delivery systems due to their hydrophilic polymer network. They mimic the conditions of native tissue. However, the complex crosslinking and chemical conjugation of the biomolecules hinder the hydrogel's potential to be used as drug delivery vehicles. This obstacle can be overcome by introducing aptamers into the hydrogel<sup>222</sup>. Aptamers have stable structures that can bind to other molecules with high binding specificity and affinity. Aptamers can undergo hybridization, i.e., combine with complementary DNA strands to form a network or release a bound molecule<sup>222</sup>. The following are examples of two DNA hydrogels synthesized using DNA oligonucleotides and natural polymers, such as chitosan and hyaluronic acid, that are used to deliver biomolecules.

Zhang *et al.* designed aptamer-functionalized hydrogels that could capture and release specific proteins<sup>222</sup>. The proteins investigated were Platelet-Derived Growth Factor BB (PDGF-BB) and Vascular Endothelial Growth Factor (VEGF)<sup>222</sup>. The hydrogel was formed by several sequential reactions. Firstly, a polymeric solution of Allyl Chitosan was formed by reacting allyl chloride with chitosan in a basic solution. Allyl Chitosan was crosslinked by using epichlorohydrin as the crosslinker, which formed the hydrogel (**Fig. 21A**). The hydrogel was dried to obtain a film. Aptamer sequences specific to PDGF-BB and VEGF, with sulfhydryl groups at one end and dye molecules at the other end, were used to enhance, also called functionalize, the hydrogel film. The PDGF-BB aptamer was labelled with green fluorescent dye and the VEGF aptamer was labelled with a red fluorescent dye. Photocoupling was carried out by using 365 nm wavelength UV light in the presence of a photoinitiator. As a result of photocoupling, bonds were formed between the sulfhydryl groups of the aptamers and the C=C double bonds of allyl chitosan. Subsequently, the hydrogels were patterned with the aptamers. The PDGF-BB aptamer was coupled first, followed by the VEGF aptamer. These aptamer-patterned hydrogel films could capture VEGF and PDGF-BB proteins (**Fig. 21B**) and showed sustained release over time. Upon the addition of the complementary DNA, all bound proteins were released.

In another study, hyaluronic acid (HA) hydrogels were functionalized with antisense oligonucleotides, which are short chain DNA molecules, to obtain a sustained release of anti-NgR aptamers<sup>223</sup>. The release pattern has been demonstrated in **Fig. 21C**. Anti-NgR aptamers bind to the cell surface protein called the nogo receptor. The binding of the anti-NgR aptamer to the nogo receptor prevents myelin inhibitors from binding to this surface protein. The prevention

of this myelin inhibitor binding is used to treat spinal cord injuries. The binding affinity between the antisense oligonucleotides and the anti-NgR aptamers has been taken advantage of in this hydrogel for the aptamer's controlled release. Here, two HA hydrogels, namely methacrylated HA hydrogels (implantable) and thiol HA hydrogels (injectable), were investigated. Oligonucleotides were functionalized onto the thiol HA hydrogels by an oxidation reaction resulting in the formation of a disulfide linkage between the thiol groups on the HA hydrogel and the oligonucleotide. 1-ethyl-3-(3-dimethylaminopropyl) carbodiimide-N-hydroxysulfosuccinimide, called EDC-NHS, coupling reaction was used to functionalize the methacrylated HA hydrogels, which resulted in the formation of an amide bond between the carboxylic groups on the HA hydrogel and the amine groups on the oligonucleotides. The HA hydrogels showed a sustained release of the anti-NgR aptamers, and higher affinity hydrogels were found to release the anti-NgR aptamers for up to 28 days (**Fig. 21D**). These hydrogels could be designed to deliver both proteins and aptamers.

**4.4.3. Delivery of Antigens.** Antigens are substances that can induce an immune response in the body by activating B cells, which leads to the production of antibodies against the antigen<sup>224</sup>. Once an immune response is induced, a memory of the antigen is created in the form of memory B and T cells. On successive exposure to the antigen, the body can mount a faster response by rapid activation and proliferation of these memory cells. This concept is exploited to make vaccines where antigens are combined with adjuvants and introduced into the body. DNA hydrogels are being investigated as delivery vehicles for antigens due to their biocompatibility, high binding affinity to peptides and nucleotide sequences, sustained release of antigens, and self-assembling property. Shao *et al.* designed a DNA supramolecular hydrogel vaccine system containing two immunogenic components<sup>225</sup> as depicted in **Fig. 22A**. Firstly, short-stranded DNA of unmethylated cytosine-phosphate-guanine (CpG), which activates the innate immunity against pathogens and initiates the production of proinflammatory cytokines. Secondly, the P1 peptide, which consists of two peptides (tumor-associated and tetanus toxoid antigens) linked sequentially. The hydrogel system consisted of two building blocks: a Y-scaffold made of three partially complementary short-stranded DNA and a linker DNA duplex with sticky ends. The CpG sequences were assembled onto the linker sequence stoichiometrically and the P1 antigen was incorporated into the hydrogel network via electrostatic interactions. The hydrogel network self-assembled by hybridization. It was found that the CpG oligonucleotide and P1 antigen were distributed uniformly in the hydrogel network, and they could activate the immune system and showed an anti-tumor effect (**Fig. 22B**). In a similar work, the DNA self-assembly was initiated by varying the concentration of salts in the DNA preparations, and the resulting hydrogel was used to deliver bioactive materials<sup>226</sup>. The above studies demonstrate the effectiveness of DNA hydrogels to deliver therapeutic molecules.

#### 4.5. DNA-Based Hydrogels in Tissue Engineering

Tissue engineering can be defined as "an interdisciplinary field that applies the principles of engineering and the life sciences toward the development of biological substitutes that restore, maintain, or improve tissue function"<sup>227</sup>. Various natural and synthetic polymers have been used to synthesize matrices such as scaffolds to facilitate the growth of different cells and tissues for repair and healing<sup>228,229</sup>. Biocompatibility, ability to promote cell migration and adhesion, mechanical properties that mimic native tissue, permeability for molecular transport, and degradation rate comparable to the

regeneration rate of cells are some of the essential characteristics of the biomaterials used<sup>227,230,231</sup>.

Hydrogels are being extensively studied for the synthesis of scaffold materials<sup>232</sup>. They are biocompatible, and their high-water content allows them to mimic the mechanical properties of tissues<sup>230</sup>. By the incorporation of biomolecules, specificity to cells and improved migration and adhesion rates are achieved. Such migration of cell is necessary for tissue repair. However, their high permeability does not allow for good binding and the long-term retention of these biomolecules. DNA hydrogels are being developed to address these drawbacks. By the incorporation of nucleotide sequences specific to the biomolecules, adhesion of peptides and other biomarkers, scaffold specificity, and function could be improved<sup>230,233</sup>. Towards that direction, Chen *et al.* synthesized aptamer-functionalized poly(ethylene glycol) (PEG) hydrogels mimicking the extracellular matrix for the adhesion of cells<sup>230</sup>. Poly (ethylene glycol) diacrylate solution and acrydite-functionalized aptamer mixture formed the reaction solution to synthesize the hydrogel (**Fig. 23A**). This solution was poured over a glass slide and covered with a silanized glass slide. The acrylate groups on the silanized glass slide got incorporated into the polymer network. This incorporation resulted in the hydrogel getting attached to the silanized glass slide. The aptamers were incorporated into the hydrogel by the formation of a double bond between the acrydite group of the aptamers and the polymer by radical polymerization. Here, the aptamer used was Sgc8c, which is specific to a T lymphoblastoid cell line called CCRF-CEM. It was found that the Sgc8c-functionalized aptamer showed improved recruitment of the lymphoblastoid cells when compared to the native PEG hydrogel (**Fig. 23B**). The aptamer concentration, seeding time of cells, and spacer length could be varied to regulate the level of cell adhesion.

Following a similar strategy, an acrylamide hydrogel with acrydite-modified adapter sequences was also developed<sup>234</sup>. However, to further mimic the native environment of biological systems, polyvalent DNA polymers were functionalized onto the hydrogels' surface. The ligands on polyvalent polymers can bind to different receptors on the target molecule, enabling stronger binding<sup>235</sup>. For carrying out the functionalization of the polyvalent DNA sequences, three steps were carried out. First, the hydrogels functionalized with the adapter sequences were incubated with DNA initiator sequences. The initiator sequence was partially complementary to the adapter sequence and hence, linked with it. Second, two DNA monomers were incubated with the hydrogel from the previous step. One of the monomers was partially complementary to the DNA initiator and partly to the other monomer, resulting in a structure where part of the second monomer was unbound. Third, the aptamer sequence specific to the target and complementary to the unbound monomer was incubated with the hydrogel. As a result, the polyvalent aptamer-functionalized films were formed. These were found to increase cell adhesion in dynamic flow.

Galli *et al.* synthesized PEG diacrylate-thiolated HA hydrogels functionalized with anti-fibronectin aptamers to improve cell adhesion on scaffolds (**Fig. 23C**)<sup>233</sup>. Fibronectin is a glycoprotein that enhances cell adhesion and formation of extracellular matrix during wound healing<sup>236</sup>. By functionalizing the hydrogel with an anti-fibronectin aptamer, the fibronectin in the serum would be recruited, which would promote and improve the recruitment and adhesion of cells to the hydrogel matrix. The anti-fibronectin aptamer used was modified to contain biotin on the 5' end and one S-S bond on the 3' end. These aptamers were reduced to give free thiol groups and purified. The hydrogel scaffold was prepared similar to the preparation of thiolated HA hydrogels by Wang *et al.*<sup>237</sup>. Firstly,

the aptamers were added to the PEG diacrylate solution. The aptamers were immobilized to the hydrogel network by forming a bond between the acrylates in the polymer and the thiols at the 3' end of the aptamers. Secondly, thiolated HA was added, which resulted in the formation of the final hydrogel. It was found that cell adhesion increased *in vitro* using this DNA hydrogel as a scaffold (**Fig. 23D**).

More recently, an aptamer-functionalized scaffold made of silk fibroin and HA to recruit Mesenchymal Stem Cells was prepared<sup>237</sup>. Silk fibroin is extracted from silkworm (*Bombyx mori*) cocoons and is a biopolymer used in cartilage tissue engineering. HA was incorporated to improve chondrogenesis, and an aptamer, Apt19s, that has been found to label pluripotent stem cells was introduced to promote the recruitment of mesenchymal stem cells. The fibroin sponge was functionalized with amino-modified Apt19s sequences by the EDC-NHS coupling reaction. For synthesizing the hydrogel reinforced with the sponge, HA-tyramine conjugates were prepared first by EDC-NHS reaction. The fibroin bound with aptamer sponge was immersed into a solution of HA-tyramine and silk fibroin. The HA-tyramine and silk fibroin were enzymatically crosslinked in the presence of horseradish peroxidase and H<sub>2</sub>O<sub>2</sub>, which formed di-tyrosine crosslinks between the silk fibroin and HA-tyramine. Thus, the gel was crosslinked. When implanted in a disease model, it was found that this hydrogel showed slow degradation rate, increased stem cell recruitment, and increased repair of osteochondral defects. Another interesting area of research involves bioprinted scaffolds using DNA-based hydrogels. **Fig. 24A** displays a strategy for developing such scaffolds for tissue engineering applications<sup>238</sup>. Here, the primary network was made of a polypeptide-DNA conjugate, whereas the crosslinker was a double stranded DNA linker with sticky ends that were complimentary to the primary network's DNA. These two components were printed at the same location, where the DNA rapidly crosslinked to form the tissue constructs. Furthermore, the developed hydrogel could also be actively degraded with enzymes. **Fig. 24B** shows the appearance of the bioprinted hydrogel. Additionally, the accompanying chart demonstrates the elasticity of the hydrogel. Finally, **Fig. 24C** proves the degradability of this DNA-based hydrogel with protease enzyme and DNA restriction enzyme. Overall, from the above studies, we can conclude that DNA hydrogels show great potential in the field of tissue engineering due to their ability to recruit molecules and cells that promote the repair of damaged tissues and organs, and their ability to form mechanically resilient scaffolds.

#### 4.6. DNA-Based Hydrogels as Biosensors

Biosensors are inexpensive, movable devices that can detect analytes in solution<sup>239</sup>. The analytes are usually pathogens, proteins, biomarkers, or any other harmful substances whose detection in the patient can lead to an early diagnosis and subsequent treatment. Many of these analytes had previously been detected using analytical techniques such as high-performance liquid chromatography (HPLC) or gas chromatography-mass spectrometry (GC-MS). These techniques require expensive equipment and specific skill sets. To address this issue, hydrogel-based sensors have emerged as a new alternative in diagnostics technologies<sup>240</sup>. Because of their high selectivity and specificity, DNA-based hydrogels are being increasingly used for diverse biosensing purposes<sup>241</sup>. They are relatively cheap to make, biofriendly, and easy to use. Different techniques have been employed to sense various analytes such as pathogens, small molecules, proteins, and biomolecules. This section will cover some of the latest developments in the field of DNA hydrogel-based biosensors.

**4.6.1. Detection of Small Molecules.** Small molecule drugs are effective in treating diseases for their ability to enter cells easily<sup>242</sup>. However, some drugs or the accumulation of drugs can be harmful to both the human body<sup>243</sup>. The following are some examples of DNA hydrogels being used as biosensing mechanisms for small molecules. One standard method for preparing biosensors to detect the presence of small molecules is using aptamer-based hydrogels. At times, aptamers are incorporated in the sensors as crosslinkers<sup>244</sup>. This design heavily relies on the competitive binding of the target molecule to the DNA aptamers. Again, the high specificity of aptamers drastically reduces the chances of getting false signals. Aptamers are also easy to make, and because small quantities are effective, they are cheap. Yang *et al.* were the first to develop an aptamer-based hydrogel for the detection of the organic compound, adenosine<sup>244</sup>. Adenosine is a nucleoside that is biologically important and is also considered as a biomarker for cancer<sup>245</sup>. Yang *et al.* linked two acrydite-modified DNA strands to a polyacrylamide chain<sup>244</sup>. As indicated in **Fig. 25A**, the crosslinker was designed in three sections. The first segment hybridized with Strand A. The second segment hybridized with the last five nucleotides of Strand B. The third segment, which was the aptamer sequence for adenosine, hybridized with the seven nucleotides of Strand B. Therefore, in the presence of adenosine, the aptamer segment of the crosslinker would competitively bind to adenosine, and detach from Strand B. The binding of the aptamer segment to adenosine dissociated the hydrogel. Gold nanoparticles were trapped inside the hydrogel, and in the presence of adenosine, the trapped nanoparticles released to the solution. The release of the nanoparticles turned the solution red in color (**Fig. 25B**). Using aptamers, this work presented a simple yet very effective technique in detecting the presence of analytes visually. The simplicity of this technique relies on the fact that by using aptamers, a vast majority of analytes can be tested. A similar strategy was employed to detect a harmful drug, cocaine<sup>246</sup>. An aptamer sequence specific to cocaine was used in this case. Here, instead of using gold nanoparticles, the enzyme amylase was trapped inside the hydrogel. When cocaine bound to the aptamer, the entrapped amylase was released. This led to the breakdown of the surrounding polysaccharide, amylose, to sugar. With iodine in the mixture, the breakdown of amylose caused a change in color. This change in color with enzyme is highly sensitive. However, colorimetric techniques have their limitations<sup>247</sup>. The presence of background signals may cause errors in such cases. Tan *et al.* devised an improved method where a fluorescence signal was used as the parameter for detection<sup>247</sup>. The components of the hydrogel along with its function has been depicted in **Fig. 25C**. Graphene oxide sheets, adenosine, and an aptamer specific to oxytetracycline were physically mixed to prepare the hydrogel. Oxytetracycline is an antibiotic that is toxic to the aquatic environment<sup>248</sup>. Adenosine and aptamer served as co-crosslinkers, whereas graphene oxide formed the backbone of the hydrogel. The aptamer was also tagged with a fluorescent dye. Steric hindrance caused the aptamer to detach from the dye once the aptamer bound to the antibiotic. Finally, the degree of fluorescence was measured to quantify the amount of drug in the solution (**Fig. 25D**).

**4.6.2. Detection of Biomolecules.** Abnormal quantities of specific proteins and biomolecules are indicators of cancers and other diseases<sup>249,250</sup>. Their presence in the blood are often exploited for early detection of diseases. Moreover, the detection of these molecules can also be used to capture cells. As stated previously, these molecules can include proteins, carbohydrates, lipids, nucleic acids, metabolites, and natural products. The following are examples

of DNA-based hydrogels used as biomarkers for cancer and for cell capture.

Yao *et al.* developed a system that can detect as well as release analytes (**Fig. 26A**)<sup>251</sup>. They used double-rolling circle amplification to prepare two elongated DNA chains with the aptamer sequence embedded within them. The DNA chains also consisted of sequences that were complementary to each other. Therefore, with the help of these complementary bindings, the two chains crosslinked. The aptamer sequence, Apt19s, specific to a protein found on the surface of bone marrow stem cells, formed a part of the hydrogel. Bone marrow stem cells are essential for tissue engineering and wound repair applications. This hydrogel could capture the stem cells when the aptamers bound to the proteins. The process of capturing cells is termed "cell fishing". Since the aptamers were not crosslinkers, the hydrogels did not break in the presence of the analyte. However, by enzymatic degradation, the DNA hydrogel could be broken, thereby releasing the trapped cells. Thus, this technique is efficient in detecting, capturing (**Fig. 26B**), and releasing cells.

As discussed earlier in the environmental section, DNAzyme-based biosensors have gained popularity in detecting various analytes<sup>252</sup>. Recently, a DNAzyme-based hydrogel was synthesized to detect circulating tumor DNA, which is a biomarker for cancer<sup>253</sup>. As shown in **Fig. 26C**, this method uses a padlock probe DNA, which is a highly specific circular DNA. This DNA can target the biomarker, which is a circulating tumor DNA. The binding of padlock DNA with the biomarker initiated rolling circle amplification. A second DNA template was paired with the amplified mixture. The pairing with the second DNA template resulted in the formation of a hydrogel. Therefore, the hydrogel could only form in the presence of the biomarker. This hydrogel was designed in such a way that a G-quadruplex developed within the structure, which coupled with hemin catalytically oxidized a chromogenic substrate. The oxidized substrate produced a change in color and a quantitative analysis by UV-Vis absorption (**Fig. 26D**) ensure the visual detection of the biomarker. Aptamers can also be integrated with DNAzymes to prepare highly specific biosensors. This concept has been used to construct DNA nanoassemblies to detect cancer cells<sup>254</sup>.

Electrochemical sensors are also being employed for sensing biomolecules<sup>255</sup>. Unlike their visual-sensing counterparts, electroconductive biosensors with DNA-based materials do not suffer from the limitation of semi-quantitative approaches, as shown by Liu *et al.*<sup>256</sup>. Here, an electrochemical based sensor was used to detect miR-21 microRNAs. MicroRNAs are a class of short ribonuclease molecules that serve as biomarkers for cancer, and miR-21 is associated with lung cancer<sup>257</sup>. Overexpressed miR-21 in lung cancer needs to be detected quickly and with ease, and DNA hydrogels were used to do so<sup>256</sup>. Here, two acrydite-linked DNA strands were polymerized with acrylamide. The mixture was crosslinked with a ferrocene-tagged DNA probe to form the hydrogel. Ferrocene is an organometallic compound used in electrochemistry<sup>258</sup>. This DNA hydrogel was fixed on a silanized titanium indium oxide electrode for final electrochemical measurements. The primary objective of the DNA probe was to bind competitively to the target, miR-21. Once the ferrocene trapped DNA hydrogel was exposed to the target, parts of the hydrogel dissolved. This breaking of the hydrogel released some of the ferrocene molecules from within. The resultant current from the broken gel was shown to be less than that of the intact hydrogel. Such a reduction in current indicated the amount of miR-21 present in the solution. The high specificity of the DNA to miR-21 plays a crucial role in enabling the DNA hydrogel sensor to avoid showing incorrect results.

**4.6.3. Detection of Pathogens.** Pathogens are disease causing agents that can spread quickly through various modes of transmission, such as through the exchange of bodily fluids<sup>259</sup>. They are classified as viruses, bacteria, fungi, protozoa, and helminths (worms)<sup>259</sup>. Detecting pathogens is critical for improved healthcare. DNA-based hydrogels have been used as biosensors to detect pathogens and the following are examples of such hydrogel biosensors.

Xu *et al.* used an aptamer-based DNA hydrogel to detect the presence of avian influenza virus (AIV), a pathogen that causes avian influenza<sup>260</sup>. The aptamer was used to specifically bind to the virus, whereas quantum dots were used to obtain fluorescent signals (**Fig. 27A**). Quantum dots are nanosized fluorophores comprising of a core, a shell, and a component that can bind to preferred biomolecules. The quantum dots used in this study consisted of a cadmium selenide core, a zinc sulfide shell, and a streptavidin protein that can bind to DNA. When excited with UV light, the quantum dots emitted a fluorescent signal. However, in the presence of a quencher, the signal was absent. This property of the quantum dots, combined with the specificity of the aptamer, was exploited to design the hydrogel. One end of the aptamer was linked to an acrydite molecule, which could bind to polyacrylamide. The other end of the aptamer was bound to a quencher. Two single-stranded DNA chains were selected, and both the strands could partially bind to the aptamer. One of the strands was also functionalized with acrydite for crosslinking with polyacrylamide. The other strand was attached to quantum dots via the streptavidin protein. With the help of the acrydite molecules, the aptamer and the DNA strand could bind to polyacrylamide, forming the hydrogel. The structure of the hydrogel was designed in such a way that the quencher was close to the quantum dot, which reduced the fluorescent signal. However, in the presence of the target virus, the aptamer selectively bound to the virus, thereby releasing the DNA strand attached to the quantum dot. This release of the quantum dot elicited a fluorescent signal, which was used to determine the presence of the virus (**Fig. 27B**) as well as prove the specificity of the hydrogel (**Fig. 27C**).

Interestingly, polymerization techniques were also employed in designing biosensors to detect pathogens<sup>261</sup>. In a real-time polymerase chain reaction, also called q-PCR or quantitative PCR, fluorescent tags were used to quantify the amount of DNA after each chain elongation cycle. This quantitative approach was used to detect pathogens. By taking advantage of the chemical properties of DNA-based hydrogels, a portable q-PCR-based system was designed to detect the sexually transmitted bacteria, *Neisseria gonorrhoeae*<sup>262</sup>.

The above examples capture the various advantages of using DNA-based materials for detection of different analytes. These studies were examples of mainly biomedical applications. However, as discussed earlier, such sensors find substantial use in environmental applications as well.

#### 4.7. DNA-Based Hydrogels for Biomolecule Production

Synthesis of biomolecules, like proteins, are essential for biomedical applications. Proteins are usually produced in living cells (**Fig. 28A**)<sup>263</sup>. However, novel methods with DNA-based hydrogels have been able to synthesize proteins without using living cells<sup>263</sup>. The underlying strategy in these hydrogels is using DNA that contains genetic information for producing proteins. Here, the hydrogel was prepared using X-shaped DNA as the primary building block for the hydrogel. The X-shaped DNA is a branched, 3-dimensional DNA molecule with a complementary sticky end on each arm<sup>264</sup>. Sticky ends are short, single-stranded segments that can bind to complementary base pairs, and in this case, the sticky ends had palindromic nucleotide sequences. Palindromic sequences have inverted symmetry and

occur when the bases are arranged in such a way that their complementary strand bases are arranged in the exact reverse order. Using the enzyme DNA ligase, the X-DNA can bind to each other forming hydrogels. In the case of hydrogels capable of producing proteins, the X-DNA were ligated with linear plasmids, which contain genetic information for the said protein. The gel with the plasmids was then incubated with cell lysates. These lysates contain all the necessary material required for protein production. Therefore, the hydrogel could synthesize the protein. However, a high quantity of DNA is needed to prepare this hydrogel, which makes it expensive. Recently, a cheaper alternative was designed for cell-free protein synthesis<sup>265</sup>. **Fig. 28B** shows a polyethylene glycol diacrylate polymer was crosslinked with acrydite-modified DNA. The DNA was synthesized from a linear plasmid by polymerization reaction, which contained the genetic information needed for protein synthesis. The resulting hydrogel was incubated with the necessary material required for protein production. Thus, a cheaper system was designed here to produce proteins. However, the chemicals needed for preparing the polyethylene glycol polymer are toxic and need to be carefully removed from the hydrogel before further use. A similar strategy with plasmid DNA has also been used to produce siRNA, which is a short ribonucleic acid fragment that can interfere with genetic functions<sup>266</sup>. Therefore, in the past two decades, DNA hydrogels have also become useful in the production of biomolecules.

Although clinical trials have not been conducted with DNA-based hydrogels, nucleic acids as therapeutic agents have recently found commercial success. In the following section, we illustrate the clinical and commercial success of nucleic acids, hoping that this evidence would make the readers hopeful about the fate of DNA-based hydrogels.

#### 5. Are Nucleic Acids Viable for Commercial Applications?

In addition to being used as a component of hydrogels, DNA has been used as components of therapeutic agents, gene therapy, vaccines, and adjuvants. Their high specificity to target sequences and receptors, bioavailability, immunogenicity, and reduced toxicity make them ideal candidates for the above applications<sup>74,75,267-272</sup>. Many of these DNA-based studies have proceeded to the clinical trials. **Fig. 29** represents the DNA that have already found clinical success and ones that are likely to become successful in advanced healthcare. The following are examples of DNA-based therapeutics that are commercially available.

DNA-based drugs make use of either antisense oligonucleotides (ASOs) or DNA aptamers<sup>267,268</sup>. ASOs and aptamers are single stranded nucleic acid sequences. They function by binding to mRNA or other target nucleic acids and prevent abnormal protein expression or disease pathogenesis<sup>267,268</sup>. Fomivirsen was the first ASO drug that was approved<sup>268</sup>. It was an antiviral drug that became commercially available in 1998 but was later withdrawn due to the emergence of more effective antiretroviral drugs. Mipomersen is another commercially available ASO drug that is effectively used to treat a genetic disorder called familial hypercholesterolemia.

Another well known clinical application of DNA is in gene therapy. Gene therapy is the process by which a mutated gene is replaced by a normal gene<sup>269</sup>. Viral vectors and genome editing tools are commonly used to deliver or modify genes<sup>269,270</sup>. Imlygic, Kymriah, Luxturna, and Zolgensma are examples of gene therapy drugs that are approved and commercially available<sup>270</sup>. They are used to treat different types of cancers and genetic disorders<sup>270</sup>.

A new and quickly rising application of DNA with prospects for clinical use is genomic editing in the form of the clustered regularly

interspaced short palindromic repeats (CRISPR)-Cas9 system<sup>273</sup>. Discovered in the bacterial genome, CRISPR sequences consist of repeat DNA fragments separated by non-repeating units called spacers<sup>274</sup>. These spacers are sequences that have been inserted in the bacterial genome after viral invasions<sup>275</sup>. Cas9, a CRISPR-associated protein, is a nuclease that forms a complex with single guide RNA (sgRNA)<sup>274</sup>. The Cas9-sgRNA complex is able to base pair with the virus-associated target DNA sequence. This target sequence is adjacent to a motif, which acts as the recognition site for the complex<sup>276</sup>. This binding event induces cleavage of the dsDNA by Cas9, providing opportunities for insertions or deletions<sup>276</sup>. Once the gene has been edited, the materials needed for repairing the DNA are recruited. By reprogramming the sgRNA sequences, the bacterial Cas9-sgRNA complex can be targeted to known gene abnormalities in mammalian cells<sup>277</sup>. Currently, clinical trials involve knocking out the programmed cell death 1 (PD-1) gene in peripheral blood lymphocytes using the CRISPR-Cas9 system. The PD-1 gene regulates T-cell activation<sup>278</sup>. By knocking out the PD-1 gene, the anti-tumor activity of T cells increases, and thereby improves the immune response<sup>278</sup>. Clinical trials for PD-1 knockouts by gene editing are currently being investigated for advanced esophageal cancer and metastatic non-small cell lung cancer.

Besides being used as therapeutic agents, DNA can also be used as vaccines and adjuvants. Although there are no DNA vaccines that have been approved for use in humans, there are several that are in clinical trials and that are approved for veterinary use<sup>271</sup>. Vaccines are frequently administered along with adjuvants, and unmethylated CpG DNA sequences have successfully been used as one. Many clinical trials involving the use of DNA as adjuvants along with antigens/anti-cancer agents were conducted. HepHisav-B is a commercially available Hepatitis B vaccine that successfully makes use of this material.

## 6. Present Limitations and Future Direction

Recent clinical success of DNA as a therapeutic agent and the rapid technological advancement discussed in this review provides hope for DNA as a nongenetic, generic polymer. Furthermore, technology has evolved to visualize DNA dynamics on live cells using atomic force microscopy, atomistic molecular dynamics simulations, fluorescence lifetime imaging microscopy<sup>279,280</sup>. Detailed understanding of the physics of double helical DNA movements including twists, turns, and coil using these new techniques may help us synthesize more advanced DNA-based nanostructures for future applications. With such advancement, we foresee that DNA-based nano and macro products will find clinical and commercial success within the next five years. However, to increase the viability of DNA, focus must be on large-scale synthesis. At present, large-scale production of DNA is laborious and expensive. One way of offsetting the cost, especially in the case of designing tissue-scaffolds, would be to use DNA in combination with FDA-approved polymers. Additionally, using DNA only as crosslinkers can reduce cost and increase selectivity of tissue-scaffolds. In this section, we will discuss the future of DNA along with their hurdles and probable solutions.

### 6.1 DNA-based additive manufacturing and tissue engineering

Additive manufacturing of biological molecules, or 3D bioprinting, is an area where DNA can be applied immediately. DNA is biocompatible, biodegradable, and non-toxic, making it suitable for bioprinting. Furthermore, by implementing simple, rational functionalization and reinforcement strategies, DNA polymer and its

nanocomposites can be made cell instructive<sup>281</sup>. However, there are certain mechanical requirements for the biomaterial to be printed, or bioink<sup>282</sup>. These mechanical requirements include low viscosity of the bioink during the printing process, such that, the bioink can be extruded through the nozzle of the printer without getting clogged. Additionally, the bioink must be able to shield the cells from shear stress. After being extruded, the bioink must maintain high shape fidelity, which is difficult for complex shapes and geometries. DNA hydrogels are mechanically weak on their own, and to overcome these challenges, nanomaterials can be infused to improve the overall printability of DNA. Nanomaterials may also be incorporated to impart unique properties to the DNA hydrogel-based bioinks. These unique properties, including light-responsiveness<sup>283</sup>, thermo-responsiveness<sup>284</sup>, magnetic field-responsiveness<sup>285</sup>, among others<sup>286</sup>, will boost the overall applicability of the bioprinted scaffolds. Increased research efforts in this area will soon enable the fabrication of stimuli-responsive, complex, DNA-based tissue mimics for both *in vivo* and *in vitro* applications.

### 6.2 DNA as a biomaterial for vaccine delivery and immune-modulation

DNA-based nanotechnology and polymer science has already started contributing towards the development of vaccines. Recently, DNA origami-based nanostructures were used as the carriers of antigen for immune cell activation<sup>138</sup>. It was observed that immune cell activation can be maximized by spatially organizing the antigens on DNA nanostructures. Furthermore, injectable DNA hydrogels containing single stranded motifs of unmethylated cytosine-phosphate-guanine can modulate the immune system<sup>225</sup>. However, vaccine development with nongenetic DNA is at its nascency. With nanoparticles, a significant challenge comes from the possibility of chronic accumulation<sup>287</sup>. The threat is amplified in the case of large nanoparticles. To assess this detrimental possibility, elimination pathways of DNA-based nanostructures must be determined to ensure patient safety. Future studies should also consider the addition of multiple functionalities to the DNA-based vaccine formulations. Nanoparticles in combination with DNA can be an effective method of enabling bioimaging or incorporating antibacterial properties. Aptamers can also be added for targeted delivery<sup>288</sup>. These improvements will increase the likelihood of commercial success of DNA-based polymers in vaccine therapy.

### 6.3 DNA sculpting and origami in nanoscale: emerging technologies

DNA nanofabrication is an emerging field where a variety of nanomaterials, such as metallic, non-metallic, metal oxide, and polymer nanomaterials, are fabricated using DNA origami<sup>289</sup>. Shani *et al.* prepared superconducting structures from gold nanoparticle DNA lattices coated with superconducting Niobium<sup>290</sup> (**Fig. 30A and 30B**). These nanofabricated devices can be used for various applications such as nanoelectronics, drug delivery, and nanosensors<sup>291,292</sup>. Among the different nanostructures being investigated, nanorulers are being studied and developed for numerous microscopy applications<sup>292</sup>. Nanorulers are DNA origami structures designed to have a specific length and are bound to dye molecules at various positions and with different patterns<sup>293</sup>. The most prominent application of these nanorulers is in super-resolution microscopy<sup>294</sup>. Nanorulers are used as reference tools, standards, and positive controls to test and validate the various parameters in this technique. Another related application of DNA origami is plasmonics. Plasmonics deals with the surface plasmon resonance of metal nanoparticles and have applications in sensing and diagnostics<sup>295</sup>. DNA origami constructs with complex and precise

patterns are used to assemble metal nanoparticles such as gold nanorods<sup>296</sup> for the plasmonics applications<sup>297</sup>. DNA origami can also be used to form nanopores, which are structures that represent natural pores on the biological membranes and can be formed by pore forming proteins or synthetic materials<sup>298</sup>. These nanopores are important for sensing and sequencing applications. Bell *et al.* developed a DNA carrier to specifically identify target protein, from a mixture of various proteins, which is an example of the detection of analytes through nanopores using DNA<sup>299</sup> (Fig. 30C-E). Another interesting and unique application of nanopores is DNA-based data storage<sup>300</sup>. Furthermore, the development of DNA origami has also introduced an interest in mechanizing DNA nanostructures. The function of these 'dynamic' nanostructures rely upon the changing of their conformations<sup>301,302</sup>. Dynamic DNA nanostructures can be applied as sensors, biological assays, cargo sorters and delivery devices, nanoscale robotic arms, and many more. Kopperger *et al.* developed a self-assembled nanoscale robotic arm controlled by electric fields using a DNA origami-based structure<sup>303</sup>.

DNA-protein nanohybrids is another emerging area of DNA-based nanotechnology. Synthesis of DNA nanostructure-protein hybrids involve the chemical conjugation, or enzymatic ligation of a native protein or a close genetically modified variant of the protein to the DNA strands<sup>304</sup>. In synthesizing DNA-protein hybrids, two parameters are closely monitored: strength and selectivity. DNA-protein interactions can be covalent, such that they are strong and irreversible, or non-covalent, such that they are weaker and can easily dissociate from the complex<sup>305</sup>. *Fu et al.* chemically crosslinked discrete glucose oxidase and horseradish peroxidase enzyme pairs on a quasi-planer DNA origami surface with controlled inter-enzyme spacing and positioning<sup>306</sup>. DNA-based nanodevices have also been used as drug delivery vehicles or diagnostic probes in living systems. However, such nanodevices face significant molecular barriers *in vivo*, including: (1) efficient delivery to the target site, (2) the stability of foreign DNA nanodevices, and (3) the potential toxicity they can introduce in the host organism<sup>307</sup>. *Batia et al.* demonstrated the first *in vivo* study of cargo-loaded designer DNA architecture that could overcome these barriers<sup>308</sup>. Future studies can procure DNA from patients to make these nanodevices personalized. However, large-scale synthesis of DNA-based products is the major limitation in all the emerging DNA nanotechnology-based applications. The next section addresses this limitation.

#### 6.4 Large-scale synthesis of DNA Polymers

Large-scale synthesis of DNA-based structures is still a substantial hindrance in the field of DNA-based nanotechnology. Only small-scale applications are economically feasible. Research efforts have been directed towards addressing this limitation. Yao *et al.* have recently shown that meta-DNA structures consisting of six-helix bundles of DNA could be used to scale up DNA origami constructs<sup>309</sup>. Moreover, biotechnological strategies can be implemented to substantially increase the yield. Departing from the traditional approach of the chemical, solid phase synthesis, single stranded DNA molecules are being biosynthesized in bacterial cells<sup>310,311</sup>. Recently, liquid *Escherichia coli* cultures were used to mass produce short single-stranded DNA sequences, which can self-assemble into the desired origami shape<sup>312</sup>. Here, target DNA sequences were cloned into phagemid vectors. Subsequently, the staple phagemid was transformed into the bacterial cells. The transformation was followed by intracellular rolling circle amplification and the release

of extracellular phagemid particles containing the sequence of interest. These sequences were then isolated to mass produce short single stranded DNA molecules. Self-cleaving DNazymes were incorporated in the target sequence to eliminate the use of endonucleases to cleave the DNA of interest and make the process cost-effective. However, further studies need to be conducted to increase the complexity of the self-assembled structures. Additionally, the degree of error of the biosynthesized structures must also be evaluated.

#### 7. Conclusions and Outlook

We intend to encourage DNA as a nongenetic, polymeric material that can be implemented beyond its genetic applications. In this article, we have provided a comprehensive discussion on different chemical strategies to manipulate DNA. Applying simple, non-covalent and covalent chemical strategies, make it possible to design a vast array of highly predictable, functionalized DNA-based, polymeric materials. These strategies are widely used to form stable, self-healing, and shear-thinning crosslinked networks. Additionally, the highly predictable, self-assembling nature of DNA is exploited to create complex shapes using bottom-up, nanotechnological approaches. The widespread application of the DNA polymer has catapulted it as a well-recognized substance in the world of material science and engineering<sup>5</sup>.

The biocompatibility, biodegradability, and favorable tunability of DNA have rendered it fit for biomedical applications. DNA-based polymers are being used to deliver drugs<sup>20</sup>, encapsulate cells<sup>313</sup>, and form scaffolds for tissue engineering<sup>314</sup>. DNazymes are being implemented to detect biomolecules<sup>315</sup>, aptamers are finding use in targeted therapy<sup>316</sup> and biosensing<sup>317</sup>, Cytosine-phosphate-guanine-based DNA motifs are being used as adjuvants to vaccines<sup>318</sup>. DNA is also being used to design metamaterials, which are engineered substances having unique mechanical properties<sup>319,320</sup>. Additionally, DNA research has the potential to contribute to personalized medicine substantially. Extracted from patients, DNA can be used to prepare scaffolds for drug delivery or tissue engineering. These scaffolds will have less probability of immune rejection in the patient. Moreover, with latest advancement in human genome sequencing, we are getting closer to designing personalized medication<sup>321</sup>. Advanced sequencing will allow for tailoring patient-specific DNA for therapeutic purposes. Clinical trials must also be conducted to increase the translational potential of the DNA polymer. Before clinical trials, the cytotoxicity of functionalized DNA must be carefully assessed. Such current and probable applications show the relevance of DNA polymer in the biomedical field.

Finally DNA biomaterials have proved to be an extremely useful scaffold fabrication tool in nanotechnology. Here, bottom-up, self-assembling design strategies have simplified as well as reduced the cost of fabricating nanostructures<sup>10</sup>. Three principle designs, including tile-based, origami-based, and brick-based fabrication methods, are implemented for manufacturing complex shapes and geometries of varying dimensions and sizes. These technological advances have found a breakthrough in electronics<sup>322</sup>, photonics<sup>295</sup>, plasmonics<sup>323</sup>, drug delivery<sup>324,325</sup>, vaccine delivery<sup>138</sup>, among others<sup>326</sup>. For these nanofabricated structures, there are concerns of stability and scalability. Innovative approaches must be undertaken to overcome limitations and improve DNA-based nanotechnology. These innovative approaches will demand interdisciplinary efforts from chemists, biologists, material scientists, pharmaceutical scientists, physicists, computer scientists, and engineers. With the current rate of progress and more research efforts initiated, we predict that DNA polymer's applicability is bound to surge.

## 8. Conflicts of Interest.

Authors declare no conflicts of interest.

## 9. Acknowledgements.

A.P. would like to gratefully acknowledge the funding and supports from Canada Research Chairs Program of the Natural Sciences and Engineering Research Council (NSERC) of Canada, NSERC Discovery Grant, NSERC Discovery Accelerator Supplements (DAS), New Frontiers in Research Fund (NFRF) - Exploration Stream, and Wolfe-Western Fellowship At-Large for Outstanding Newly Recruited Research Scholar. C.C. likes to acknowledge the Summer 2020 NSERC Undergraduate Student Research Award. The authors declare that there is no conflict of interest regarding the publication of this article. The authors would like to acknowledge BioRender and freepik companies. Some of the images and illustrations were created with BioRender.com and freepik.com.

## 10. References.

- 1 R. D. Wells, T. M. Jacob, S. A. Narang and H. G. Khorana, *J. Mol. Biol.*, 1967, **27**, 237–263.
- 2 J. Gačanin, C. V Synatschke and T. Weil, *Adv. Funct. Mater.*, 2020, **30**, 1906253.
- 3 J. S. Kahn, Y. Hu and I. Willner, *Acc. Chem. Res.*, 2017, **50**, 680–690.
- 4 N. C. Seeman, *Nature*, 2003, **421**, 427–431.
- 5 Y. Hu and C. M. Niemeyer, *Adv. Mater.*, , DOI:10.1002/adma.201806294.
- 6 M. H. Caruthers, *Science (80-. )*, 1985, **230**, 281–285.
- 7 E. Sonveaux, *Bioorg. Chem.*, 1986, **14**, 274–325.
- 8 R. Bischoff, J. M. Coull and F. E. Regnier, *Anal. Biochem.*, 1987, **164**, 336–344.
- 9 M. Bathe and P. W. K. Rothmund, *MRS Bull.*, 2017, **42**, 882–888.
- 10 N. C. Seeman and H. F. Sleiman, *Nat. Rev. Mater.*, 2017.
- 11 S. Nummelin, J. Kommeri, M. A. Kostianen and V. Linko, *Adv. Mater.*, , DOI:10.1002/adma.201703721.
- 12 F. Hong, F. Zhang, Y. Liu and H. Yan, *Chem. Rev.*, 2017, **117**, 12584–12640.
- 13 S. Basu, S. Pacelli and A. Paul, *Acta Biomater.*, 2020, **105**, 159–169.
- 14 S. Basu, S. Pacelli, Y. Feng, Q. Lu, J. Wang and A. Paul, *ACS Nano*, 2018, **12**, 9866–9880.
- 15 S. Basu, A. R. Alkhwani, S. Pacelli and A. Paul, *ACS Appl. Mater. Interfaces*, 2019, **11**, 34621–34633.
- 16 C. K. Lee, S. R. Shin, J. Y. Mun, S. S. Han, I. So, J.-H. Jeon, T. M. Kang, S. I. Kim, P. G. Whitten, G. G. Wallace, G. M. Spinks and S. J. Kim, *Angew. Chemie - Int. Ed.*, 2009, **48**, 5116–5120.
- 17 C. K. Lee, S. R. Shin, S. H. Lee, J. H. Jeon, I. So, T. M. Kang, S. I. Kim, J. Y. Mun, S. S. Han, G. M. Spinks, G. G. Wallace and S. J. Kim, *Angew. Chemie - Int. Ed.*, 2008, **47**, 2470–2474.
- 18 H. Qi, M. Ghodousi, Y. Du, C. Grun, H. Bae, P. Yin and A. Khademhosseini, *Nat. Commun.*, 2013, **4**, 1–10.
- 19 A. Arcella, G. Portella, R. Collepardo-Guevara, D. Chakraborty, D. J. Wales and M. Orozco, *J. Phys. Chem. B*, 2014, **118**, 8540–8548.
- 20 S. Singh, A. Mishra, R. Kumari, K. K. Sinha, M. K. Singh and P. Das, *Carbon N. Y.*, 2017, **114**, 169–176.
- 21 Z. Zhang, J. Han, Y. Pei, R. Fan and J. Du, *ACS Appl. Bio Mater.*, 2018, **1**, 1206–1214.
- 22 C. Li, C. Guo, V. Fitzpatrick, A. Ibrahim, M. J. Zwieterstra, P. Hanna, A. Lechtig, A. Nazarian, S. J. Lin and D. L. Kaplan, *Nat. Rev. Mater.*, 2020, **5**, 61–81.
- 23 Y. Eguchi, T. Kato, T. Tanaka and T. Maruyama, *Chem. Commun.*, 2017, **53**, 5802–5805.
- 24 W. Guo, R. Orbach, I. Mironi-Harpaz, D. Seliktar and I. Willner, *Small*, 2013, **9**, 3748–3752.
- 25 Y. Xu, Q. Wu, Y. Sun, H. Bai and G. Shi, *ACS Nano*, 2010, **4**, 7358–7362.
- 26 X. Ji, J. Wang, S. Niu and C. Ding, *Chem. Commun.*, 2019, **55**, 5243–5246.
- 27 T. Liedl, H. Dietz, B. Yurke and F. Simmel, *Small*, 2007, **3**, 1688–1693.
- 28 Y. Hu, D. Rehnlund, E. Klein, J. Gescher and C. M. Niemeyer, *ACS Appl. Mater. Interfaces*, 2020, **12**, 14806–14813.
- 29 J. Song, K. Im, S. Hwang, J. Hur, J. Nam, G. O. Ahn, S. Hwang, S. Kim and N. Park, *Nanoscale*, 2015, **7**, 9433–9437.
- 30 X. Xiong, C. Wu, C. Zhou, G. Zhu, Z. Chen and W. Tan, *Macromol. Rapid Commun.*, 2013, **34**, 1271–1283.
- 31 Z. G. Wang and B. Ding, *Adv. Mater.*, 2013, **25**, 3905–3914.
- 32 Y. Hoon Roh, R. C. H. Ruiz, S. Peng, J. B. Lee and D. Luo, *Chem. Soc. Rev.*, 2011, **40**, 5730–5744.
- 33 J. Li, L. Mo, C. H. Lu, T. Fu, H. H. Yang and W. Tan, *Chem. Soc. Rev.*, 2016, **45**, 1410–1431.
- 34 M. Nishikawa, S. Rattanakit and Y. Takakura, *Adv. Drug Deliv. Rev.*, 2010, **62**, 626–632.
- 35 M. J. Campolongo, S. J. Tan, J. Xu and D. Luo, *Adv. Drug Deliv. Rev.*, 2010, **62**, 606–616.
- 36 Z. G. Wang, C. Song and B. Ding, *Small*, 2013, **9**, 2210–2222.
- 37 M.-A. Shahbazi, T. Bauleth-Ramos and H. A. Santos, *Adv. Ther.*, 2018, **1**, 1800042.
- 38 Y. Zhang, J. Tu, D. Wang, H. Zhu, S. K. Maity, X. Qu, B. Bogaert, H. Pei and H. Zhang, *Adv. Mater.*, , DOI:10.1002/adma.201703658.
- 39 S. Liu, Q. Jiang, Y. Wang and B. Ding, *Adv. Healthc. Mater.*, 2019, **8**, 1801658.
- 40 N. Dai and E. T. Kool, *Chem. Soc. Rev.*, 2011, **40**, 5756–5770.
- 41 X. Lin, X. Sun, S. Luo, B. Liu and C. Yang, *TrAC - Trends Anal. Chem.*, 2016, **80**, 132–148.
- 42 J. B. Lee, M. J. Campolongo, J. S. Kahn, Y. H. Roh, M. R. Hartman and D. Luo, *Nanoscale*, 2010, **2**, 188–197.
- 43 T. M. H. Lee and I. M. Hsing, *Anal. Chim. Acta*, 2006, **556**, 26–37.
- 44 G. Liang, Y. Man, A. Li, X. Jin, X. Liu and L. Pan, *Microchem. J.*, 2017, **131**, 145–153.
- 45 J. Chao, D. Zhu, Y. Zhang, L. Wang and C. Fan, *Biosens. Bioelectron.*, 2016, **76**, 68–79.

- 46 D. Sadighbayan, K. Sadighbayan, A. Y. Khosroushahi and M. Hasanzadeh, *TrAC - Trends Anal. Chem.*, 2019, **119**, 115609.
- 47 J. Bath and A. J. Turberfield, *Nat. Nanotechnol.*, 2007, **2**, 275–284.
- 48 C. Song, Z. G. Wang and B. Ding, *Small*, 2013, **9**, 2382–2392.
- 49 J. Pan, F. Li, T. G. Cha, H. Chen and J. H. Choi, *Curr. Opin. Biotechnol.*, 2015, **34**, 56–64.
- 50 E. Braun and K. Keren, *Adv. Phys.*, 2004, **53**, 441–496.
- 51 K. Wang, *J. Funct. Biomater.*, 2018, **9**, 8.
- 52 Y. Ye, L. Chen, X. Liu and U. J. Krull, *Anal. Chim. Acta*, 2006, **568**, 138–145.
- 53 J. W. Bruce Alberts, Dennis Bray, Julian Lewis, Martin Raff, Keith Roberts, *Molecular Biology of the Cell*, Garland Science, New York, 2002.
- 54 J. D. Watson and F. H. C. Crick, *Nature*, 1953, **171**, 737–738.
- 55 N. C. Seeman, J. M. Rosenberg and A. Rich, *Proc. Natl. Acad. Sci. U. S. A.*, 1976, **73**, 804–808.
- 56 J. A. Subirana and M. Soler-López, *Annu. Rev. Biophys. Biomol. Struct.*, 2003, **32**, 27–45.
- 57 S. Mikkola, T. Lönnberg and H. Lönnberg, *Beilstein J. Org. Chem.*, 2018, **14**, 803–837.
- 58 R. J. Bauer, T. J. Jurkiw, T. C. Evans and G. J. S. Lohman, *Biochemistry*, 2017, **56**, 1117–1129.
- 59 R. Molina, S. Stella, P. Redondo, H. Gomez, M. J. Marcaida, M. Orozco, J. Prieto and G. Montoya, *Nat. Struct. Mol. Biol.*, 2015, **22**, 65–72.
- 60 K. M. Burkin, O. L. Bodulev, A. V. Gribas and I. Y. Sakharov, *Enzyme Microb. Technol.*, 2019, **131**, 109419.
- 61 D. Rhodes and H. J. Lipps, *Nucleic Acids Res.*, 2015, **43**, 8627–8637.
- 62 L. Garibyan and N. Avashia, *J. Invest. Dermatol.*, 2013, **133**, 1–4.
- 63 A. J. Berdis, *Chem. Rev.*, 2009, **109**, 2862–2879.
- 64 M. M. Ali, F. Li, Z. Zhang, K. Zhang, D. K. Kang, J. A. Ankrum, X. C. Le and W. Zhao, *Chem. Soc. Rev.*, 2014, **43**, 3324–3341.
- 65 W. Zhao, C. H. Cui, S. Bose, D. Guo, C. Shen, W. P. Wong, K. Halvorsen, O. C. Farokhzad, G. S. L. Teo, J. A. Phillips, D. M. Dorfman, R. Karnik and J. M. Karp, *Proc. Natl. Acad. Sci. U. S. A.*, 2012, **109**, 19626–19631.
- 66 T. Gao, T. Chen, C. Feng, X. He, C. Mu, J. ichi Anzai and G. Li, *Nat. Commun.*, 2019, **10**, 1–10.
- 67 A. Kellett, Z. Molphy, C. Slator, V. McKee and N. P. Farrell, *Chem. Soc. Rev.*, 2019, **48**, 971–988.
- 68 J. M. Benevides and G. J. Thomas, *Biochemistry*, 2005, **44**, 2993–2999.
- 69 A. R. Bahrami, M. J. Dickman, M. M. Matin, J. R. Ashby, P. E. Brown, M. J. Conroy, G. J. S. Fowler, J. P. Rose, Q. I. Sheikh, A. T. Yeung and D. P. Hornby, *Anal. Biochem.*, 2002, **309**, 248–252.
- 70 K. Liu, L. Zheng, C. Ma, R. Göstl and A. Herrmann, *Chem. Soc. Rev.*, 2017, **46**, 5147–5172.
- 71 O. Boussif, F. LezoualC'H, M. A. Zanta, M. D. Mergny, D. Scherman, B. Demeneix and J. P. Behr, *Proc. Natl. Acad. Sci. U. S. A.*, 1995, **92**, 7297–7301.
- 72 D. D. Dunlap, A. Maggi, M. R. Soria and L. Monaco, *Nucleic Acids Res.*, 1997, **25**, 3095–3101.
- 73 A. Baker, M. Saltik, H. Lehrmann, I. Killisch, V. Mautner, G. Lamm, G. Christofori and M. Gotten, *Gene Ther.*, 1997, **4**, 773–782.
- 74 A. M. Krieg, *Nat. Rev. Drug Discov.*, 2006, **5**, 471–484.
- 75 H. Shirota and D. M. Klinman, *Expert Rev. Vaccines*, 2014, **13**, 299–312.
- 76 Y. Yoshizaki, E. Yuba, N. Sakaguchi, K. Koiwai, A. Harada and K. Kono, *Biomaterials*, 2017, **141**, 272–283.
- 77 Y. Xiang and Y. Lu, *Inorg. Chem.*, 2014, **53**, 1925–1942.
- 78 S. Javani, R. Lorca, A. Latorre, C. Flors, A. L. Cortajarena and Á. Somoza, *ACS Appl. Mater. Interfaces*, 2016, **8**, 10147–10154.
- 79 M. Madsen and K. V. Gothelf, *Chem. Rev.*, 2019, 119.
- 80 A. V. Azhayev and M. L. Antopolsky, *Tetrahedron*, 2001, **57**, 4977–4986.
- 81 M. H. Caruthers, A. D. Barone, S. L. Beaucage, D. R. Dodds, E. F. Fisher, L. J. McBride, M. Matteucci, Z. Stabinsky and J. Y. Tang, *Methods Enzymol.*, 1987, **154**, 287–313.
- 82 J. Telsner, K. A. Cruickshank, L. E. Morrison and T. L. Netzel, *J. Am. Chem. Soc.*, 1989, **111**, 6966–6976.
- 83 Y. Zhang, H. Zhao, Z. Wu, Y. Xue, X. Zhang, Y. He, X. Li and Z. Yuan, *Biosens. Bioelectron.*, 2013, **48**, 180–187.
- 84 D. E. Draper, *Nucleic Acids Res.*, 1984, **12**, 989–1002.
- 85 I. C. Gillam and G. M. Tener, *Anal. Biochem.*, 1986, **157**, 199–207.
- 86 G. B. Dreyer and P. B. Dervan, *Proc. Natl. Acad. Sci. U. S. A.*, 1985, **82**, 968–972.
- 87 B. A. Connolly and P. Rider, *Nucleic Acids Res.*, 1985, **13**, 4485–4502.
- 88 R. Zuckermann, D. Corey and P. Schultz, *Nucleic Acids Res.*, 1987, **15**, 5305–5321.
- 89 M. J. Robins and P. J. Barr, *J. Org. Chem.*, 1983, **48**, 1854–1862.
- 90 E. Trévisiol, A. Renard, E. Defrancq and J. Lhomme, *Tetrahedron Lett.*, 1997, **38**, 8687–8690.
- 91 A. V. Kachalova, D. A. Stetsenko, E. A. Romanova, V. N. Tashlitsky, M. J. Gait and T. S. Oretskaya, *Helv. Chim. Acta*, 2002, **85**, 2409–2416.
- 92 J. N. Kremsky, J. L. Wooters, J. P. Dougherty, R. E. Meyers, M. Collins and E. L. Brown, *Nucleic Acids Res.*, 1987, **15**, 2891–2909.
- 93 G. W. Cline and S. B. Hanna, *J. Am. Chem. Soc.*, 1987, **109**, 3087–3091.
- 94 D. J. Hnatowich, P. Winnard, F. Virzi, M. Fogarasi, T. Sano, C. L. Smith, C. R. Cantor and M. Rusckowski, *J. Nucl. Med.*, 1995, **36**, 2306–2314.
- 95 W. H. Heath, F. Palmieri, J. R. Adams, B. K. Long, J. Chute, T.

- W. Holcombe, S. Zieren, M. J. Truitt, J. L. White and C. G. Willson, *Macromolecules*, 2008, **41**, 719–726.
- 96 A. Sánchez, E. Pedroso and A. Grandas, *Org. Lett.*, 2011, **13**, 4364–4367.
- 97 R. Lartia, P. Murat, P. Dumy and E. Defrancq, *Org. Lett.*, 2011, **13**, 5672–5675.
- 98 M. F. Jacobsen, J. B. Ravnsbaek and K. V. Gothelf, *Org. Biomol. Chem.*, 2010, **8**, 50–52.
- 99 A. Dallmann, A. H. El-Sagheer, L. Dehmel, C. Mügge, C. Griesinger, N. P. Ernsting and T. Brown, *Chem. - A Eur. J.*, 2011, **17**, 14714–14717.
- 100 G. Zhu, G. Niu and X. Chen, *Bioconjug. Chem.*, 2015, **26**, 2186–2197.
- 101 A. H. El-Sagheer and T. Brown, *Chem. Soc. Rev.*, 2010, **39**, 1388–1405.
- 102 H. C. Kolb, M. G. Finn and K. B. Sharpless, *Angew. Chemie - Int. Ed.*, 2001, **40**, 2004–2021.
- 103 T. S. Seo, Z. Li, H. Ruparel and J. Ju, *J. Org. Chem.*, 2003, **68**, 609–612.
- 104 M. Kollaschinski, J. Sobotta, A. Schalk, T. Frischmuth, B. Graf and S. Serdjukow, *Bioconjug. Chem.*, 2020, **31**, 507–512.
- 105 N. C. Seeman, *Mater. Today*, 2003, **6**, 24–29.
- 106 S. Modi, C. Nizak, S. Surana, S. Halder and Y. Krishnan, *Nat. Nanotechnol.*, 2013, **8**, 459–467.
- 107 Y. Yan, Y. Sun, H. Yu, H. Xu and J. R. Lu, *Soft Matter*, 2015, **11**, 1748–1754.
- 108 Y. A. Jodat, P. Lotfi, P. P. S. S. Abadi, J. Y. Mun, J. Seo, E. A. Shin, S. M. Jung, C. K. Lee and S. R. Shin, *ACS Appl. Nano Mater.*, 2018, **1**, 6630–6640.
- 109 J. L. Seifter and H.-Y. Chang, *Kidney Dis.*, 2016, **2**, 170–186.
- 110 S. Modi, M. G. Swetha, D. Goswami, G. D. Gupta, S. Mayor and Y. Krishnan, *Nat. Nanotechnol.*, 2009, **4**, 325–330.
- 111 S. Saha, K. Chakraborty and Y. Krishnan, *Chem. Commun.*, 2012, **48**, 2513–2515.
- 112 X. Yan, S. Huang, Y. Wang, Y. Tang and Y. Tian, *Nanomaterials*, 2020, **10**, 2047.
- 113 J. Chen and N. C. Seeman, *Nature*, 1991, **350**, 631–633.
- 114 J. Zheng, J. J. Birktoft, Y. Chen, T. Wang, R. Sha, P. E. Constantinou, S. L. Ginell, C. Mao and N. C. Seeman, *Nature*, 2009, **461**, 74–77.
- 115 C. G. Evans and E. Winfree, *Chem. Soc. Rev.*, 2017, **46**, 3808–3829.
- 116 J. E. Padilla, W. Liu and N. C. Seeman, in *Natural Computing*, Springer, 2012, vol. 11, pp. 323–338.
- 117 A. Mohammed, E. Czeizler and E. Czeizler, *Theor. Comput. Sci.*, 2017, **701**, 203–215.
- 118 E. Winfree, F. Liu, L. A. Wenzler and N. C. Seeman, *Nature*, 1998, **394**, 539–544.
- 119 Y. Wang, W. Ge, B. Lu, J. J. Zhu and S. J. Xiao, *Nanoscale*, 2020, **12**, 19597–19603.
- 120 B. Wei, M. Dai and P. Yin, *Nature*, 2012, **485**, 623–626.
- 121 X. Wang, A. R. Chandrasekaran, Z. Shen, Y. P. Ohayon, T. Wang, M. E. Kizer, R. Sha, C. Mao, H. Yan, X. Zhang, S. Liao, B. Ding, B. Chakraborty, N. Jonoska, D. Niu, H. Gu, J. Chao, X. Gao, Y. Li, T. Ciengshin and N. C. Seeman, *Chem. Rev.*, 2019, **119**, 6273–6289.
- 122 F. Hong, S. Jiang, X. Lan, R. P. Narayanan, P. Šulc, F. Zhang, Y. Liu and H. Yan, *J. Am. Chem. Soc.*, 2018, **140**, 14670–14676.
- 123 A. Heuer-Jungemann and T. Liedl, *Trends Chem.*, 2019, **1**, 799–814.
- 124 H. Zhang, Y. Wang, H. Zhang, X. Liu, A. Lee, Q. Huang, F. Wang, J. Chao, H. Liu, J. Li, J. Shi, X. Zuo, L. Wang, L. Wang, X. Cao, C. Bustamante, Z. Tian and C. Fan, *Nat. Commun.*, 2019, **10**, 1–11.
- 125 L. N. Green, A. Amodio, H. K. K. Subramanian, F. Ricci and E. Franco, *Nano Lett.*, 2017, **17**, 7283–7288.
- 126 D. Woods, D. Doty, C. Myhrvold, J. Hui, F. Zhou, P. Yin and E. Winfree, *Nature*, 2019, **567**, 366–372.
- 127 A. Tandon, Y. Song, S. B. Mitta, S. Yoo, S. Park, S. Lee, M. T. Raza, T. H. Ha and S. H. Park, *ACS Nano*, 2020, **14**, 5260–5267.
- 128 C. Xing, J. Dai, Y. Huang, Y. Lin, K. Zhang, C. Lu and H. Yang, *Small*, 2019, **15**, 1901795.
- 129 Q. Hu, H. Li, L. Wang, H. Gu and C. Fan, *Chem. Rev.*, 2019, **119**, 6459–6506.
- 130 X. Liu, Y. Zhao, P. Liu, L. Wang, J. Lin and C. Fan, *Angew. Chemie Int. Ed.*, 2019, **58**, 8996–9011.
- 131 Y. Ke, L. L. Ong, W. M. Shih and P. Yin, *Science (80-. )*, 2012, **338**, 1177–1183.
- 132 Y. Ke, L. L. Ong, W. Sun, J. Song, M. Dong, W. M. Shih and P. Yin, *Nat. Chem.*, 2014, **6**, 994–1002.
- 133 A. Reinhardt and D. Frenkel, *Soft Matter*, 2016, **12**, 6253–6260.
- 134 A. Reinhardt and D. Frenkel, *Phys. Rev. Lett.*, 2014, **112**, 238103.
- 135 Y. Zhang, A. Reinhardt, P. Wang, J. Song and Y. Ke, *Angew. Chemie*, 2020, **132**, 8672–8678.
- 136 Y. Kim and P. Yin, *Angew. Chemie Int. Ed.*, 2020, **59**, 700–703.
- 137 L. L. Ong, N. Hanikel, O. K. Yaghi, C. Grun, M. T. Strauss, P. Bron, J. Lai-Kee-Him, F. Schueder, B. Wang, P. Wang, J. Y. Kishi, C. Myhrvold, A. Zhu, R. Jungmann, G. Bellot, Y. Ke and P. Yin, *Nature*, 2017, **552**, 72–77.
- 138 R. Veneziano, T. J. Moyer, M. B. Stone, E. C. Wamhoff, B. J. Read, S. Mukherjee, T. R. Shepherd, J. Das, W. R. Schief, D. J. Irvine and M. Bathe, *Nat. Nanotechnol.*, 2020, 1–8.
- 139 R. M. Zadegan and M. L. Norton, *Int. J. Mol. Sci.*, 2012, **13**, 7149–7162.
- 140 P. W. K. Rothmund, *Nature*, 2006, **440**, 297–302.
- 141 C. E. Castro, F. Kilchherr, D. N. Kim, E. L. Shiao, T. Wauer, P. Wortmann, M. Bathe and H. Dietz, *Nat. Methods*, 2011, **8**, 221–229.
- 142 N. C. Seeman, *J. Theor. Biol.*, 1982, **99**, 237–247.
- 143 J. F. Berengut, J. C. Berengut, J. P. K. Doye, D. Prešern, A. Kawamoto, J. Ruan, M. J. Wainwright and L. K. Lee, *Nucleic*

- Acids Res.*, 2019, **47**, 11963–11975.
- 144 T. Zhang, C. Hartl, K. Frank, A. Heuer-Jungemann, S. Fischer, P. C. Nickels, B. Nickel and T. Liedl, *Adv. Mater.*, 2018, **30**, 1800273.
- 145 S. Julin, A. Korpi, Nonappa, B. Shen, V. Liljeström, O. Ikkala, A. Keller, V. Linko and M. A. Kostiaainen, *Nanoscale*, 2019, **11**, 4546–4551.
- 146 H. Jun, X. Wang, W. P. Bricker and M. Bathe, *Nat. Commun.*, 2019, **10**, 1–9.
- 147 P. Piskunen, S. Nummelin, B. Shen, M. A. Kostiaainen and V. Linko, *Molecules*, 2020, **25**, 1823.
- 148 V. Linko and M. A. Kostiaainen, *Nat. Biotechnol.*, 2016, **34**, 826–827.
- 149 E. Benson, A. Mohammed, J. Gardell, S. Masich, E. Czeizler, P. Orponen and B. Högberg, *Nature*, 2015, **523**, 441–444.
- 150 G. Tikhomirov, P. Petersen and L. Qian, *Nature*, 2017, **552**, 67–71.
- 151 S. Jia, J. Wang, M. Xie, J. Sun, H. Liu, Y. Zhang, J. Chao, J. Li, L. Wang, J. Lin, K. V. Gothelf and C. Fan, *Nat. Commun.*, 2019, **10**, 1–9.
- 152 Y. Tian, J. R. Lhermitte, L. Bai, T. Vo, H. L. Xin, H. Li, R. Li, M. Fukuto, K. G. Yager, J. S. Kahn, Y. Xiong, B. Minevich, S. K. Kumar and O. Gang, *Nat. Mater.*, 2020, **19**, 789–796.
- 153 B. Uprety, T. Westover, M. Stoddard, K. Brinkerhoff, J. Jensen, R. C. Davis, A. T. Woolley and J. N. Harb, *Langmuir*, 2017, **33**, 726–735.
- 154 D. Balakrishnan, G. D. Wilkens and J. G. Heddle, *Nanomedicine*, 2019, **14**, 911–925.
- 155 L. Zhou, X. Jiao, S. Liu, M. Hao, S. Cheng, P. Zhang and Y. Wen, *J. Mater. Chem. B*, 2020, **8**, 1991–2009.
- 156 Y. Dong, C. Yao, Y. Zhu, L. Yang, D. Luo and D. Yang, *Chem. Rev.*, 2020, acs.chemrev.0c00294.
- 157 F. Li, J. Tang, J. Geng, D. Luo and D. Yang, *Prog. Polym. Sci.*, 2019, **98**, 101163.
- 158 F. Li, D. Lyu, S. Liu and W. Guo, *Adv. Mater.*, 2020, **32**, 1806538.
- 159 J. Bush, C.-H. Hu and R. Veneziano, *Appl. Sci.*, 2021, **11**, 1885.
- 160 N. A. Peppas, P. Bures, W. Leobandung and H. Ichikawa, *Eur. J. Pharm. Biopharm.*, 2000, **50**, 27–46.
- 161 Y. S. Zhang and A. Khademhosseini, *Science (80-. )*, 2017, 356.
- 162 S. Van Vlierberghe, P. Dubruel and E. Schacht, *Biomacromolecules*, 2011, **12**, 1387–1408.
- 163 A. K. Gaharwar, I. Singh and A. Khademhosseini, *Nat. Rev. Mater.*, 2020, 1–20.
- 164 A. C. Daly, L. Riley, T. Segura and J. A. Burdick, *Nat. Rev. Mater.*, 2020, **5**, 20–43.
- 165 J. Li and D. J. Mooney, *Nat. Rev. Mater.*, , DOI:10.1038/natrevmats.2016.71.
- 166 T. R. Hoare and D. S. Kohane, *Polymer (Guildf.)*, 2008, **49**, 1993–2007.
- 167 A. K. Gaharwar, N. A. Peppas and A. Khademhosseini, *Biotechnol. Bioeng.*, 2014, **111**, 441–453.
- 168 J. Whitlow, S. Pacelli and A. Paul, *Macromol. Chem. Phys.*, 2016, **217**, 1245–1259.
- 169 A. Paul, A. Hasan, H. Al Kindi, A. K. Gaharwar, V. T. S. Rao, M. Nikkhah, S. R. Shin, D. Krafft, M. R. Dokmeci, D. Shum-Tim and A. Khademhosseini, *ACS Nano*, 2014, **8**, 8050–8062.
- 170 J. Li, E. Weber, S. Guth-Gundel, M. Schuleit, A. Kuttler, C. Halleux, N. Accart, A. Doelemeyer, A. Basler, B. Tigani, K. Wuersch, M. Fornaro, M. Kneissel, A. Stafford, B. R. Freedman and D. J. Mooney, *Adv. Healthc. Mater.*, , DOI:10.1002/adhm.201701393.
- 171 A. K. Gaharwar, L. M. Cross, C. W. Peak, K. Gold, J. K. Carrow, A. Brokesh and K. A. Singh, *Adv. Mater.*, 2019, **31**, 1900332.
- 172 D. Chimene, D. L. Alge and A. K. Gaharwar, *Adv. Mater.*, 2015, **27**, 7261–7284.
- 173 S. R. Shin, S. M. Jung, M. Zalabany, K. Kim, P. Zorlutuna, S. B. Kim, M. Nikkhah, M. Khabiry, M. Azize, J. Kong, K. T. Wan, T. Palacios, M. R. Dokmeci, H. Bae, X. Tang and A. Khademhosseini, *ACS Nano*, 2013, **7**, 2369–2380.
- 174 W. Zhou, F. Wang, J. Ding and J. Liu, *ACS Appl. Mater. Interfaces*, 2014, **6**, 14795–14800.
- 175 S. Wang, C. M. McGuirk, M. B. Ross, S. Wang, P. Chen, H. Xing, Y. Liu and C. A. Mirkin, *J. Am. Chem. Soc.*, 2017, **139**, 9827–9830.
- 176 S. Wang, Y. Chen, S. Wang, P. Li, C. A. Mirkin and O. K. Farha, *J. Am. Chem. Soc.*, 2019, **141**, 2215–2219.
- 177 P. Horcajada, T. Chalati, C. Serre, B. Gillet, C. Sebrie, T. Baati, J. F. Eubank, D. Heurtaux, P. Clayette, C. Kreuz, J. S. Chang, Y. K. Hwang, V. Marsaud, P. N. Bories, L. Cynober, S. Gil, G. Férey, P. Couvreur and R. Gref, *Nat. Mater.*, 2010, **9**, 172–178.
- 178 A. Dolatshahi-Pirouz, M. Nikkhah, A. K. Gaharwar, B. Hashmi, E. Guermani, H. Aliabadi, G. Camci-Unal, T. Ferrante, M. Foss, D. E. Ingber and A. Khademhosseini, *Sci. Rep.*, 2015, **4**, 1–9.
- 179 D. López Barreiro, Z. Martín-Moldes, J. Yeo, S. Shen, M. J. Hawker, F. J. Martin-Martinez, D. L. Kaplan and M. J. Buehler, *Adv. Mater.*, 2019, **31**, 1904720.
- 180 S. R. Shin, C. K. Lee, I. So, J. H. Jeon, T. M. Kang, C. Kee, S. I. Kim, G. M. Spinks, G. G. Wallace and S. J. Kim, *Adv. Mater.*, 2008, **20**, 466–470.
- 181 S. R. Shin, K. S. Jin, C. K. Lee, S. I. Kim, G. M. Spinks, I. So, J. H. Jeon, T. M. Kang, J. Y. Mun, S. S. Han, M. Ree and S. J. Kim, *Adv. Mater.*, 2009, **21**, 1907–1910.
- 182 Y. Hu and C. M. Niemeyer, *J. Mater. Chem. B*, 2020, **8**, 2250–2255.
- 183 S. H. Lee, C. K. Lee, S. R. Shin, B. K. Gu, S. I. Kim, T. M. K. Kang and S. J. Kim, *Sensors Actuators, B Chem.*, 2010, **145**, 89–92.
- 184 J. Song, S. Hwang, K. Im, J. Hur, J. Nam, S. Hwang, G. O. Ahn, S. Kim and N. Park, *J. Mater. Chem. B*, 2015, **3**, 1537–1543.
- 185 X. Zhang, M. R. Servos and J. Liu, *J. Am. Chem. Soc.*, 2012, **134**, 7266–7269.

- 186 W. Guo, X. J. Qi, R. Orbach, C. H. Lu, L. Freage, I. Mironi-Harpaz, D. Seliktar, H. H. Yang and I. Willner, *Chem. Commun.*, 2014, **50**, 4065–4068.
- 187 L. Järup, *Br. Med. Bull.*, 2003, **68**, 167–182.
- 188 J. J. Zhang, F. F. Cheng, J. J. Li, J. J. Zhu and Y. Lu, *Nano Today*, 2016, **11**, 309–329.
- 189 R. J. Lake, Z. Yang, J. J. Zhang and Y. Lu, *Acc. Chem. Res.*, 2019, **52**, 3275–3286.
- 190 N. Dave, M. Y. Chan, P. J. J. Huang, B. D. Smith and J. Liu, *J. Am. Chem. Soc.*, 2010, **132**, 12668–12673.
- 191 J. Li and Y. Lu, *J. Am. Chem. Soc.*, 2000, **122**, 10466–10467.
- 192 Y. Wang, Y. Zhu, Y. Hu, G. Zeng, Y. Zhang, C. Zhang and C. Feng, *Small*, 2018, **14**, 1703305.
- 193 H. Lin, Y. Zou, Y. Huang, J. Chen, W. Y. Zhang, Z. Zhuang, G. Jenkins and C. J. Yang, *Chem. Commun.*, 2011, **47**, 9312–9314.
- 194 J. Zheng, *J. Environ. Anal. Toxicol.*, 2012, **02**, 1–4.
- 195 Y. Huang, Y. Ma, Y. Chen, X. Wu, L. Fang, Z. Zhu and C. J. Yang, *Anal. Chem.*, 2014, **86**, 11434–11439.
- 196 A. Ono and H. Togashi, *Angew. Chemie - Int. Ed.*, 2004, **43**, 4300–4302.
- 197 Z. G. Wang, Y. Li, H. Wang, K. Wan, Q. Liu, X. Shi and B. Ding, *Chem. - A Eur. J.*, 2019, **25**, 12576–12582.
- 198 K. Van Nguyen, Y. Holade and S. D. Minteer, *ACS Catal.*, 2016, **6**, 2603–2607.
- 199 E. Kuah, S. Toh, J. Yee, Q. Ma and Z. Gao, *Chem. - A Eur. J.*, 2016, **22**, 8404–8430.
- 200 S. Wang, R. Cazelles, W. C. Liao, M. Vázquez-González, A. Zoabi, R. Abu-Reziq and I. Willner, *Nano Lett.*, 2017, **17**, 2043–2048.
- 201 G. J. Cao, X. Jiang, H. Zhang, T. R. Croley and J. J. Yin, *RSC Adv.*, 2017, **7**, 52210–52217.
- 202 F. W. Krainer and A. Glieder, *Appl. Microbiol. Biotechnol.*, 2015, **99**, 1611–1625.
- 203 J. Kosman and B. Juskowiak, *Anal. Chim. Acta*, 2011, **707**, 7–17.
- 204 H. Zhao, G. Jiang, J. Weng, Q. Ma, H. Zhang, Y. Ito and M. Liu, *J. Mater. Chem. B*, 2016, **4**, 4648–4651.
- 205 S. Uchida, Y. Satoh, N. Yamashiro and T. Satoh, *J. Nucl. Sci. Technol.*, 2004, **41**, 898–906.
- 206 N. Näther, L. M. Juárez, R. Emmerich, J. Berger, P. Friedrich and M. J. Schöning, *Sensors*, 2006, **6**, 308–317.
- 207 M. B. Grisham, *Comp. Biochem. Physiol. - A Mol. Integr. Physiol.*, 2013, **165**, 429–438.
- 208 J. Meier, E. Hofferber, J. A. Stapleton and N. M. Iverson, *Chemosensors*, 2019, **7**, 64.
- 209 Y. Huang, W. Xu, G. Liu and L. Tian, *Chem. Commun.*, 2017, **53**, 3038–3041.
- 210 A. Guiseppi-Elie, *Biomaterials*, 2010, **31**, 2701–2716.
- 211 Z. Shi, X. Gao, M. W. Ullah, S. Li, Q. Wang and G. Yang, *Biomaterials*, 2016, **111**, 40–54.
- 212 X. Mao, D. Mao, T. Chen, M. Jalalah, M. S. Al-Assiri, F. A. Harraz, X. Zhu and G. Li, *ACS Appl. Mater. Interfaces*, 2020, [acsami.0c08064](https://doi.org/10.1021/acsami.0c08064).
- 213 B. E. Logan, *Nat. Rev. Microbiol.*, 2009, **7**, 375–381.
- 214 S. R. Shin, C. K. Lee, T. W. Eom, S. H. Lee, C. H. Kwon, I. So and S. J. Kim, *Sensors Actuators, B Chem.*, 2012, **162**, 173–177.
- 215 H. Janocha, *Actuators: Basics and Applications*, Springer-Verlag Berlin Heidelberg, Berlin, Heidelberg, 2004.
- 216 K. Tapio, D. Shao, S. Auer, J. Tuppurainen, M. Ahlskog, V. P. Hytönen and J. J. Toppari, *Nanoscale*, 2018, **10**, 19297–19309.
- 217 G. Tiwari, R. Tiwari, S. Bannerjee, L. Bhati, S. Pandey, P. Pandey and B. Sriwastawa, *Int. J. Pharm. Investig.*, 2012, **2**, 2.
- 218 N. Ren, R. Sun, K. Xia, Q. Zhang, W. Li, F. Wang, X. Zhang, Z. Ge, L. Wang, C. Fan and Y. Zhu, *ACS Appl. Mater. Interfaces*, 2019, **11**, 26704–26710.
- 219 Y. Ma, H. Liu, Q. Mou, D. Yan, X. Zhu and C. Zhang, *Nanoscale*, 2018, **10**, 8367–8371.
- 220 W. C. Liao, S. Lilienthal, J. S. Kahn, M. Riutin, Y. S. Sohn, R. Nechushtai and I. Willner, *Chem. Sci.*, 2017, **8**, 3362–3373.
- 221 R. M. Dirks and N. A. Pierce, *Proc. Natl. Acad. Sci. U. S. A.*, 2004, **101**, 15275–15278.
- 222 Z. Zhang, C. Liu, C. Yang, Y. Wu, F. Yu, Y. Chen and J. Du, *ACS Appl. Mater. Interfaces*, 2018, **10**, 8546–8554.
- 223 N. K. Agrawal, P. Allen, Y. H. Song, R. A. Wachs, Y. Du, A. D. Ellington and C. E. Schmidt, *Acta Biomater.*, 2020, **102**, 315–325.
- 224 Z. Hua and B. Hou, *Immunol. Rev.*, 2020, **296**, 24–35.
- 225 Y. Shao, Z. Y. Sun, Y. Wang, B. D. Zhang, D. Liu and Y. M. Li, *ACS Appl. Mater. Interfaces*, 2018, **10**, 9310–9314.
- 226 M. Nishikawa, K. Ogawa, Y. Umeki, K. Mohri, Y. Kawasaki, H. Watanabe, N. Takahashi, E. Kusuki, R. Takahashi, Y. Takahashi and Y. Takakura, *J. Control. Release*, 2014, **180**, 25–32.
- 227 R. Langer and J. Vacanti, *J. Pediatr. Surg.*, 2016, **51**, 8–12.
- 228 A. A. Chaudhari, K. Vig, D. R. Baganizi, R. Sahu, S. Dixit, V. Dennis, S. R. Singh and S. R. Pillai, *Int. J. Mol. Sci.*, , DOI:10.3390/ijms17121974.
- 229 R. D. Pedde, B. Mirani, A. Navaei, T. Styan, S. Wong, M. Mehrali, A. Thakur, N. K. Mohtaram, A. Bayati, A. Dolatshahi-Pirouz, M. Nikkhah, S. M. Willerth and M. Akbari, *Adv. Mater.*, 2017, 29.
- 230 N. Chen, Z. Zhang, B. Soontornworajit, J. Zhou and Y. Wang, *Biomaterials*, 2012, **33**, 1353–1362.
- 231 J. A. Hubbell, *Bio/Technology*, 1995, **13**, 565–576.
- 232 X. Zhang, M. R. Battig, N. Chen, E. R. Gaddes, K. L. Duncan and Y. Wang, *Biomacromolecules*, 2016, **17**, 778–787.
- 233 C. Galli, L. Parisi, M. Piergianni, A. Smerieri, G. Passeri, S. Guizzardi, F. Costa, S. Lumetti, E. Manfredi and G. M. Macaluso, *Acta Biomater.*, 2016, **42**, 147–156.
- 234 E. R. Gaddes, G. Gydush, S. Li, N. Chen, C. Dong and Y. Wang, *Biomacromolecules*, 2015, **16**, 1382–1389.
- 235 M. Mammen, S. Choi and G. M. Whitesides, *Angew. Chemie Int. Ed.*, 1998, **37**, 2754–2794.

- 236 E. A. Lenzelink, *Int. Wound J.*, 2015, **12**, 313–316.
- 237 X. Wang, X. Song, T. Li, J. Chen, G. Cheng, L. Yang and C. Chen, *Am. J. Sports Med.*, 2019, **47**, 2316–2326.
- 238 C. Li, A. Faulkner-Jones, A. R. Dun, J. Jin, P. Chen, Y. Xing, Z. Yang, Z. Li, W. Shu, D. Liu and R. R. Duncan, *Angew. Chemie - Int. Ed.*, 2015, **54**, 3957–3961.
- 239 J. Tavakoli and Y. Tang, *Polymers (Basel)*, , DOI:10.3390/polym9080364.
- 240 I. Y. Jung, J. S. Kim, B. R. Choi, K. Lee and H. Lee, *Adv. Healthc. Mater.*, , DOI:10.1002/adhm.201601475.
- 241 S. Khajouei, H. Ravan and A. Ebrahimi, *Adv. Colloid Interface Sci.*, 2019, **275**, 102060.
- 242 J. Mosquera, I. García and L. M. Liz-Marzán, *Acc. Chem. Res.*, 2018, **51**, 2305–2313.
- 243 M. A. Perazella, *Clin. J. Am. Soc. Nephrol.*, 2018, **13**, 1897–1908.
- 244 H. Yang, H. Liu, H. Kang and W. Tan, *J. Am. Chem. Soc.*, 2008, **130**, 6320–6321.
- 245 Y. Hu, J. Liu, X. You, C. Wang, Z. Li and W. Xie, *Sensors (Switzerland)*, , DOI:10.3390/s17102246.
- 246 Z. Zhu, C. Wu, H. Liu, Y. Zou, X. Zhang, H. Kang, C. J. Yang and W. Tan, *Angew. Chemie - Int. Ed.*, 2010, **49**, 1052–1056.
- 247 B. Tan, H. Zhao, L. Du, X. Gan and X. Quan, *Biosens. Bioelectron.*, 2016, **83**, 267–273.
- 248 B. Kolar, L. Arnuš, B. Jeretin, A. Gutmaher, D. Drobne and M. K. Durjava, *Chemosphere*, 2014, **115**, 75–80.
- 249 T. Otsoshi, T. Nagano, M. Tachihara and Y. Nishimura, *Cancers (Basel)*, 2019, **11**, 935.
- 250 Z. Zhang, T. Yang and J. Xiao, *EBioMedicine*, 2018, **34**, 267–274.
- 251 C. Yao, H. Tang, W. Wu, J. Tang, W. Guo, D. Luo and D. Yang, *J. Am. Chem. Soc.*, 2020, **142**, 3422–3429.
- 252 L. Gong, Z. Zhao, Y. F. Lv, S. Y. Huan, T. Fu, X. B. Zhang, G. L. Shen and R. Q. Yu, *Chem. Commun.*, 2015, **51**, 979–995.
- 253 X. Mao, S. Pan, D. Zhou, X. He and Y. Zhang, *Sensors Actuators, B Chem.*, 2019, **285**, 385–390.
- 254 A. Norouzi, H. Ravan, A. Mohammadi, E. Hosseinzadeh, M. Norouzi and T. Fozooni, *Anal. Chim. Acta*, 2018, **1017**, 26–33.
- 255 I. H. Cho, D. H. Kim and S. Park, *Biomater. Res.*, 2020, **24**, 6.
- 256 S. Liu, W. Su, Y. Li, L. Zhang and X. Ding, *Biosens. Bioelectron.*, 2018, **103**, 1–5.
- 257 Y. H. Feng and C. J. Tsao, *Biomed. Reports*, 2016, **5**, 395–402.
- 258 D. Astruc, *Eur. J. Inorg. Chem.*, 2017, **2017**, 6–29.
- 259 J. CA, T. P and W. M, *Immunobiology*, Garland Science, New York, 5th edn., 2001.
- 260 L. Xu, R. Wang, L. C. Kelso, Y. Ying and Y. Li, *Sensors Actuators, B Chem.*, 2016, **234**, 98–108.
- 261 P. Kralik and M. Ricchi, *Front. Microbiol.*, 2017, **8**, 108.
- 262 S. R. Perera, A. Taheri, N. H. Khan, R. P. Parti, S. Stefura, P. Skiba, J. P. Acker, I. Martin, A. Kusalik and J. A. R. Dillon, *Antibiotics*, , DOI:10.3390/antibiotics7030070.
- 263 N. Park, S. H. Um, H. Funabashi, J. Xu and D. Luo, *Nat. Mater.*, 2009, **8**, 432–437.
- 264 S. H. Um, J. B. Lee, N. Park, S. Y. Kwon, C. C. Umbach and D. Luo, *Nat. Mater.*, 2006, **5**, 797–801.
- 265 J. Cui, D. Wu, Q. Sun, X. Yang, D. Wang, M. Zhuang, Y. Zhang, M. Gan and D. Luo, *Front. Chem.*, , DOI:10.3389/fchem.2020.00028.
- 266 J. Song, M. Lee, T. Kim, J. Na, Y. Jung, G. Y. Jung, S. Kim and N. Park, *Nat. Commun.*, 2018, **9**, 1–11.
- 267 C. Rinaldi and M. J. A. Wood, *Nat. Rev. Neurol.*, 2018, **14**, 9–22.
- 268 K. Sridharan and N. J. Gogtay, *Br. J. Clin. Pharmacol.*, 2016, **82**, 659–672.
- 269 D. P. Wolf, P. A. Mitalipov and S. M. Mitalipov, *Nat. Med.*, 2019, **25**, 890–897.
- 270 J. Daley, *Nature*, 2019, **576**, S12–S13.
- 271 Z. Cui, *Adv. Genet.*, 2005, **54**, 257–289.
- 272 D. Hobernik and M. Bros, *Int. J. Mol. Sci.*, 2018, **19**, 3605.
- 273 P. D. Hsu, E. S. Lander and F. Zhang, *Cell*, 2014, **157**, 1262–1278.
- 274 M. Adli, *Nat. Commun.*, 2018, **9**, 1–13.
- 275 J. A. Soppe and R. J. Lebbink, *Trends Microbiol.*, 2017, **25**, 833–850.
- 276 H. Wang, M. La Russa and L. S. Qi, *Annu. Rev. Biochem.*, 2016, **85**, 227–264.
- 277 L. Cong, F. A. Ran, D. Cox, S. Lin, R. Barretto, N. Habib, P. D. Hsu, X. Wu, W. Jiang, L. A. Marraffini and F. Zhang, *Science (80-. )*, 2013, **339**, 819–823.
- 278 Z. Zhao, L. Shi, W. Zhang, J. Han, S. Zhang, Z. Fu and J. Cai, *Oncotarget*, 2018, **9**, 5208–5215.
- 279 A. L. B. Pyne, A. Noy, K. H. S. Main, V. Velasco-Berrelleza, M. M. Piperakis, L. A. Mitchenall, F. M. Cugliandolo, J. G. Beton, C. E. M. Stevenson, B. W. Hoogenboom, A. D. Bates, A. Maxwell and S. A. Harris, *Nat. Commun.*, 2021, **12**, 1053.
- 280 P. A. Summers, B. W. Lewis, J. Gonzalez-Garcia, R. M. Porreca, A. H. M. Lim, P. Cadinu, N. Martin-Pintado, D. J. Mann, J. B. Edel, J. B. Vannier, M. K. Kuimova and R. Vilar, *Nat. Commun.*, 2021, **12**, 1–11.
- 281 Y. Hu, C. M. Domínguez, J. Bauer, S. Weigel, A. Schipperges, C. Oelschlaeger, N. Willenbacher, S. Keppler, M. Bastmeyer, S. Heißler, C. Wöll, T. Scharnweber, K. S. Rabe and C. M. Niemeyer, *Nat. Commun.*, , DOI:10.1038/s41467-019-13381-1.
- 282 K. A. Deo, K. A. Singh, C. W. Peak, D. L. Alge and A. K. Gaharwar, *Tissue Eng. - Part A*, , DOI:10.1089/ten.tea.2019.0298.
- 283 J. Pang, Z. Gao, H. Tan, X. Mao, J. Xu, J. Kong and X. Hu, *Front. Chem.*, , DOI:10.3389/fchem.2019.00620.
- 284 S. Khoee and M. R. Karimi, *Polymer (Guildf)*, , DOI:10.1016/j.polymer.2018.03.022.
- 285 S. F. Bakshi, N. Guz, A. Zakharchenko, H. Deng, A. V. Tumanov, C. D. Woodworth, S. Minko, D. M. Kolpashchikov and E. Katz, *Nanoscale*, , DOI:10.1039/c7nr08581h.

- 286 M. Grzelczak, L. M. Liz-Marzán and R. Klajn, *Chem. Soc. Rev.*, 2019.
- 287 W. Poon, Y. N. Zhang, B. Ouyang, B. R. Kingston, J. L. Y. Wu, S. Wilhelm and W. C. W. Chan, *ACS Nano*, , DOI:10.1021/acsnano.9b01383.
- 288 G. Zhu and X. Chen, *Adv. Drug Deliv. Rev.*, 2018.
- 289 F. Liu, Y. Shang, Z. Wang, Y. Jiao, N. Li and B. Ding, *APL Mater.*, , DOI:10.1063/5.0025776.
- 290 L. Shani, A. N. Michelson, B. Minevich, Y. Flegler, M. Stern, A. Shaulov, Y. Yeshurun and O. Gang, *Nat. Commun.*, , DOI:10.1038/s41467-020-19439-9.
- 291 Y. Shang, N. Li, S. Liu, L. Wang, Z. G. Wang, Z. Zhang and B. Ding, *Adv. Mater.*, , DOI:10.1002/adma.202000294.
- 292 M. Scheckenbach, J. Bauer, J. Zähringer, F. Selbach and P. Tinnefeld, *APL Mater.*, , DOI:10.1063/5.0022885.
- 293 M. Raab, I. Jusuk, J. Molle, E. Buhr, B. Bodermann, D. Bergmann, H. Bosse and P. Tinnefeld, *Sci. Rep.*, , DOI:10.1038/s41598-018-19905-x.
- 294 L. Schermelleh, A. Ferrand, T. Huser, C. Eggeling, M. Sauer, O. Biehlaier and G. P. C. Drummen, *Nat. Cell Biol.*, 2019.
- 295 A. Kuzyk, R. Jungmann, G. P. Acuna and N. Liu, *ACS Photonics*, 2018.
- 296 M. Wang, J. Dong, C. Zhou, H. Xie, W. Ni, S. Wang, H. Jin and Q. Wang, *ACS Nano*, , DOI:10.1021/acsnano.9b06734.
- 297 P. Wang, J. H. Huh, H. Park, D. Yang, Y. Zhang, Y. Zhang, J. Lee, S. Lee and Y. Ke, *Nano Lett.*, , DOI:10.1021/acs.nanolett.0c04055.
- 298 B. Shen, P. Piskunen, S. Nummelin, Q. Liu, M. A. Kostianen and V. Linko, *ACS Appl. Bio Mater.*, 2020.
- 299 N. A. W. Bell and U. F. Keyser, *J. Am. Chem. Soc.*, , DOI:10.1021/ja512521w.
- 300 K. Chen, J. Zhu, F. Bošković and U. F. Keyser, *Nano Lett.*, , DOI:10.1021/acs.nanolett.0c00755.
- 301 M. Deluca, Z. Shi, C. E. Castro and G. Arya, *Nanoscale Horizons*, 2020.
- 302 S. Nummelin, B. Shen, P. Piskunen, Q. Liu, M. A. Kostianen and V. Linko, *ACS Synth. Biol.*, , DOI:10.1021/acssynbio.0c00235.
- 303 E. Kopperger, J. List, S. Madhira, F. Rothfischer, D. C. Lamb and F. C. Simmel, *Science (80- )*, , DOI:10.1126/science.aao4284.
- 304 A. Jaekel, P. Stegemann and B. Saccà, *Molecules*, 2019.
- 305 D. Zhao, Y. Kong, S. Zhao and H. Xing, *Top. Curr. Chem.*, 2020.
- 306 J. Fu, M. Liu, Y. Liu, N. W. Woodbury and H. Yan, *J. Am. Chem. Soc.*, , DOI:10.1021/ja300897h.
- 307 S. Surana, A. R. Shenoy and Y. Krishnan, *Nat. Nanotechnol.*, 2015.
- 308 D. Bhatia, S. Surana, S. Chakraborty, S. P. Koushika and Y. Krishnan, *Nat. Commun.*, , DOI:10.1038/ncomms1337.
- 309 G. Yao, F. Zhang, F. Wang, T. Peng, H. Liu, E. Poppleton, P. Šulc, S. Jiang, L. Liu, C. Gong, X. Jing, X. Liu, L. Wang, Y. Liu, C. Fan and H. Yan, *Nat. Chem.*, , DOI:10.1038/s41557-020-0539-8.
- 310 C. Ducani, C. Kaul, M. Moche, W. M. Shih and B. Högberg, *Nat. Methods*, , DOI:10.1038/nmeth.2503.
- 311 J. Elbaz, P. Yin and C. A. Voigt, *Nat. Commun.*, , DOI:10.1038/ncomms11179.
- 312 F. Praetorius, B. Kick, K. L. Behler, M. N. Honemann, D. Weuster-Botz and H. Dietz, *Nature*, , DOI:10.1038/nature24650.
- 313 D. Ye, M. Li, T. Zhai, P. Song, L. Song, H. Wang, X. Mao, F. Wang, X. Zhang, Z. Ge, J. Shi, L. Wang, C. Fan, Q. Li and X. Zuo, *Nat. Protoc.*, , DOI:10.1038/s41596-020-0326-4.
- 314 S. Basu, R. Johl, S. Pacelli, S. Gehrke and A. Paul, *ACS Macro Lett.*, 2020, **9**, 1230–1236.
- 315 I. Cozma, E. M. McConnell, J. D. Brennan and Y. Li, *Biosens. Bioelectron.*, , DOI:10.1016/j.bios.2021.112972.
- 316 F. He, N. Wen, D. Xiao, J. Yan, H. Xiong, S. Cai, Z. Liu and Y. Liu, *Curr. Med. Chem.*, , DOI:10.2174/0929867325666181008142831.
- 317 L. Hong, F. Zhou, D. Shi, X. Zhang and G. Wang, *Biosens. Bioelectron.*, , DOI:10.1016/j.bios.2017.04.023.
- 318 Y. Wu, Q. Li, G. Shim and Y. K. Oh, *J. Control. Release*, , DOI:10.1016/j.jconrel.2020.12.040.
- 319 J. B. Lee, S. Peng, D. Yang, Y. H. Roh, H. Funabashi, N. Park, E. J. Rice, L. Chen, R. Long, M. Wu and D. Luo, *Nat. Nanotechnol.*, 2012, **7**, 816–820.
- 320 K. O'Brien, H. Suchowski, J. Rho, A. Salandrino, B. Kante, X. Yin and X. Zhang, *Nat. Mater.*, 2015, **14**, 379–383.
- 321 P. Ebert, P. A. Audano, Q. Zhu, B. Rodriguez-Martin, D. Porubsky, M. J. Bonder, A. Sulovari, J. Ebler, W. Zhou, R. Serra Mari, F. Yilmaz, X. Zhao, P. Hsieh, J. Lee, S. Kumar, J. Lin, T. Rausch, Y. Chen, J. Ren, M. Santamarina, W. Höps, H. Ashraf, N. T. Chuang, X. Yang, K. M. Munson, A. P. Lewis, S. Fairley, L. J. Tallon, W. E. Clarke, A. O. Basile, M. Byrska-Bishop, A. Corvelo, U. S. Evani, T.-Y. Lu, M. J. P. Chaisson, J. Chen, C. Li, H. Brand, A. M. Wenger, M. Ghareghani, W. T. Harvey, B. Raeder, P. Hasenfeld, A. A. Regier, H. J. Abel, I. M. Hall, P. Flicek, O. Stegle, M. B. Gerstein, J. M. C. Tubio, Z. Mu, Y. I. Li, X. Shi, A. R. Hastie, K. Ye, Z. Chong, A. D. Sanders, M. C. Zody, M. E. Talkowski, R. E. Mills, S. E. Devine, C. Lee, J. O. Korbel, T. Marschall and E. E. Eichler, *Science (80- )*, 2021, eabf7117.
- 322 B. R. Aryal, D. R. Ranasinghe, T. R. Westover, D. G. Calvopiña, R. C. Davis, J. N. Harb and A. T. Woolley, *Nano Res.*, , DOI:10.1007/s12274-020-2672-5.
- 323 Y. Huang, M. K. Nguyen, A. K. Natarajan, V. H. Nguyen and A. Kuzyk, *ACS Appl. Mater. Interfaces*, , DOI:10.1021/acsmi.8b19153.
- 324 F. Xu, Q. Xia and P. Wang, *Front. Chem.*, 2020.
- 325 Q. Jiang, S. Liu, J. Liu, Z. G. Wang and B. Ding, *Adv. Mater.*, , DOI:10.1002/adma.201804785.
- 326 Y. Wang, Y. Shao, X. Ma, B. Zhou, A. Faulkner-Jones, W. Shu and D. Liu, *ACS Appl. Mater. Interfaces*, 2017, **9**, 12311–12315.

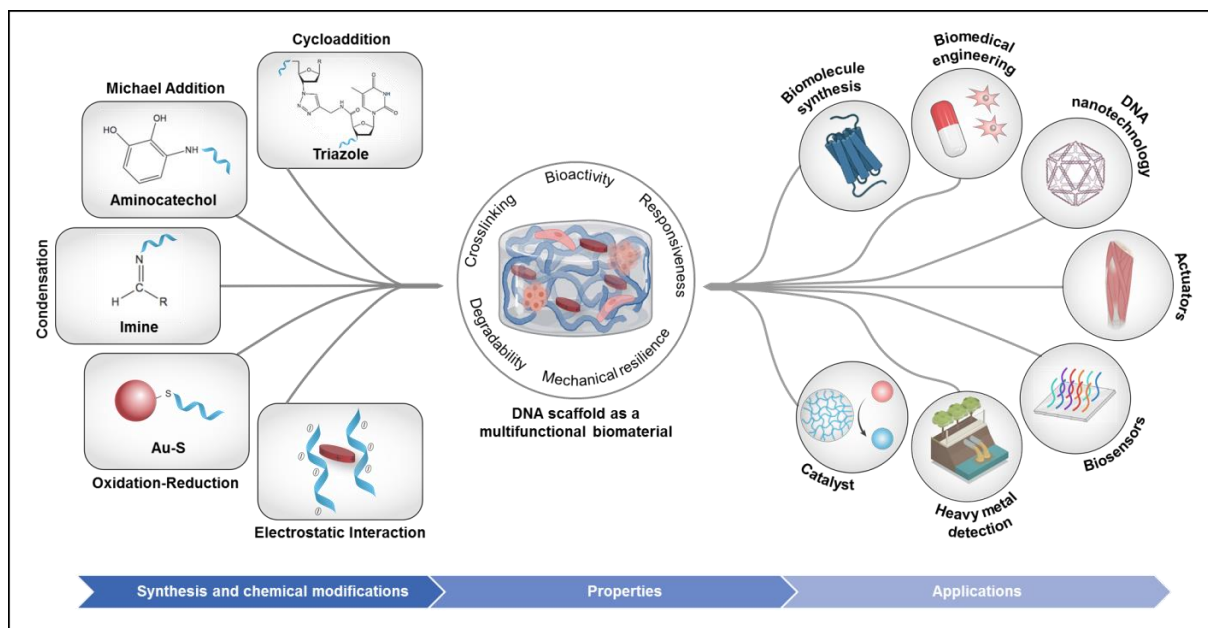


**Fig. 1** Overview of the chemical modifications, properties, and applications of DNA as a multifunctional biomaterial.

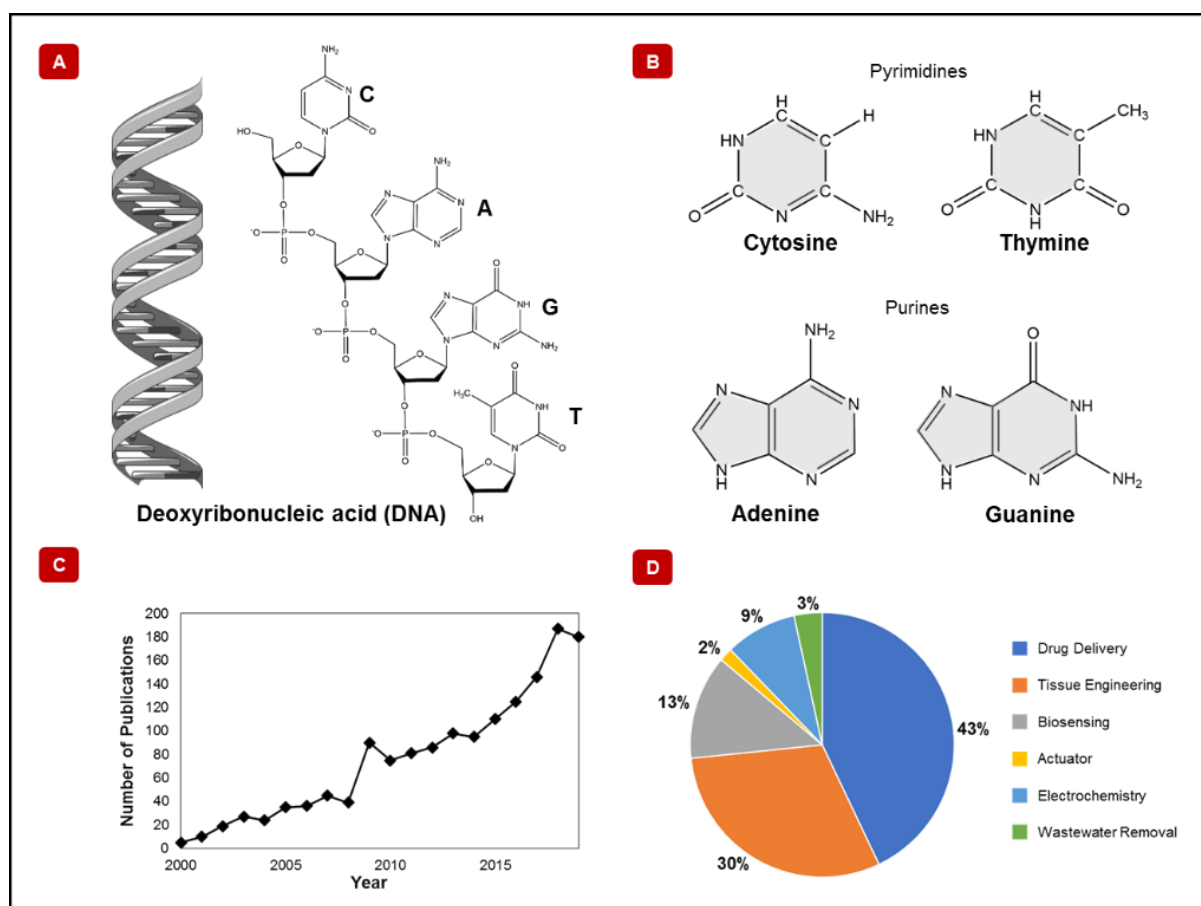


**Fig. 2** The shape and chemical structure of DNA along with the trend in publication of papers on DNA-based hydrogels. (A) The shape of a double-stranded DNA has been shown along with its chemical composition. (B) The chemical structure of the nucleotides has been depicted. (C) A search in the Web of Science database with the keywords “DNA hydrogels” demonstrates a rise in the number of publications over the last two decades (2000-2019). (D) Pie chart showing the different fields in which DNA hydrogels have found use between the years (2000 – 2020). The data has been represented as a percentage of publications based on 785 total publications. Biomedical applications found the most use. The keywords in Web of Science included both DNA-based hydrogels and the desired application.

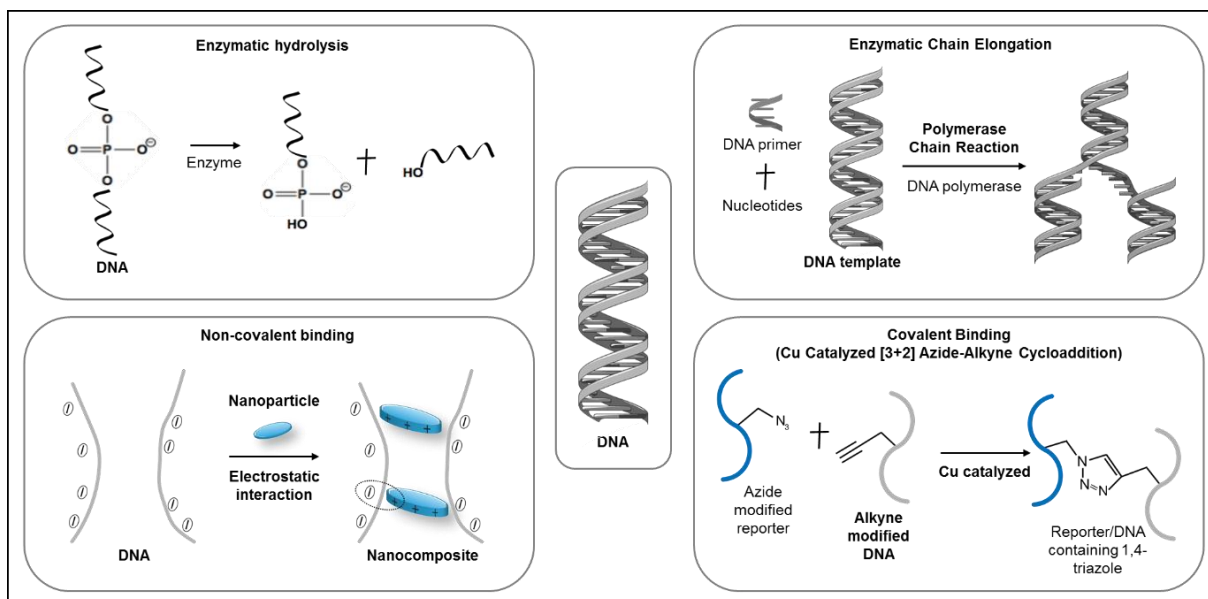


**Fig. 3** Four different schemes of DNA manipulation. The top panels focus on enzymatic tools that are frequently employed to break or elongate DNA. The bottom panels outline the non-enzymatic approaches. Both non-covalent and covalent binding are crucial in synthesizing useful DNA structures.

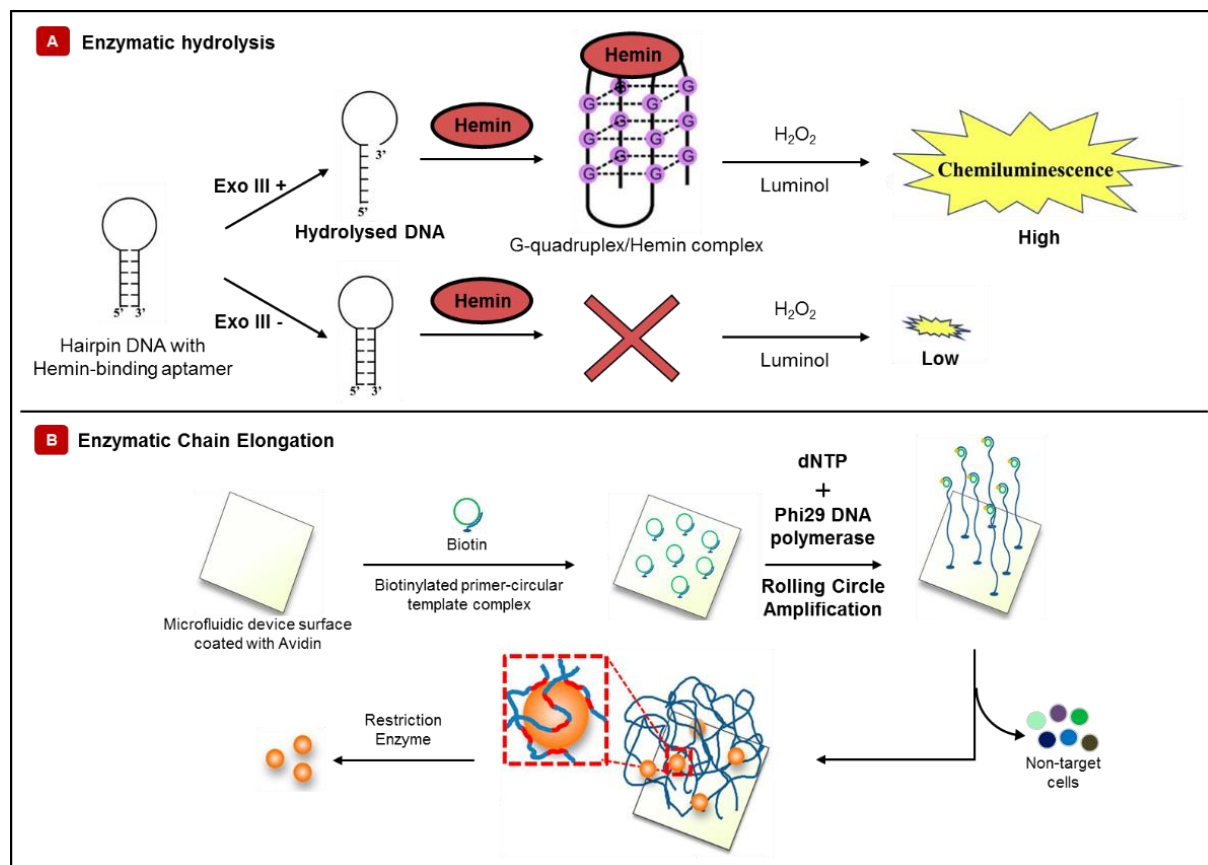


**Fig. 4** Enzymatic modifications of DNA. (A) A hairpin DNA (black hairpin) containing a hemin-binding aptamer was hydrolytically cleaved with the enzyme, Exo III. The resulting DNA formed a G-quadruplex and bonded with the iron containing hemin (red ellipse). This structure acted as a DNAzyme capable of oxidizing the chemiluminescent substrate, luminol, in the presence of hydrogen peroxide. However, in the absence of the enzyme, no G-quadruplex formed. Therefore, only in the presence of the enzyme, chemiluminescence was observed. Adapted<sup>60</sup>. Copyright pending 2019, Elsevier. (B) An enzymatically elongated DNA was used to capture and release target cells. Biotinylated circular templates/primers for the rolling circle amplification was attached to an avidin-coated microfluidic device. Rolling circle amplification was carried out with the DNA polymerase enzyme, phi29, in the presence of the substrate, deoxynucleoside triphosphate. The resulting DNA-network had repetitive sequences of aptamer that could bind to the protein, tyrosine kinase-7, expressed on the surface of cancer cells. Therefore, cells expressing the protein were captured by the DNA network. Finally, the captured cells were released by cleaving the DNA strands with restriction enzymes. Adapted<sup>65</sup>. Copyright pending 2012, National Academy of Sciences.

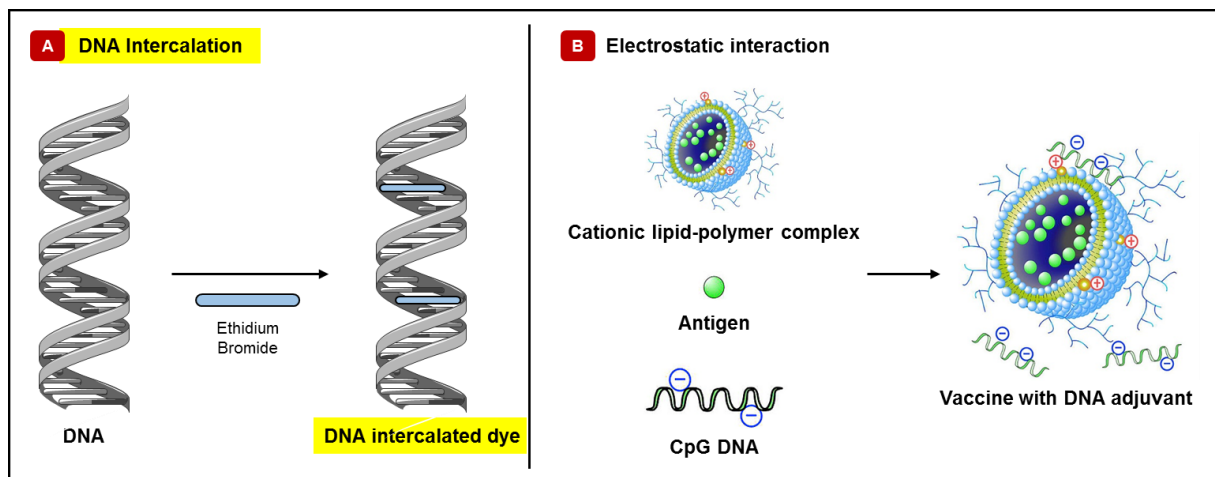


**Fig. 5** Non-covalent interactions with DNA. (A) Some molecules, like the fluorescent dye ethidium bromide, can penetrate the DNA and form Van der Waals interactions with the nucleotides. Such interactions are called intercalation. (B) The negative charge of DNA helps in binding with positively charged materials by electrostatic forces. Here, an antigen delivering vaccine has been shown. The antigen was trapped inside a cationic liposome modified by a pH sensitive synthetic polymer. DNA consisting of cytosine-guanine-phosphate (CpG) motifs was added to the cationic liposomes to enhance immune response. CpG DNA can interact with antigen presenting cells (APCs) to invoke an immune response. Therefore, CpG serves as an adjuvant to vaccines. Adapted<sup>76</sup>. Copyright pending 2017, Elsevier.



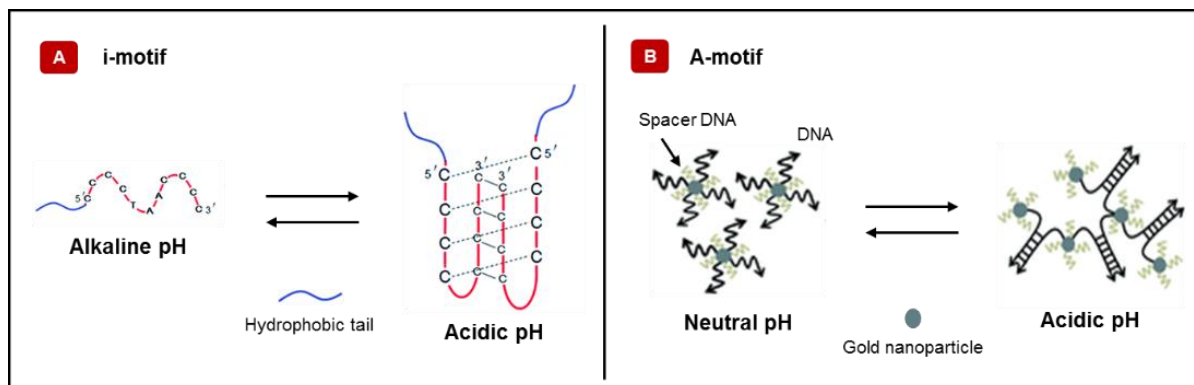


**Fig. 7** DNA polymers as self-assembled nanodevices. (A) The diagram shows the reversible nature of a pH responsive DNA polymer. The cytosine-rich DNA was covalently attached to a hydrophobic alkyl chain making the DNA amphiphilic. Transitioning from alkaline to acidic pH, the DNA formed an i-motif structure. However, reversing the pH disrupted the i-motif. Adapted<sup>107</sup>. Copyright pending 2015, RSC. (B) A colorimetric, pH sensing DNA device is shown here. Thiolated DNA (black line) was conjugated to gold nanoparticles. At acidic pH, the adenine-rich DNA hybridized to form A-motifs, subsequently aggregating the gold nanoparticles, which lead to the change in solution color. At neutral pH, the DNA could revert to its original form. Additionally, thiolated DNA, referred to as a spacer, was conjugated with gold to control the density of the mixture. Adapted<sup>111</sup>. Copyright pending 2012, RSC.

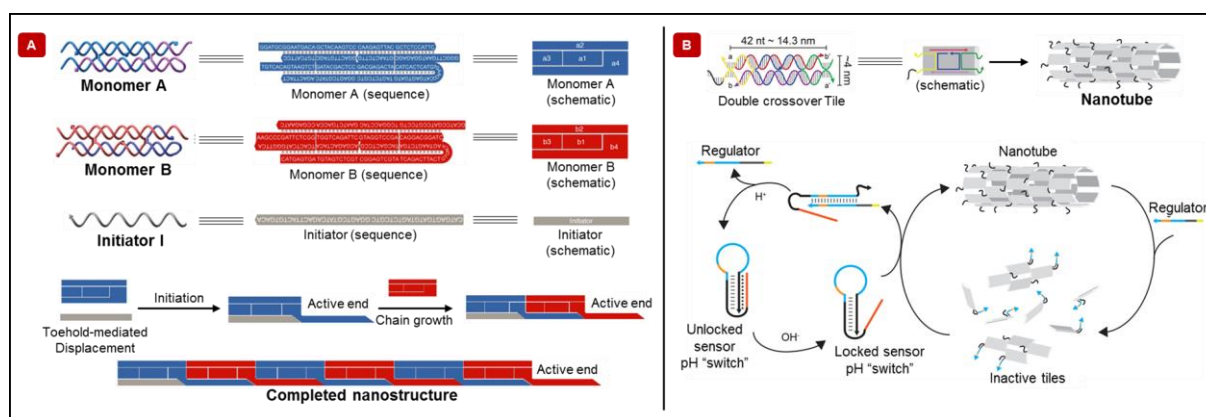


**Fig. 8** Tile-based DNA nanotechnology. (A) The schematic displays a copolymerization method of constructing 1D DNA nanofilaments using hairpin tiles. Monomer A and monomer B consists of four single stranded DNA sequences. These strands form double crossover motifs that are held together by two crossover junctions as can be seen in the diagram. These monomers contain the hairpin domains, a4 and b4. These hairpin sequences have sticky ends that act as toeholds. The corresponding sequences and simplified sketches have been shown in the top panel. The initiator sequence has been selected such that toehold-mediated strand displacement reaction can allow the initiator to hybridize with monomer A. This reaction sets off a polymeric chain growth, where monomer A hybridizes with monomer B, leaving an active end open for the continuation of polymerization. The completed nanostructure is obtained when the monomers are depleted off from the reaction mixture. Adapted<sup>124</sup>. Copyright pending 2019, Nature. (B) The image shows a pH responsive, self-assembled DNA nanotube. The tile consists of five single stranded DNA sequences and they self-assemble at room temperature to form the DNA nanotube. The bottom panel elaborates the mechanism of pH response. The tiles contain actuation domains that can interact with rationally designed, single stranded assembly regulators. This interaction results in prompt disassembly. The design also consists of a pH-responsive, DNA “switch” that can interact with the regulator. At acidic pH, the switch forms an intramolecular triplex hairpin that cannot hybridize with the regulator. Therefore, at acidic pH, the nanoassembly disassembles. However, at basic pH, the switch can interact with the regulator, thereby keeping the nanoassembly intact. Adapted<sup>125</sup>. Copyright pending 2017, ACS.

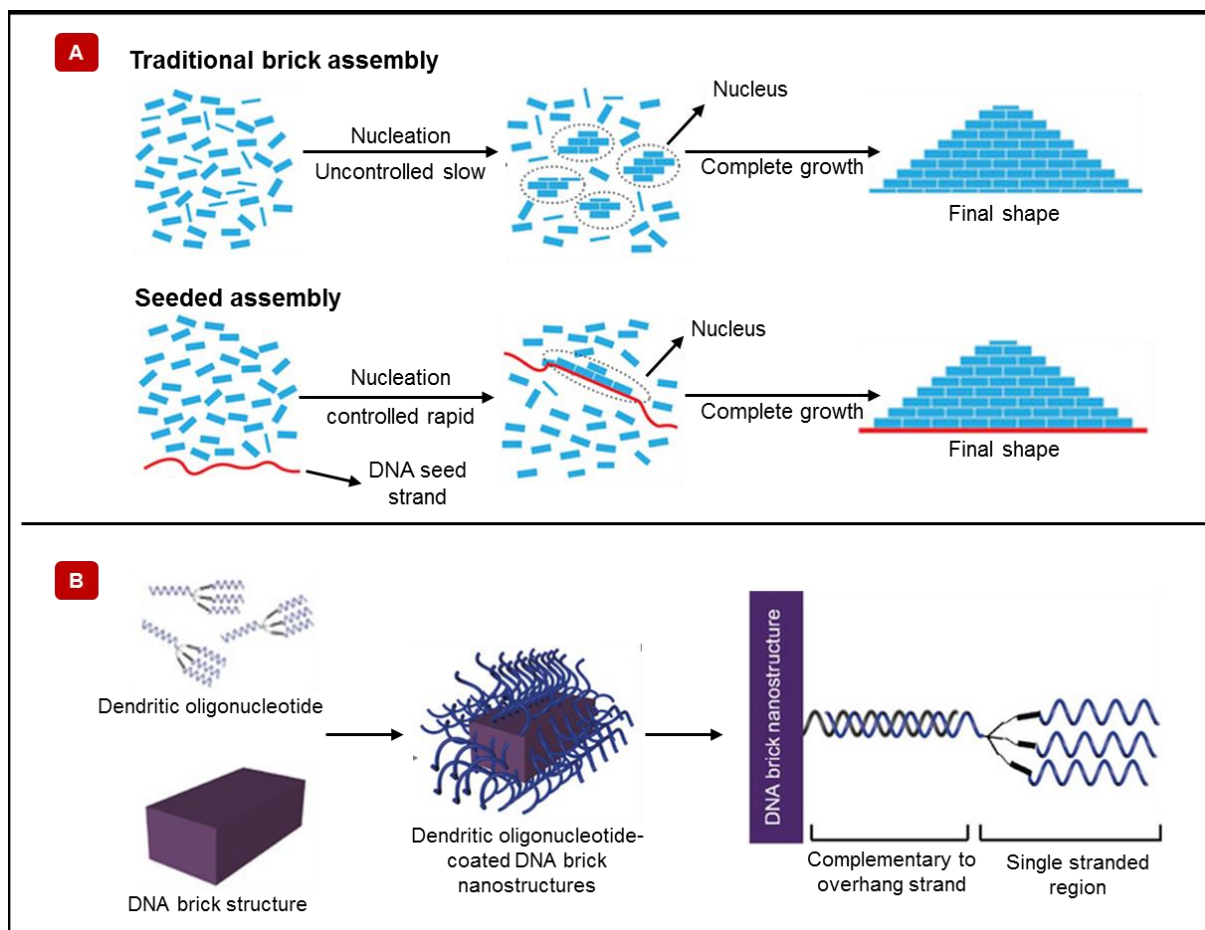


**Fig. 9** Brick-based DNA nanotechnology. (A) The sketch highlights the traditional (top panel) and a new approach (bottom panel) for synthesizing DNA brick-based assemblies. DNA bricks are traditionally assembled by uncontrolled, random nucleation followed by their subsequent growth to higher-ordered structures. However, the nucleation step is slow because the likelihood of formation of similar nucleated structures from different DNA sequences is small. To increase the rate of synthesis, a single stranded DNA seed strand can be included into the mixture. The nucleation in such process is fast and controlled. Therefore, this seeding strategy could significantly reduce the time needed for synthesis. Adapted<sup>135</sup>. Copyright pending 2020, Wiley. (B) A stable DNA brick-based assembly scheme has been shown in the diagram. The design intends on improving the stability of DNA-based nanostructures by functionalizing them with dendritic oligonucleotides such that the biocompatibility of the material is not compromised. The resulting steric hindrance caused by the functionalization prevents nuclease enzymes from digesting the DNA nanostructures. Each DNA brick consists of single stranded overhangs that can hybridize with dendritic oligonucleotides. Adapted<sup>136</sup>. Copyright pending 2019, Wiley.

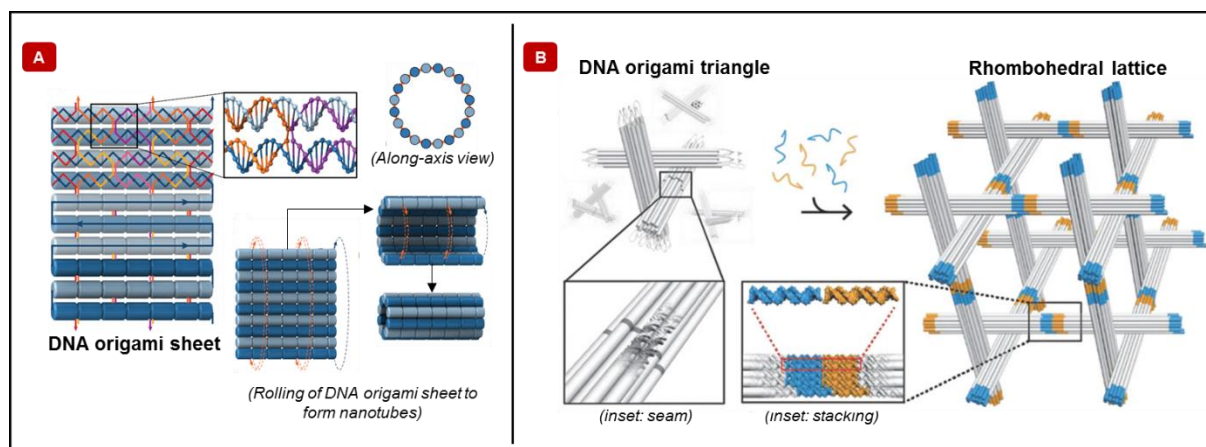


**Fig. 10** Origami-based DNA nanotechnology. (A) The illustration represents the fabrication of DNA nanotubes by implementing DNA origami-based approach. The DNA origami sheet consists of a long single stranded DNA scaffold hybridized with short staple strands. Inset represents the double crossover of staple strands. These crossover junction holds the origami sheet together. This sheet can be rolled into a nanotube by connecting the two ends of the sheet using hybridizable staple strands. Both the length and diameter of the nanotubes can be adjusted. The length can be controlled by changing the number of basepairs between two crossovers, whereas the diameter can be controlled by selecting the density of attachment along the axis. Adapted<sup>143</sup>. Copyright pending 2019, Oxford academic. (B) Schematic represents a DNA-origami nanostructure build with tensegrity triangular motifs. The motif provides structural integrity. All the three struts of the triangle consist of one scaffold DNA. The inset image for the triangle shows a seam where the scaffold no longer continues, and the structure ends with oligonucleotides. By adding additional oligonucleotides that can connect the triangles by non-covalent stacking interactions (inset), a rhombohedral lattice can be fabricated. Adapted<sup>144</sup>. Copyright pending 2018, Wiley.

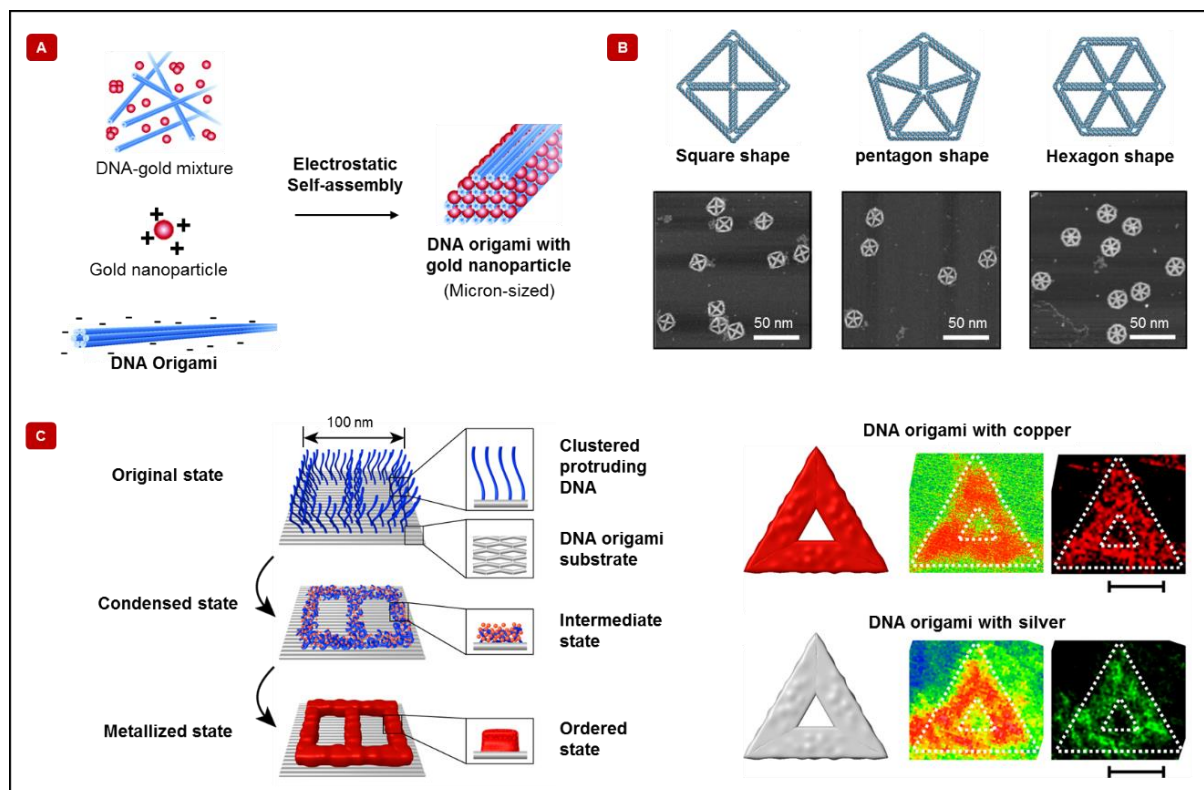


**Fig. 11** Self-assembled DNA origami. (A) A gold nanoparticle associated DNA origami has been shown. Electrostatic interaction between positively charged gold nanoparticles and negatively charged DNA was used to prepare the micron-sized, higher-order arrangement. Adapted<sup>145</sup>. Copyright pending 2019, RSC. (B) Illustrations represent nanosized, wireframe DNA origami objects. Two dimensional, self-assembled squares, pentagons, and hexagons were synthesized. The shape and size of the nanomaterials were characterized by atomic force microscopy. The lower panel shows the micrographs with the defined structures. Adapted<sup>146</sup>. Copyright pending 2019, Nature. (C) The figure displays condensation and metallization reactions on two-dimensional DNA origami substrate. Double-stranded DNA assembly formed the reaction site. Clustered protruding DNA, comprising of three single stranded DNA chains, were placed at specified locations on the origami substrate. Condensation of the clustered protruding DNA occurred with the addition of copper ions. Subsequently, a reducing agent was added to initiate metallization, coating the surface of the substrate with copper. Scanning transmission electron microscopy was performed on triangular DNA origami substrates to visualize the metallization on the surface. Additionally, elemental mapping proved the presence of copper. Scale bar denotes 50 nm. Adapted<sup>151</sup>. Copyright pending 2019, Nature.

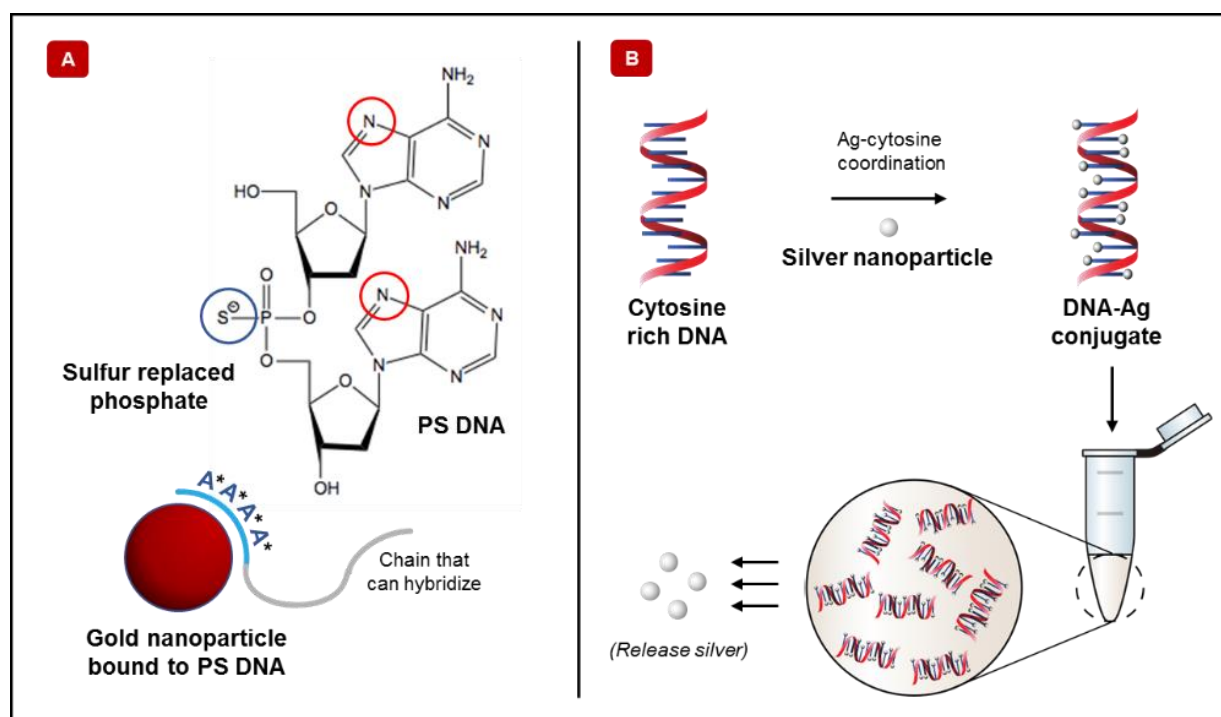


**Fig. 12** Interaction of DNA with nanoparticles. (A) DNA can be used to functionalize gold nanoparticles through different routes<sup>174</sup>. Gold can attach to the nitrogen (N-7 position) on adenosine (circled). In this example, sulfur replaced a non-bridging oxygen in the phosphate group located between adenosine nucleotides. Therefore, the adenosine with modified phosphate groups (A\*) in the DNA sequence, referred to as PS DNA, adsorbed to gold. The remaining chain was free to hybridize. (B) The diagram shows the interaction of silver nanoparticles with cytosine-rich DNA<sup>78</sup>. Silver nanoparticles form coordination complexes with cytosine. Therefore, clusters of silver nanoparticles can be stabilized with DNA. Silver nanoparticles have antibacterial properties, and the silver released from these clusters can be used to prevent bacterial infection.

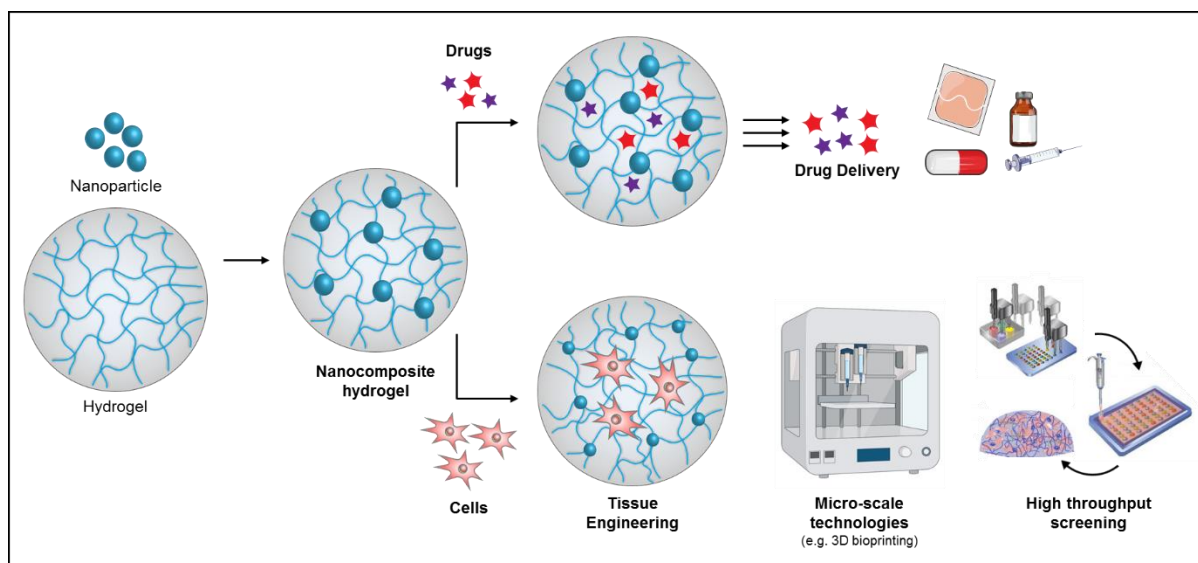


**Fig. 13** Biomedical applications of DNA nanocomposite hydrogels. The schematic displays drug delivery and tissue engineering applications of DNA-based hydrogels incorporated with nanoparticles. The diagram also highlights micro-scale techniques (such as 3D bioprinting) and high throughput screening for analyzing biomaterials (Adapted<sup>178</sup>), which are two emerging approaches in the field of tissue engineering.

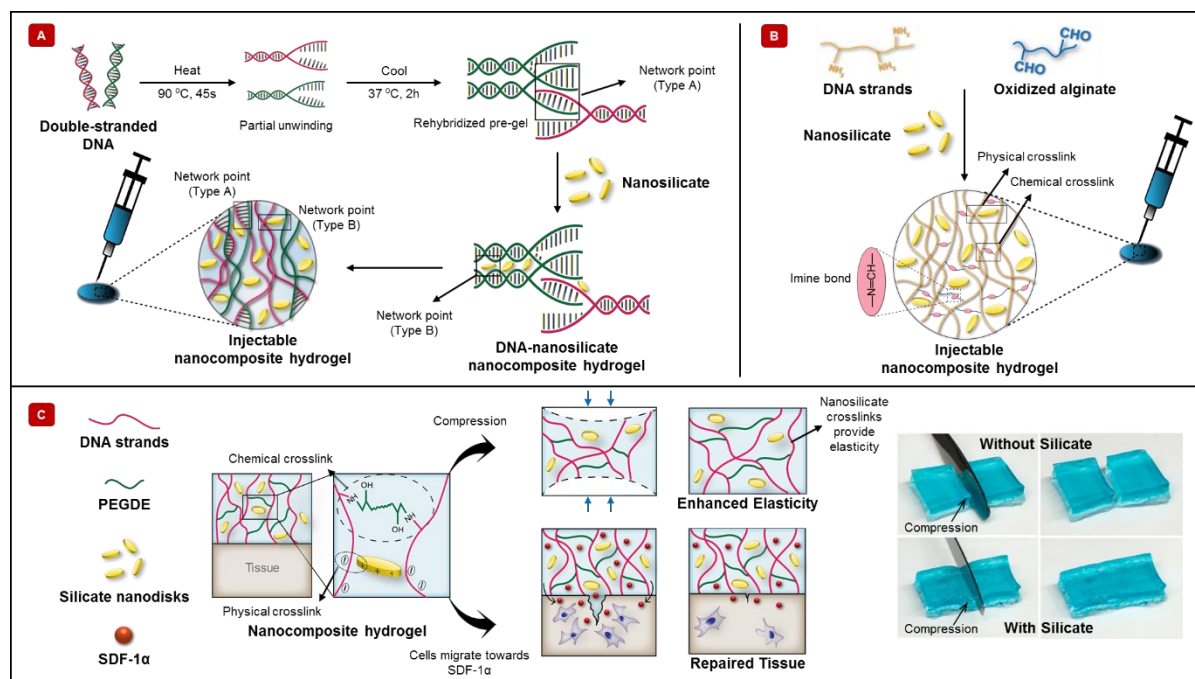


**Fig. 14** Using nanosilicate disks to prepare DNA nanocomposite hydrogels. (A) An injectable DNA nanocomposite hydrogel has been shown. Two double-stranded DNA sequences were denatured and cooled to form a weak pre-gel. This pre-gel consisted of network points between adjacent DNA strands. Two-dimensional nanosilicate disks were then introduced into the pre-gel. Nanosilicate discs are negatively charged on the top and bottom surfaces, but positively charged along the edge. The edges of the nanosilicate disks interacted with the anionic DNA backbone and increased the network points of the pre-gel and the resulting mixture was injectable. Adapted<sup>14</sup>. Copyright pending 2018, ACS. (B) An injectable DNA-based nanocomposite hydrogel with dynamic covalent crosslinks has been depicted. The nucleotide's amine groups covalently linked with the aldehyde groups of the oxidized alginate crosslinker. The resulting imine bond is reversible in nature, which can produce self-healing, injectable hydrogels. Nanosilicate disks electrostatically interacted with DNA and oxidized alginate was introduced to form the nanocomposite hydrogel. Nanosilicate disks were used to enhance the mechanical properties of the hydrogel by adding more network points and to help with the long-term delivery of the drug, simvastatin. Adapted<sup>13</sup>. Copyright pending 2020, Elsevier. (C) A tissue-repairing DNA-based nanocomposite hydrogel has been displayed. The amine groups of DNA nucleotides were chemically conjugated to the epoxides of polyethylene glycol diglycidyl ether (PEGDE) to form the hydrogel. Nanosilicate disks were added to the DNA before gelation to enhance the elasticity of the hydrogel and to control the release of the protein, stromal cell-derived factor-1 (SDF-1 $\alpha$ ), by electrostatic interaction. Together with the protein, the devised nanocomposite hydrogel could help with tissue regeneration. The photographs display the enhanced elasticity of the hydrogel when the nanosilicate disks were added. Adapted<sup>15</sup>. Copyright pending 2019, ACS.

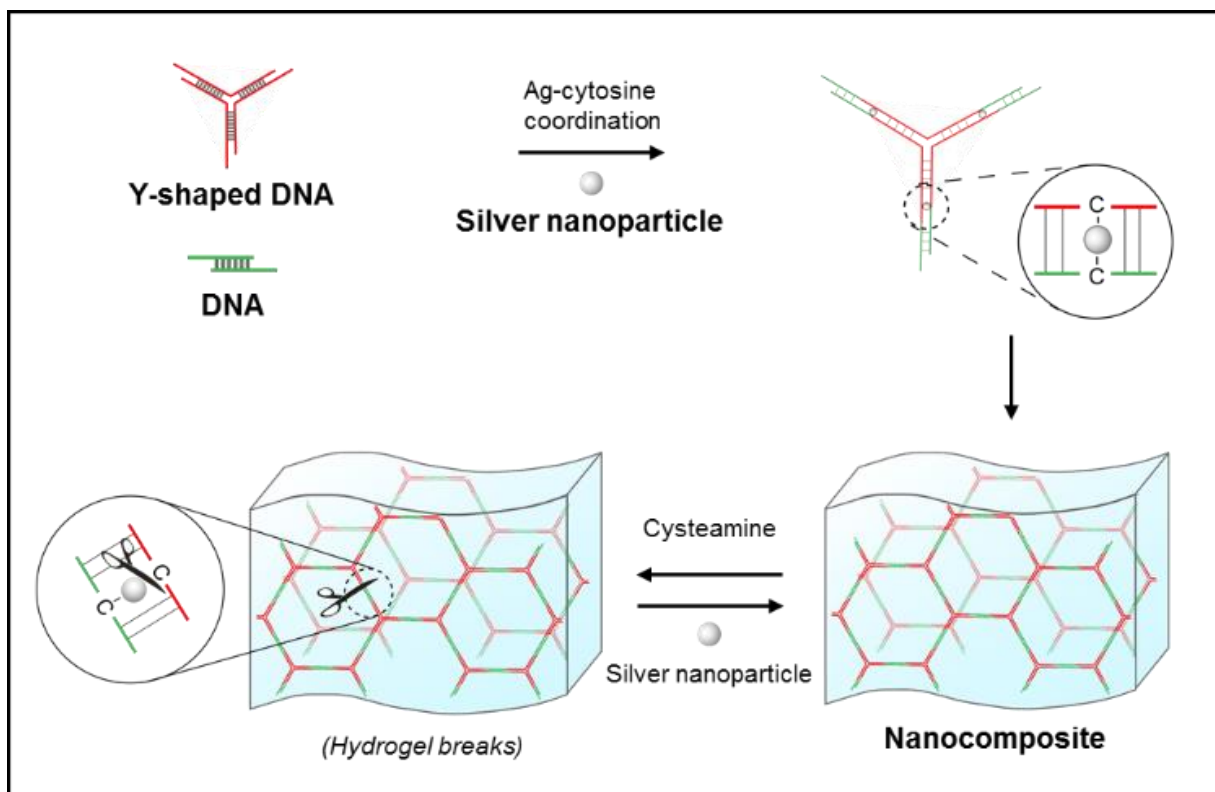


**Fig. 15** DNA-silver nanocomposite hydrogel. (A) A pure DNA hydrogel was synthesized by crosslinking with silver nanoparticles. A Y-shaped DNA and a duplex DNA were selected such that parts of both the stands were complementary to each other. However, there was one cytosine-cytosine mismatch, which prevented the polymers from forming the hydrogel upon mixing. Crosslinking was achieved only when silver was added, which formed cytosine-silver-cytosine coordination complexes. The resulting hydrogel could be reversibly dissociated by adding cysteamine. Adapted<sup>186</sup>. Copyright pending 2014, RSC.

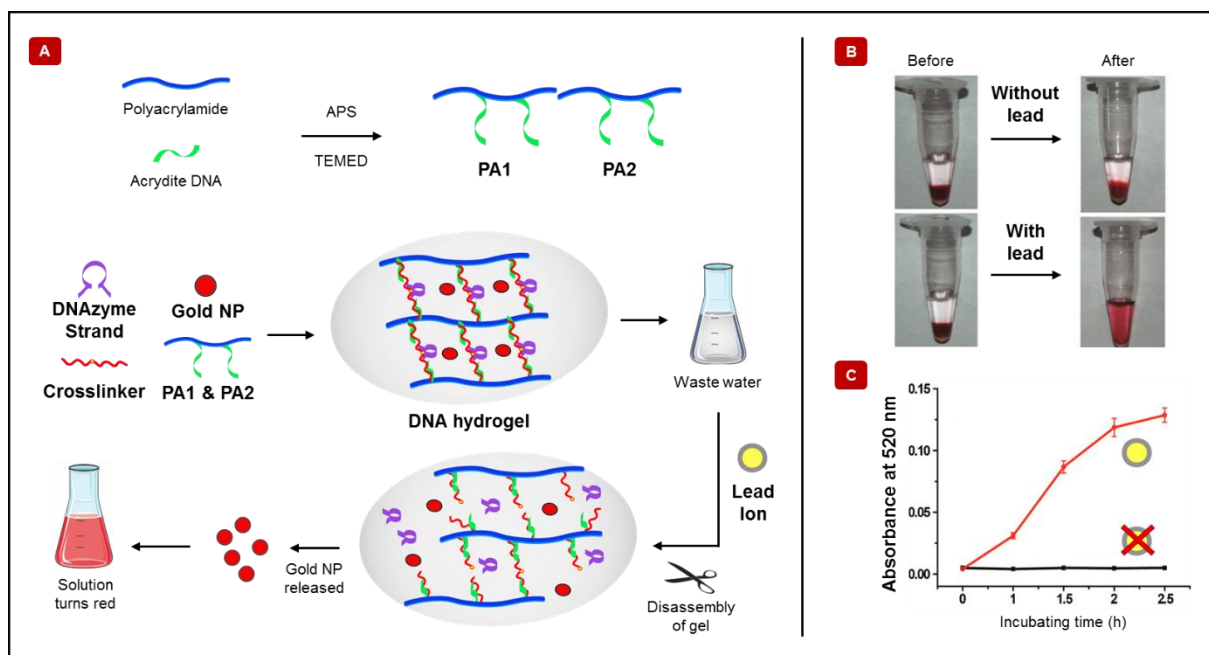


**Fig. 16** DNA-based hydrogel as a biosensor for detecting toxic heavy metal in water. (A) The schematic shows the hydrogel and its mechanism of action. Acrydite-modified, short DNA strands were copolymerized with acrylamide using the free radical initiator, ammonium persulfate (APS), and the catalyst, tetramethylethylenediamine (TEMED). The resulting polymerized polyacrylamide-DNA polymer has been represented as PA1 and PA2. A DNA sequence complementary to A1 and A2 strands was chosen as the crosslinker and served as the substrate to the DNAzyme. Therefore, the DNAzyme formed part of the crosslinker. Gold nanoparticles were trapped within the hydrogel. In the presence of lead ions, the DNAzyme could enzymatically cleave the substrate strand at the cleavage site. With this cleavage, the hydrogel collapsed, and the gold nanoparticles were released. (B) Without lead ions, the water remained colorless. However, with the addition of lead ions, gold nanoparticles were released causing the water to turn red. (C) UV-Vis spectrometry quantified the change in color. An increase in the absorbance value with incubation time indicated the presence of lead. Adapted<sup>195</sup>. Copyright pending 2014, ACS.

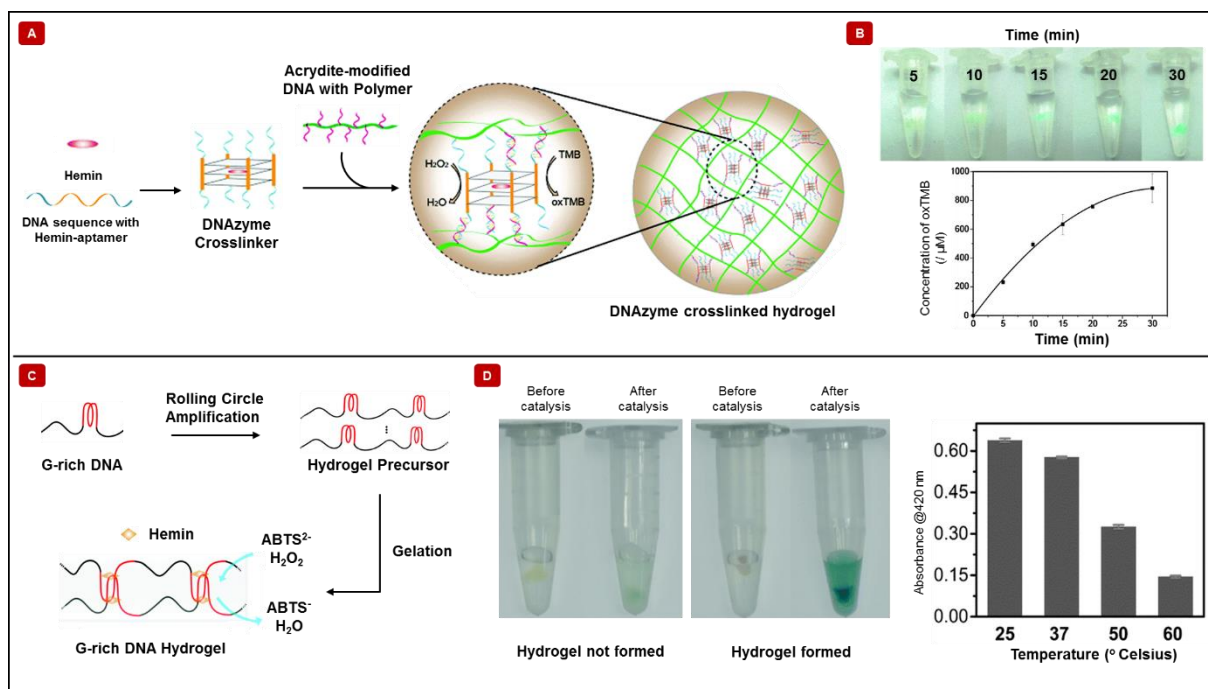


**Fig. 17** DNA-based hydrogels as biocatalysts. (A) A diagram of the catalytic sensor of hydrogen peroxide has been displayed. Hemin was used to bind with the DNA aptamer, 4c15s. The aptamer contained thymine-rich nucleotide sequences on both ends that acted as the crosslinker. The guanine-rich aptamer formed the G-quadruplex structure. This G-quadruplex formed a complex with hemin forming the DNAzyme. Acrydite-modified DNA, which hybridized with the crosslinker DNA sequence, along with polyacrylamide formed the backbone of the hydrogel. The DNAzyme in the hydrogel acted as a mimic of horseradish peroxidase by reducing hydrogen peroxide ( $H_2O_2$ ) and oxidized the chromogenic substrate, tetramethylbenzidine (TMB). (B) In the presence of  $H_2O_2$ , the TMB inside the hydrogel transitioned from colorless to blue. The brightness increased with incubation time. (C) UV-Vis spectrometry demonstrated an increase in the oxidized TMB (oxTMB) concentration with time. Adapted<sup>204</sup>. Copyright pending 2013, RSC. (C) A horseradish peroxidase mimicking, pure DNA hydrogel has been represented. Long stranded guanine-rich DNA sequence was synthesized by rolling circle amplification. The resulting polymers formed interstrand G-quadruplex structures. These interstrand G-quadruplexes served as the crosslinker for the hydrogel. Moreover, the G-quadruplex also formed a complex with hemin. In this case, the chromogenic substrate, 2,2'-Azinobis [3-ethylbenzothiazoline-6-sulfonic acid]-diammonium salt (ABTS), turned blue as it oxidized in the presence of hydrogen peroxide. (D) Hydrogels did not form without interstrand G-quadruplexes and showed weak changes in color. However, hydrogels with interstrand G-quadruplexes oxidized ABTS. The significant change in color as a function of temperature was quantified by detecting absorbance. The increase in temperature reduced the catalytic activity of the hydrogel. Adapted<sup>209</sup>. Copyright pending 2017, RSC.

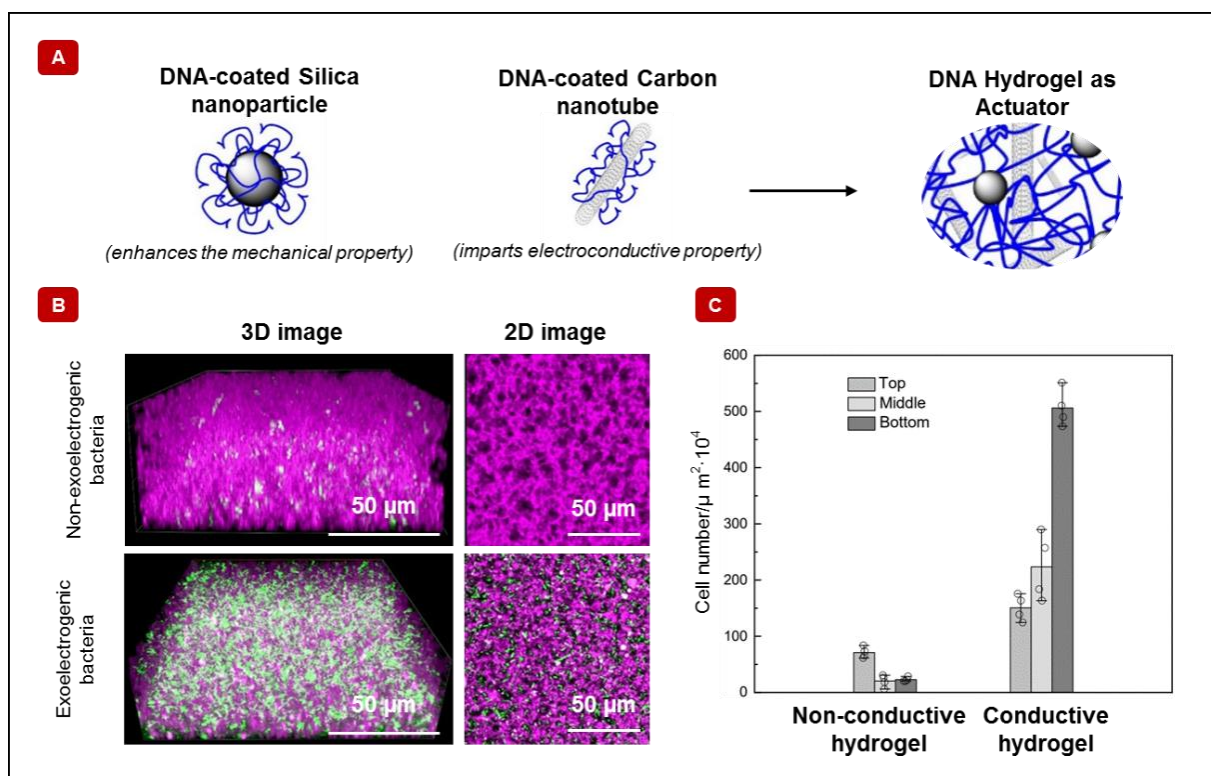


**Fig. 18** Electroconductive DNA-based hydrogel. (A) The schematic shows the formation of nanocomposite hydrogel. Rolling circle amplification was used to coat silica nanoparticles and carbon nanotubes with DNA. The primers for the DNA amplification were chemically conjugated to the nanoparticles such that the polymerization could take place on the nanoparticles. The two DNA-coated nanomaterials were mixed to form the electroconductive hydrogel. The silica nanoparticle enhanced the mechanical property of the hydrogel, whereas the carbon nanotube made the hydrogel electroconductive. (B) 3D and 2D confocal fluorescence images show that only exoelectrogenic bacteria (*S. oneidensis*) (green) grew on the electroconductive hydrogel. In the case of non-exoelectrogenic bacteria (*E. coli*), the hydrogel appeared entirely pink without any bacterial growth. (C) Cell count obtained from fluorescence images quantified the bacterial growth in the electroconductive hydrogel. The highest growth was seen at the bottom of the hydrogel, whereas the middle and the top of the hydrogels had much lesser growth. Adapted<sup>28</sup>. Copyright pending 2020, ACS.

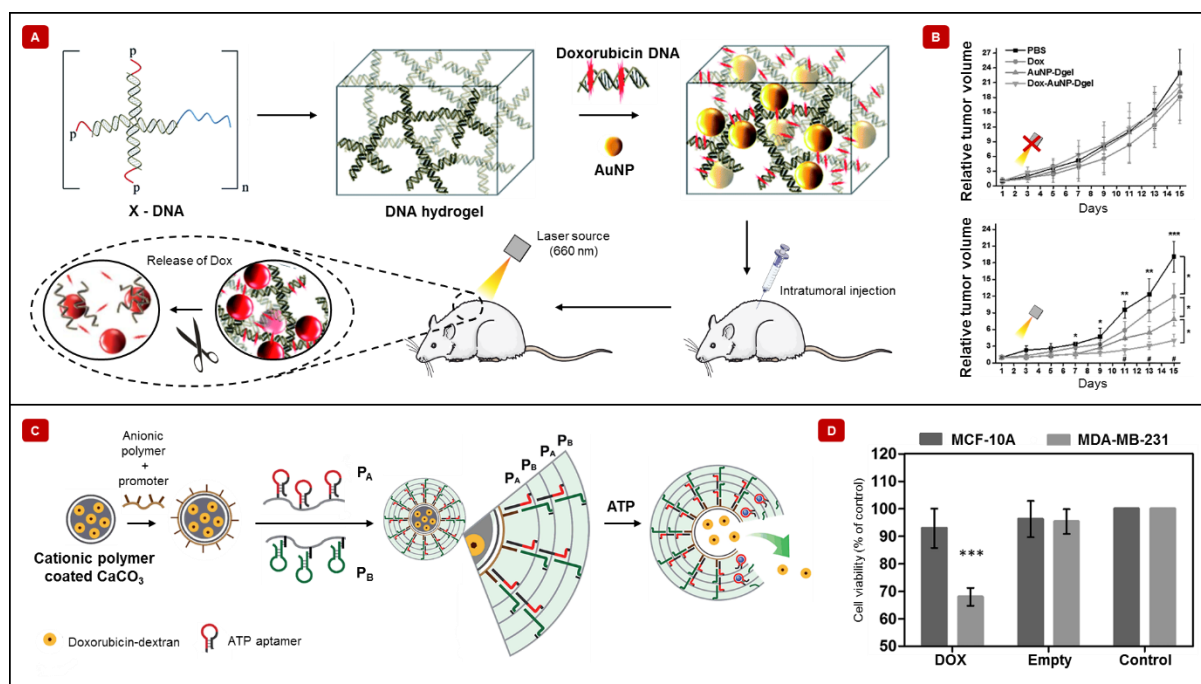


**Fig. 19** DNA-based hydrogels delivering small molecules. (A) A DNA hydrogel that can release floxuridine has been shown. Floxuridine binds with purines by complementary base pairing. Two Y-DNAs were designed in such a way that floxuridine formed part of the DNA. The mixture of Ya and Yb self-assembled to form the nanosized hydrogel. In the presence of the hydrolyzing enzyme DNase II, the hydrogel completely degraded. Floxuridine released from the broken hydrogel. The presence of DNase II in the cancer cells can then act as a trigger for the targeted release of floxuridine. (B) Mean fluorescence intensity obtained from flow cytometry studies quantified the uptake of the hydrogels inside cervical cancer cells. Flow cytometry with fluorescent-labeled DNA hydrogels revealed an increase in the mean fluorescence as the hydrogels were taken up by the cells. The cellular uptake is a key aspect for the targeted drug delivery. Adapted<sup>219</sup>. Copyright pending 2013, RSC. (C) A small molecule delivering DNA-based hydrogel has been depicted. Dexamethasone (DEX) was encapsulated within the poly(lactic-co-glycolic acid) (PLGA) polymer. The drug-nanoparticle complex was then mixed with Y-DNA and crosslinkers (blue lines), which formed the hydrogel. By a sustained release of dexamethasone, these hydrogels treated allergic conjunctivitis. (D) The concentration of dexamethasone inside the human corneal epithelial cells was determined by high performance liquid chromatography (HPLC). The hydrogel showed the highest amount of drug released after six hours of incubation. HPLC was also used to determine the concentration of drug released in the ophthalmic tissues of mice. The hydrogel showed a high initial release of the drug compared to the non-hydrogels. Adapted<sup>218</sup>. Copyright pending 2019, ACS.

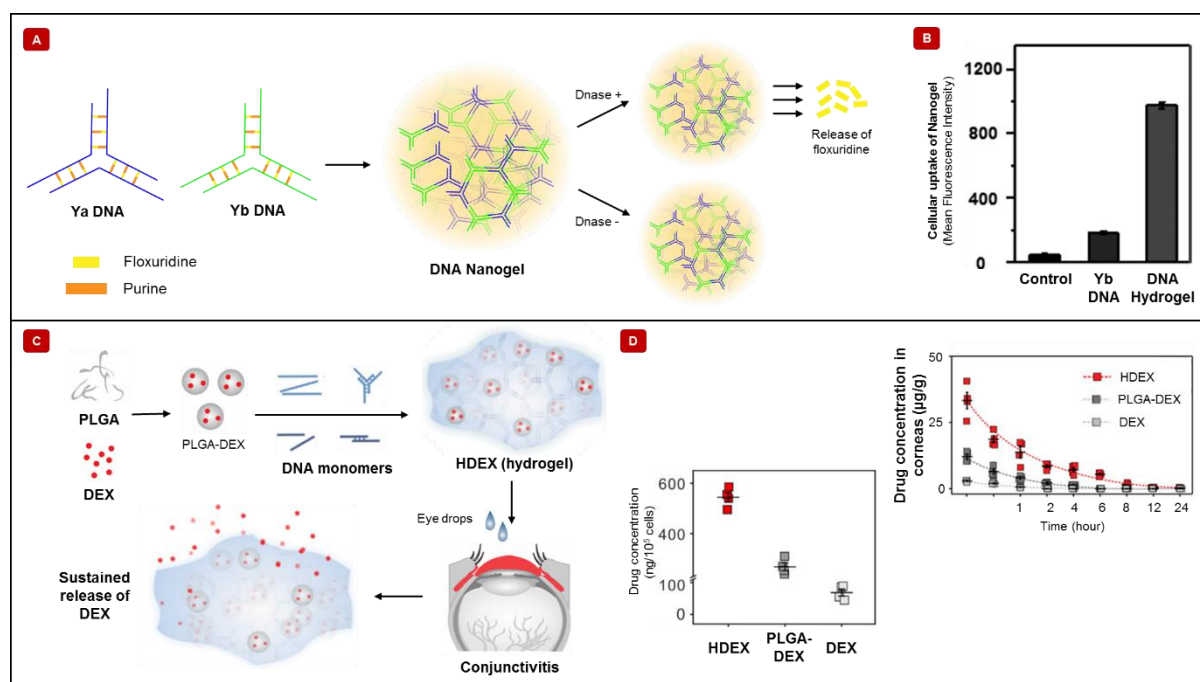


**Fig. 20** Controlled release of drugs from DNA-based hydrogels. (A) A nanocomposite, light-responsive hydrogel has been shown. The hydrogel consisted of enzymatically ligated X-DNA with four single-stranded segments. Three of the arms ended with a segment having phosphate groups and sticky ends that could hybridize with complementary base pairs. Nanosized hydrogels formed by ligation. Positively charged gold nanoparticles were loaded inside the hydrogel by electrostatic interaction, while Doxorubicin was intercalated within the DNA strands. The synthesized nanocomposite hydrogel was intratumorally injected into mice. Upon laser excitation, the heated gold nanoparticles melted the hydrogel. (B) The relative tumor volume reduced with the hydrogel treatment. Adapted<sup>184</sup>. Copyright pending 2015, RSC. (C) A doxorubicin delivering hydrogel has been depicted. Calcium carbonate microcapsules coated with the cationic polymer, poly(allylamine hydrochloride) formed the core. The drug was loaded inside the microcapsule. Anionic polyacrylic acid conjugated to a nucleic acid promoter was deposited on the microcapsule. Acrylamides P<sub>A</sub> and P<sub>B</sub> were chosen as copolymers. The acrylamides were attached to two different hairpin DNAs. Additionally, part of the hairpin, H<sub>A</sub>, had the aptamer sequence that could bind to the target ligand (ATP). The hairpin, H<sub>B</sub>, was bound to P<sub>B</sub> by an acrydite-modified strand. The polymerization was carried out by a hybridization chain reaction. The promoter bound to the sticky part of H<sub>A</sub>, opened it, and initiated the reaction. Crosslinking was achieved by H<sub>A</sub>-H<sub>B</sub> links. In the presence of ATP, the aptamer bound to ATP, opening the hydrogel and releasing the drug. (D) The released drug killed cancer cells (MCF-10A), while sparing non-cancer cells (MDA-MB-231). Adapted<sup>220</sup>. Copyright pending 2017, RSC.

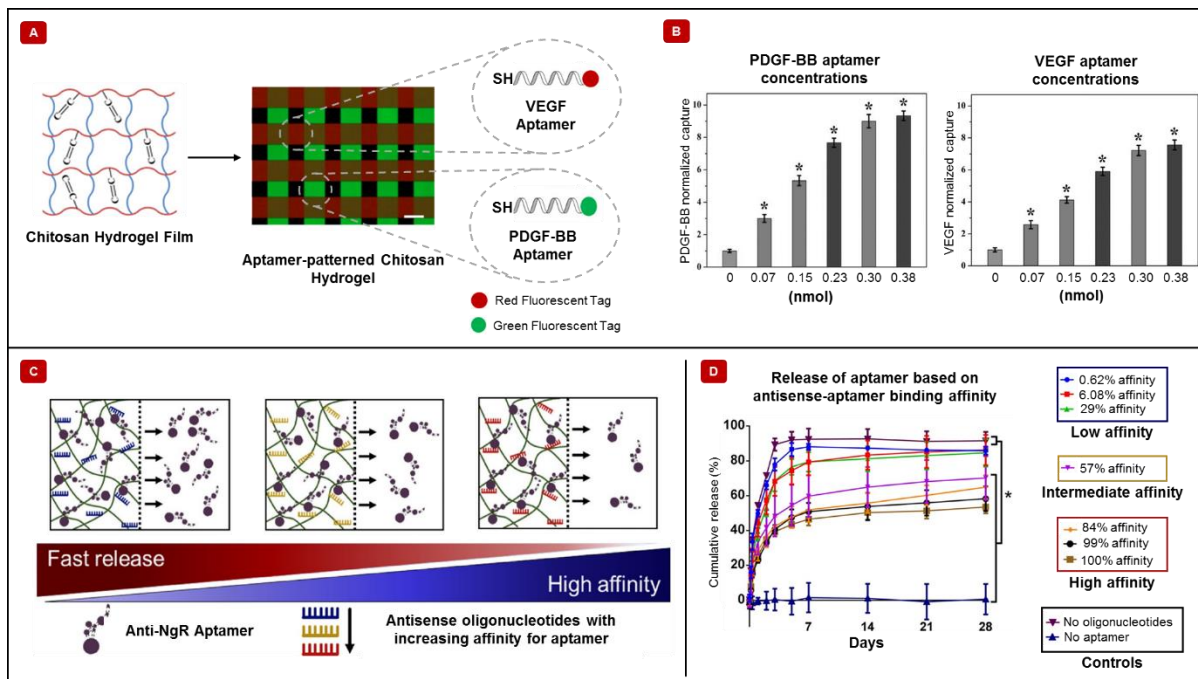


**Fig. 21** DNA-based hydrogels delivering biomolecules. (A) The figure depicts the structure of a protein delivering hydrogel. Allyl chitosan crosslinked with epichlorohydrin formed the hydrogel film. Thiolated aptamers specific to the proteins, vascular endothelial growth factor (VEGF) and platelet-derived growth factor (PDGF-BB), were attached to the hydrogel film by a photo-initiated thiol-ene reaction. VEGF was tagged with red fluorescent dye, whereas PDGF-BB was tagged with green fluorescent dye. (B) The fluorescence spectroscopy data shows the concentration dependent capture of both the proteins by the aptamer-coated hydrogel film. Adapted<sup>222</sup>. (C) Hyaluronic acid bound to antisense oligonucleotides specific to anti-NgR aptamers made up the depicted hydrogels. With the antisense oligonucleotides, the aptamers were loaded onto the hydrogels. This aptamer is useful in treating spinal cord injuries. The antisense oligonucleotides were designed such that they had low, intermediate, or high affinity for the aptamers. (D) Aptamer release kinetics showed that hydrogels with low affinity antisense quickly released their payload, whereas the hydrogels with high affinity antisense released the aptamers slowly. Adapted<sup>223</sup>. Copyright pending 2020, Elsevier.

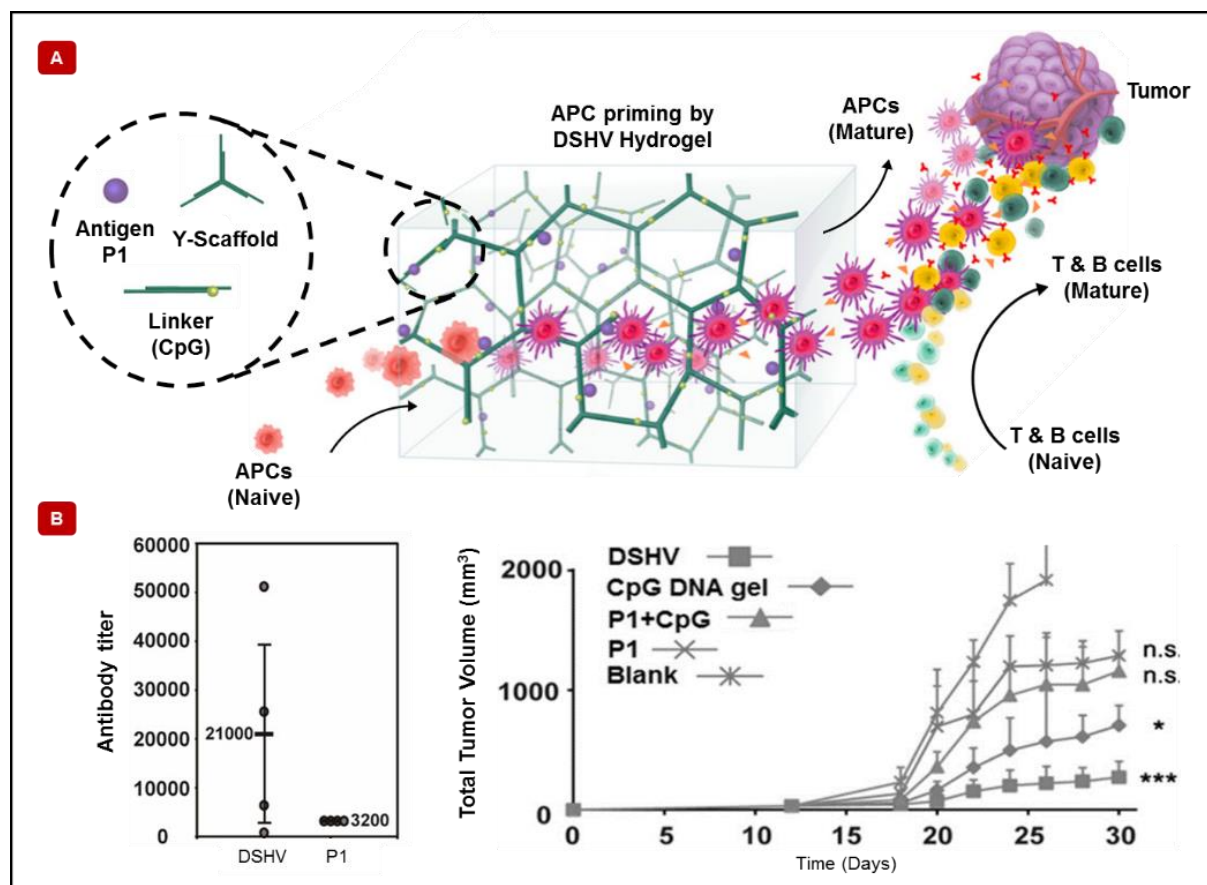


**Fig. 22** DNA-based hydrogel vaccine delivering antigens and invoking an immune response. (A) The components and mechanism of action of the hydrogel has been shown. Y-scaffolds were crosslinked with linear DNA. The Y-scaffold consisted of three single stranded DNA, and the linear linker consisted of two single stranded DNA. Prior to crosslinking, a tumor-related antigen (peptide, P1) was added to the linear linker by electrostatic interaction. Unmethylated cytosine-guanine-phosphate (CpG) motifs were added to the linker DNA by complementary base pairing. Subsequently, the injectable DNA supramolecular hydrogel vaccine (DSHV) formed by self-assembly. The antigen was used to invoke an immune response, whereas the CpG motif was used as an adjuvant. The figure depicts how the hydrogel can recruit naïve antigen presenting cells (APC), which has CpG recognizing receptors. The activated APCs mature and elicit a strong immune response by interacting with other immune cells (such as T and B cells). (B) The quantity of antibodies in the blood of mice, either treated with the injectable hydrogel or with just the peptide, was determined using enzyme-linked immunosorbent assay. A higher count of antibodies, which suggests an improved immune response, was observed with the hydrogel. Additionally, after 30 days, the tumor volume was significantly smaller in the mice treated with the injectable hydrogel compared to the ones without. Adapted<sup>225</sup>. Copyright pending 2018, ACS.

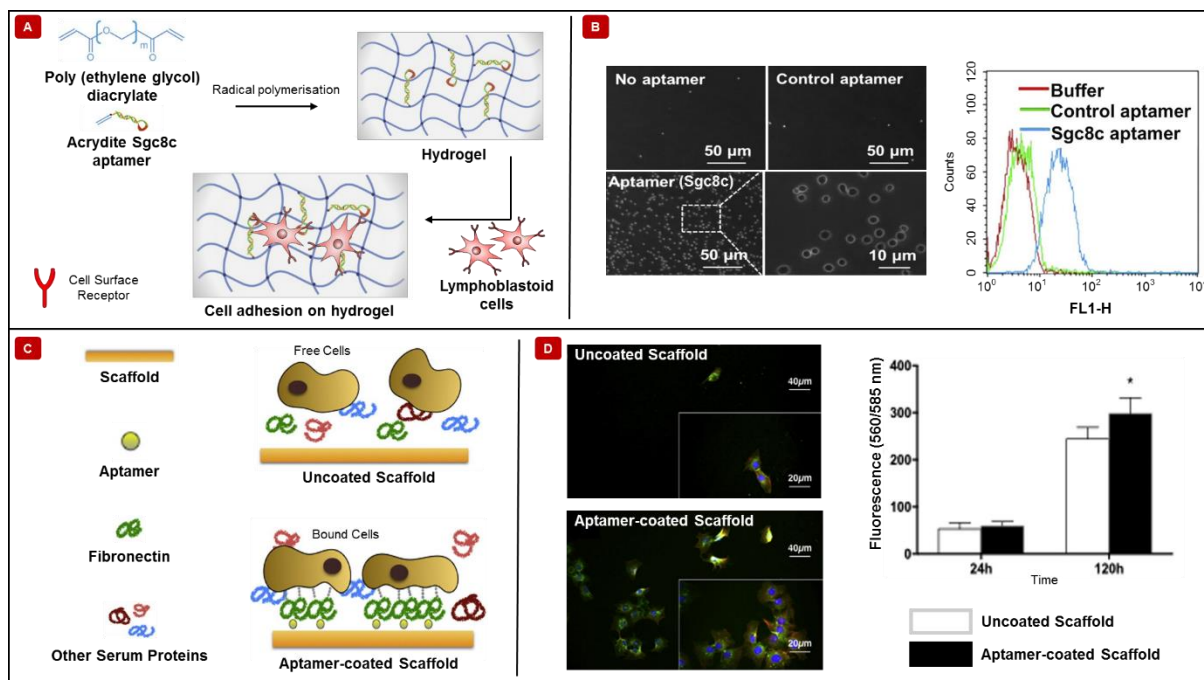


**Fig. 23** Tissue engineering application of DNA-based hydrogels. (A) The structure and function of a hydrogel designed to mimic the extracellular matrix has been depicted. Acrydite-modified aptamers (Sgc8c) and poly(ethylene glycol) diacrylate were the two components of the hydrogel. The hydrogel was synthesized by radical polymerization. The aptamer was selected such that they could bind to the surface receptors of lymphoblastoid cells. (B) Binding specificity was investigated. Images from inverted optical microscopy demonstrated that lymphoblastoid cells could only adhere to hydrogels that contained the Sgc8c aptamers specific to lymphoblastoid cell receptors. A shift in the flow cytometry data suggests stronger fluorescence in the case of hydrogels with aptamers. Adapted<sup>230</sup>. Copyright pending 2012, Elsevier. (C) A DNA-based hydrogel capable of cell adhesion has been shown. A hyaluronic acid/polyethylene glycol hydrogel was bound to aptamers specific to the protein, fibronectin. Fibronectin was chosen as it helps in wound healing. Therefore, with the aptamers, cells adhered to the hydrogel. (D) Fluorescent micrographs demonstrated the attachment of cells on the aptamer-coated hydrogels. Quantitative assays with fluorescent dyes demonstrated the efficacy of aptamer-coated hydrogels after five days of exposure. Adapted<sup>233</sup>. Copyright pending 2016, Elsevier.

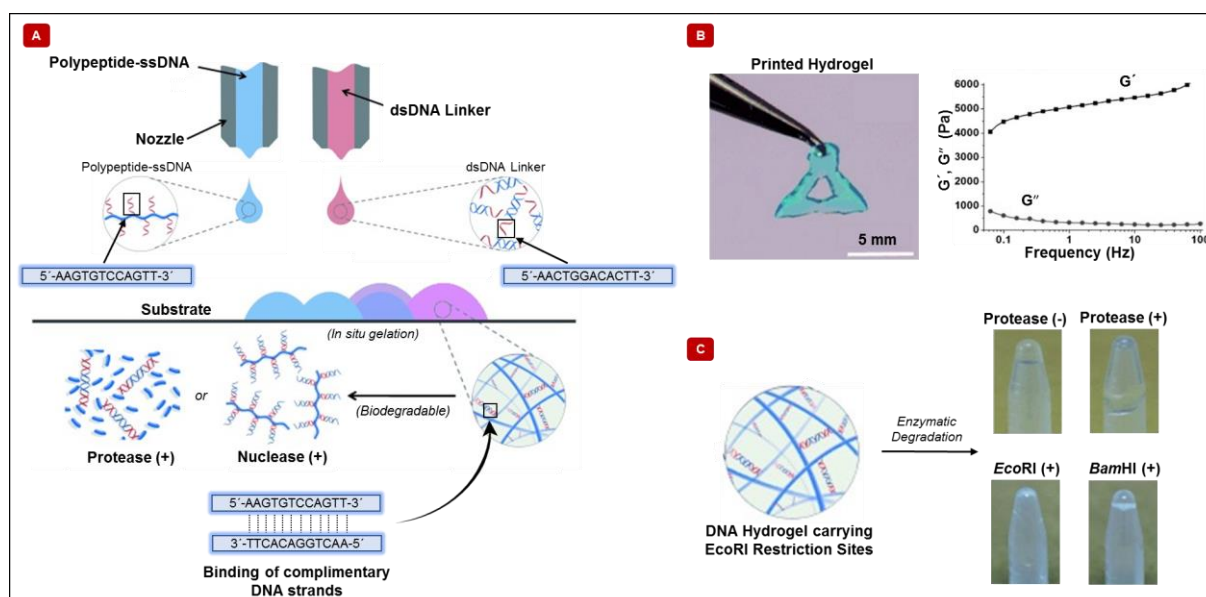


**Fig. 24** DNA-based hydrogel for printing three-dimensional tissue scaffolds. (A) The schematic outlines the concept of preparing scaffolds with DNA-based hydrogels. Two separate injectable inks were used here. The primary ink consisted of polypeptide backbones covalently attached to single stranded DNA chains. The second injectable ink comprised of double stranded DNA chains with sticky ends complementary to the DNA strands on the polypeptide backbone. The two inks were printed simultaneously at the same location to show that the double stranded DNA linker could bind with its complementary strand and rapidly crosslink the polymers. Furthermore, the hydrogels were designed such that they were prone to enzymatic degradation. (B) The picture depicts the shape of a printed hydrogel colored with a blue dye for the ease of visualization. Rheological experiments were performed to substantiate the success of gelation. The graph shows higher values of storage modulus ( $G'$ ) than loss modulus ( $G''$ ) for a range of frequencies, which is possible only for elastic materials. (C) Enzymatic degradation was brought about with both protease and DNA restriction enzymes. With no enzyme, Protease (-), the hydrogel was observed to be intact inside the microcentrifuge tube. However, in the presence of protease, Protease (+), the hydrogel degraded. Moreover, the inclusion of specific recognition sites for DNA restriction enzymes made the hydrogels susceptible to those enzymes. For example, the hydrogels containing the sites for the DNA restriction enzyme, *EcoRI*, degraded in the presence of that enzyme, *EcoRI* (+). However, the same hydrogel in the presence of the DNA restriction enzyme, *BamHI*, denoted by *BamHI* (+), remained intact. Adapted<sup>238</sup>. Copyright pending 2015, Wiley Online Library.

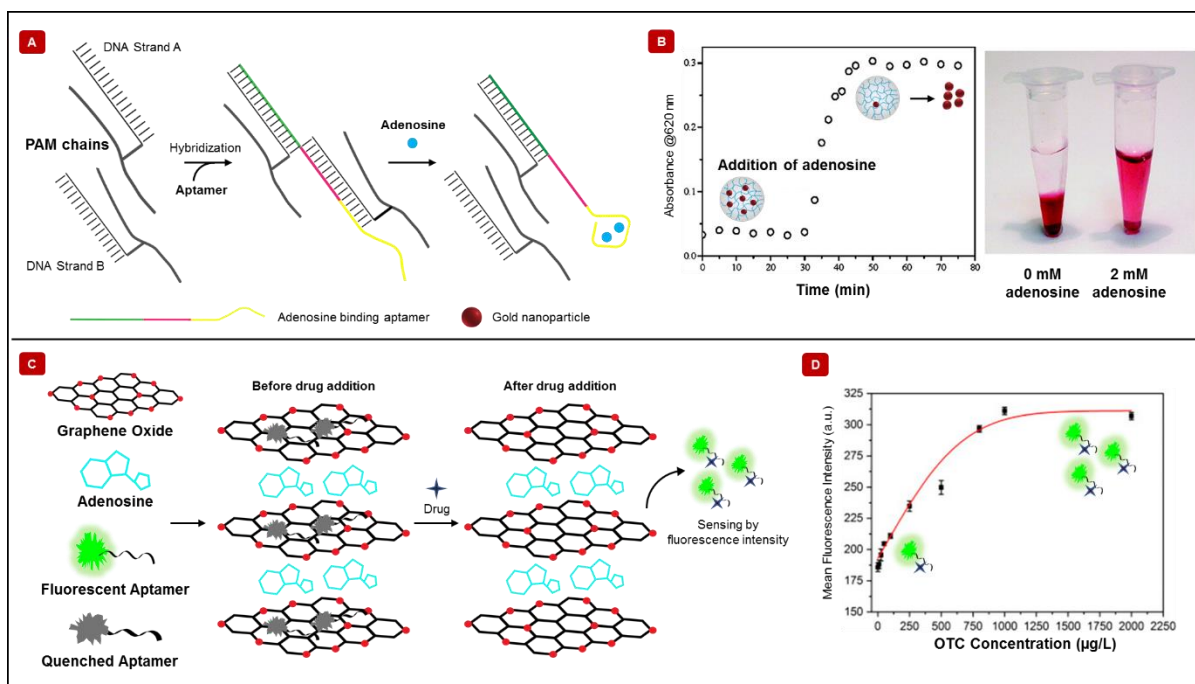


**Fig. 25** DNA-based hydrogels detecting small molecules. (A) A schematic of the hydrogel has been shown. DNA strands A and B were copolymerized with polyacrylamide (PAM). The crosslinker was designed such that a part of it hybridized with strand A and a part with strand B. The remaining section was an aptamer specific to adenosine. The hybridization reaction produced the hydrogel. Gold nanoparticles were inserted into the hydrogel. In the presence of adenosine, the aptamer preferentially bound to adenosine, thereby breaking the hydrogel, and releasing the gold nanoparticles. The released gold nanoparticles changed the color of the solution, indicating the presence of adenosine. (B) UV-Vis spectroscopy was conducted. Once the hydrogels were incubated with adenosine, there was an increase in absorption, indicating a change in color. A visible change in color has been shown in the figure. Adapted<sup>244</sup>. Copyright pending 2008, ACS. (C) A hydrogel for sensing the antibiotic drug, oxytetracycline, has been shown. The hydrogel comprised of graphene oxide sheets and adenosine. A fluorescent dye-tagged aptamer specific to the drug was added to the hydrogel by  $\pi$ - $\pi$  interactions with graphene oxide sheets. Inside the hydrogel, the fluorescence was quenched. However, in the presence of the drug, the aptamers detached from the hydrogel and bound to adenosine. This event recovered the fluorescence of the dye, which indicated the presence of adenosine. (D) The data shows an increase in fluorescence with increasing concentrations of the drug. Adapted<sup>247</sup>. Copyright pending 2016, Elsevier.

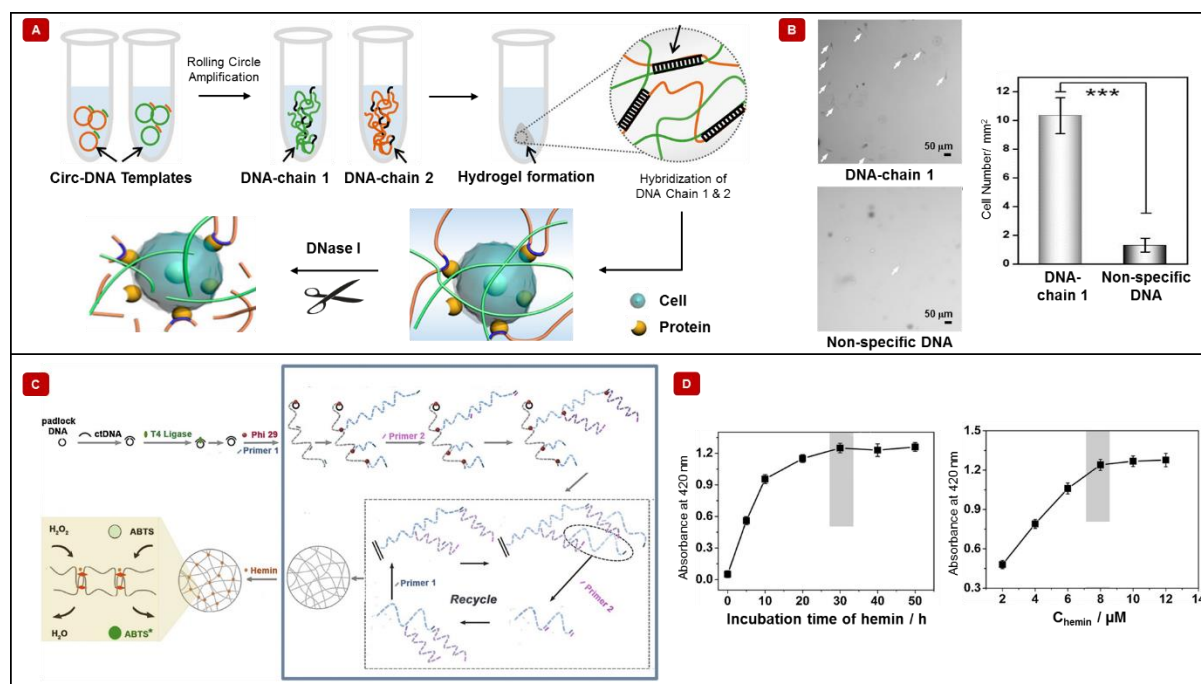


**Fig. 26** DNA-based hydrogels detecting biomolecules. (A) The schematic reveals the synthesis and mechanism of cell capture by a DNA hydrogel. Two DNA chains, DNA-chain 1 and DNA-chain 2, were formed by rolling circle amplification using circular DNA (circ-DNA) templates. The elongated DNA chains were then mixed. Hybridization of the chains resulted in the formation of the hydrogel. Chain 1 consisted of an aptamer, Apt19s, specific to a surface protein on bone marrow mesenchymal stem cells. With the help of this aptamer, the hydrogel specifically captured the target cells. The release of the cells was achieved by reacting the hydrogel with the enzyme, DNase I, which broke the hydrogel. (B) Microscopy images showed that the cells could only be captured by the hydrogel with the aptamer. A higher number of cells was observed in the aptamer-containing hydrogel. Adapted<sup>251</sup>. Copyright pending 2020, ACS. (C) A diagram of a DNA hydrogel that can detect circulating tumor DNA (ctDNA). A padlock DNA was used as the template for rolling circle amplification. The amplification process could only initiate when the circulating tumor DNA ligated the padlock DNA with the enzyme, T4 DNA ligase. Additionally, the enzyme, phi29, and the primers 1 and 2, enabled the amplification. The synthesized hydrogel formed G-quadruplexes and was bound with hemin. The resulting DNAzyme oxidized the chromogenic substrate, ABTS to ABTS\*. The change in color of the substrate visually confirmed the presence of the circulating tumor DNA. (D) The increase of UV-Vis absorbance with both incubation time and hemin concentration confirmed the formation of the G-quadruplex. The box inside the graph indicates optimum values. Adapted<sup>253</sup>. Copyright pending 2019, Elsevier.

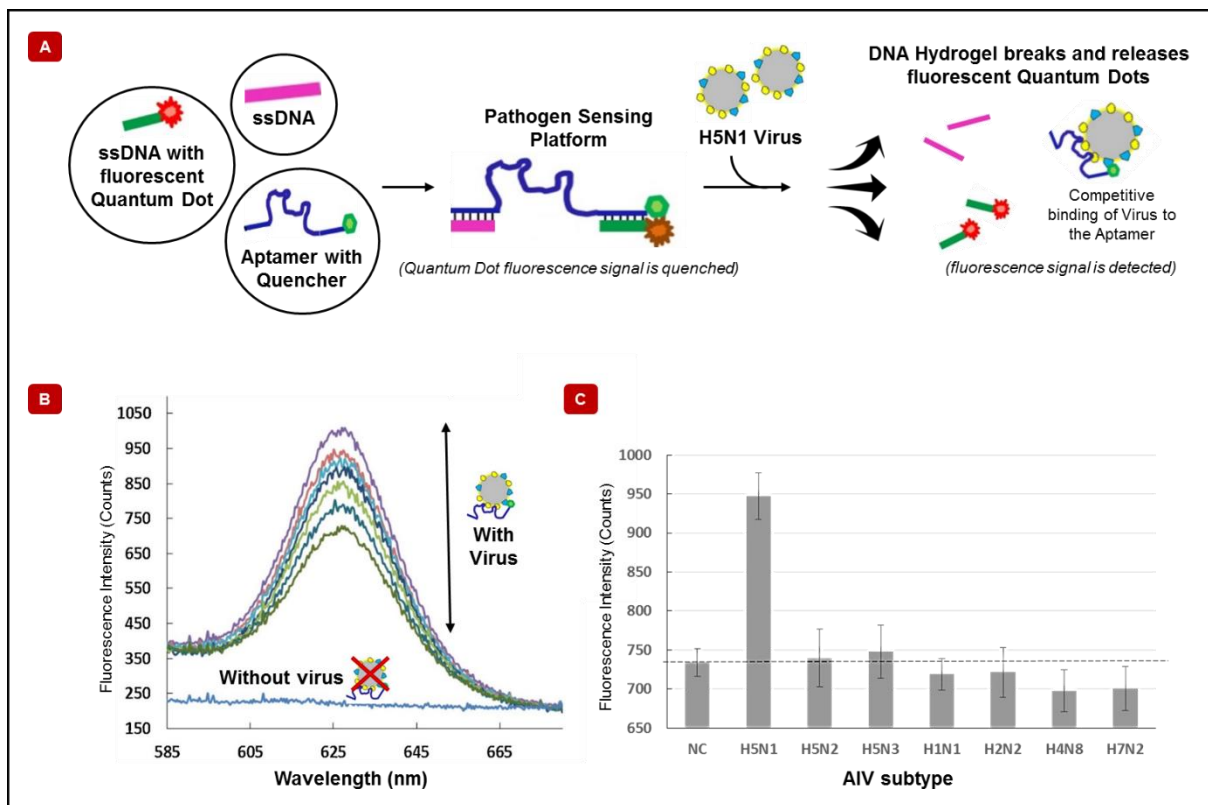


**Fig. 27** A DNA-based hydrogel detecting pathogens. (A) The various components of the hydrogel have been shown. An acrydite-modified, virus-specific aptamer was linked to a quencher molecule. A single stranded (ss) DNA was attached to a fluorescent quantum dot. Another ssDNA was modified with an acrydite molecule. The aptamer bound to both the ssDNAs to form the polyacrylamide-DNA hydrogel. Without the avian influenza virus (H5N1) the hydrogel remained intact, and the fluorescence of the quantum dot was quenched. However, in the presence of the virus, the aptamer broke the crosslink and bound to the virus instead. The breaking of the hydrogel released the quantum dots into the solution, and the resulting fluorescence indicated the presence of the virus. (B) The fluorescence intensity as a function of wavelength increased with the increasing concentrations of the virus. No fluorescence was seen in the absence of the virus. (C) The high specificity of the aptamer was demonstrated by exposing the hydrogel to different strains of influenza viruses. A strong fluorescence signal was present only in the case of H5N1. Adapted<sup>260</sup>. Copyright pending 2016, Elsevier.

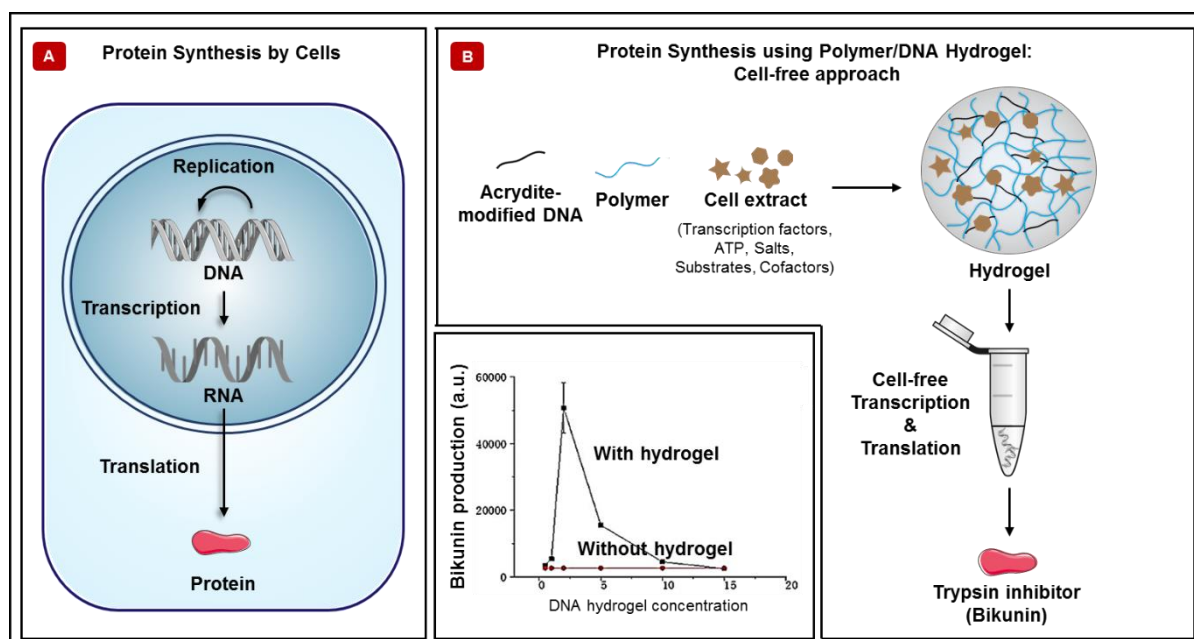


**Fig. 28** A DNA-based hydrogel for cell-free protein production. (A) The conventional scheme of protein production has been highlighted. Inside the cell, the desired DNA are replicated. This step is followed by transcription, which produces RNA. Next, the RNA is translated to protein. The cell provides all the necessary material for protein production. (B) A cell-free protein production method with a DNA-based hydrogel has been shown. Acrydite-modified DNA, along with poly(ethylene glycol) diacrylate polymer, was used to synthesize the hydrogel. The DNA contained the genetic information of a trypsin inhibiting protein, Bikunin. The hydrogel was then incubated with cell extract containing all the ingredients for protein production. Protein was successfully produced, and the yield was optimized as a function of the poly(ethylene glycol) diacrylate present in the DNA-based hydrogel. Adapted<sup>265</sup>. Copyright pending 2020, Frontiers in chemistry.

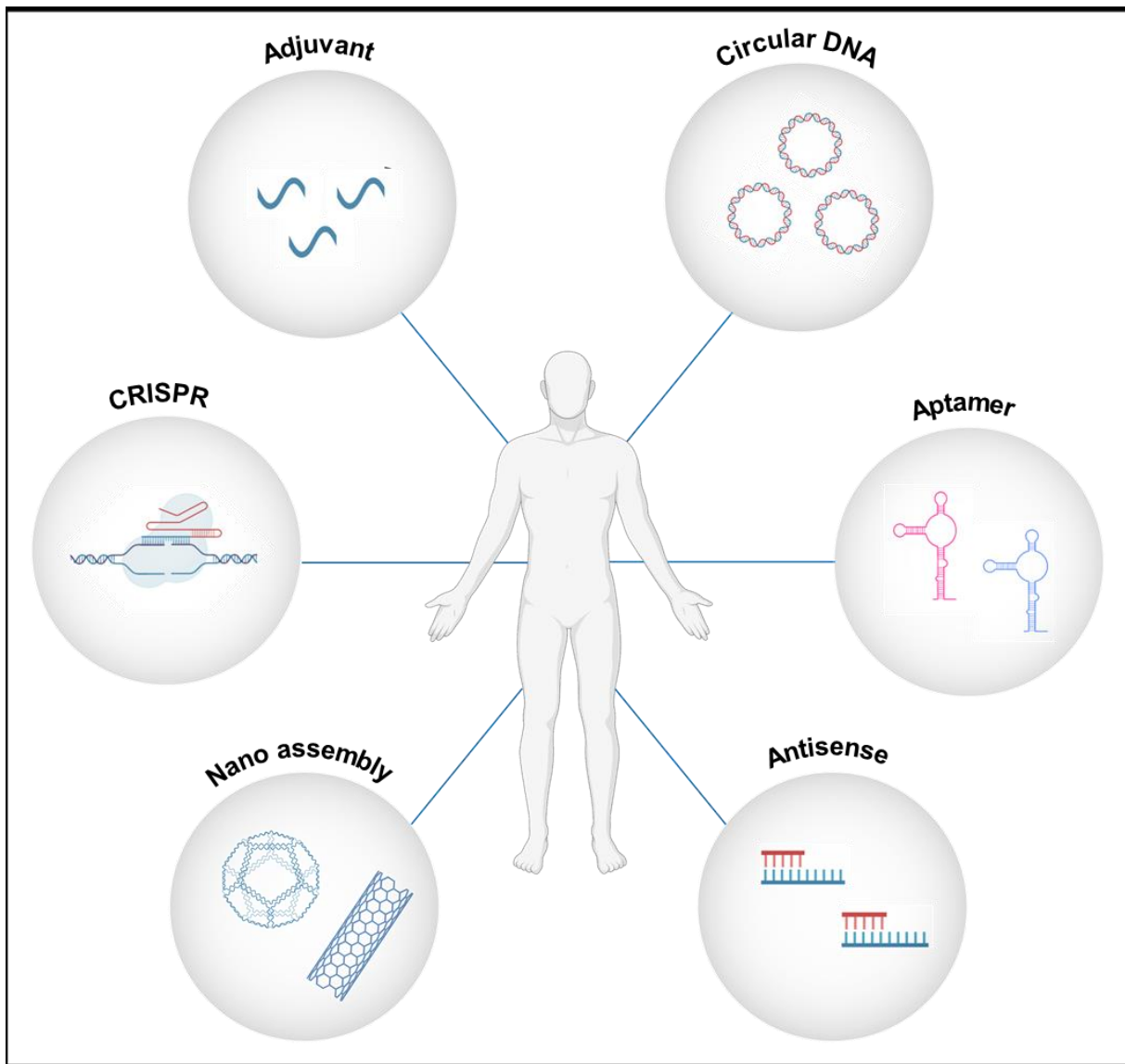


**Fig. 29** Current and future applications of DNA in biomedical science. Different DNA candidates that are commercialized or are undergoing clinical trials have been shown. Growing research in DNA nano-assemblies are highly likely to make their mark in advanced healthcare technologies in the next five years.

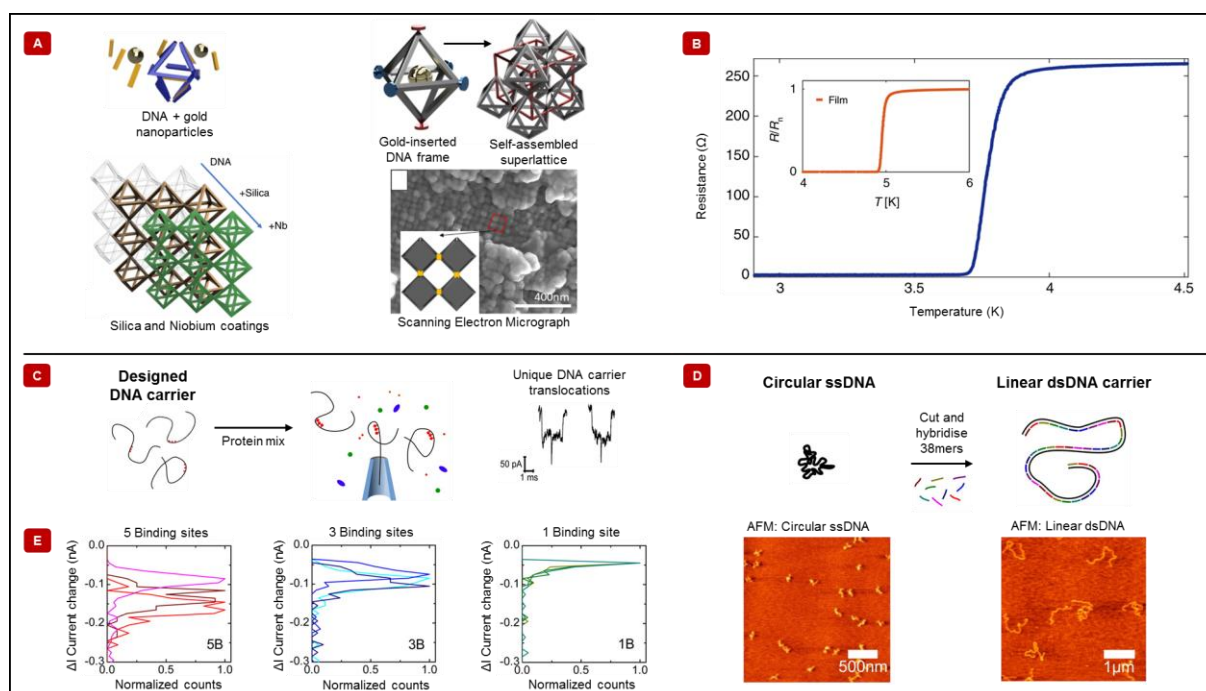


**Fig. 30** Emerging technologies by DNA sculpting. (A) DNA superconductor. DNA origami-based octahedral frames were prepared to carry gold nanoparticles. The gold-inserted frames self-assembled to form a 3D cubic superlattice of octahedra. The superlattice was next coated with silica to provide structural integrity. Finally, Niobium was coated to make the structure superconductive. Scanning electron micrograph shows the structure of the Niobium coated superlattice. Inset shows four octahedra connected by Niobium-coated sticky ends. (B) Graph demonstrates that the resistance of the designed superconductor is dependent on temperature. Inset graph with thin film of Niobium was taken as the point of reference. The material behaves as a superconductor below the transition temperature of 3.8K. Adapted<sup>290</sup>. Copyright pending 2020, Nature. (C) Nanopore-based protein detector. Illustration highlights a protein detection platform using DNA carriers and nanopores. The double stranded DNA was designed such that specific proteins bind on tailored target sites present on the DNA. Solid-state nanopores were then used to translocate proteins for detection by determining the characteristic ionic current signature of the DNA carriers. (D) Schematic shows the design of the double stranded carrier DNA. Similar to the DNA origami approach, a long, linear scaffold strand was prepared by cutting a circular single stranded genome, m13mp18. Subsequently, shorter staple strands were hybridized with the single stranded linear scaffold strand. Atomic force micrographs clearly distinguish the synthesized linear double stranded DNA from the template single stranded genome. (E) The amplitude of the protein signal was recorded for DNA carriers with varying binding sites. It was observed that the current signal was proportional to the number of binding sites. Adapted<sup>299</sup>. Copyright pending 2015, ACS.

**Table 1.** Chemical strategies for incorporating functional groups to synthetic DNA.

DNA Precursor	Functional group	Process	Reaction mechanism
2'-deoxycytidine <sup>[82]</sup> 	(a) Amine group 	Transamination	
5'-dimethoxytritylthymidine <sup>[88]</sup> 	(b) Thiol group 	Phosphorylation of thymidine with a, then nucleotide coupled to b	
5-iodo-3',5'-di- <i>o</i> - <i>p</i> -toluyl-2'-deoxyuridine <sup>[89]</sup> 	(c) Alkyne group 	S <sub>N</sub> 1	
Alkenyl containing oligonucleotide <sup>[90]</sup>  ★ alkenyl group	(d) Aldehyde group 	Oxidation of alkene to diol, oxidative cleavage of vicinal diols to give aldehyde	
Methyl ester phosphoramidite <sup>[92]</sup>  ◆ methyl ester	(e) Carboxylic acid group 	Hydrolysis	
Amino-modified ODN <sup>[94]</sup> 	(f) NHS (N-hydroxysuccinimide) derivative  ★	Conjugated with NHS derivatized hydrazinonicotinamide moiety (SHNH)  ■ SHNH	
Furan  Maleic anhydride <sup>[95]</sup> 	(g) Maleimide 	Diels-Alder reaction, then amine insertion	
Amino-modified ODN <sup>[97]</sup> 	(h) Azide group 	Diazo transfer reaction	

a: 2-chlorophenyl-O,O-bis(1-benzotriazolyl)phosphate, b: 3,3'-dithiodipropanol, c: oxidation of alkene to diol

**Table 2.** Chemical schemes and applications of nanocomposite DNA-based hydrogels.

Nanomaterial Used	DNA Origin	Reacting component	Polymer-CrosslinkerBond	Reaction Scheme	Reaction Mechanism	Application
Nanosilicates <sup>15</sup>	Natural (salmon testes)	Polyethylene glycol diglycidyl ether (PEGDE)	Covalent	Nucleophilic substitution	Amine group of DNA binds with epoxide group of PEGDE	Tissue Repair
Silicate nanodisks <sup>13</sup>	Natural (salmon testes)	Oxidized alginate	Covalent (imine bond)	Schiff base reaction	Condensation of amine group of DNA with aldehyde group of oxidized alginate	Drug delivery
Silicate nanodisks <sup>14</sup>	Natural (salmon testes)	DNA	Noncovalent	Hydrogen bonds and electrostatic interaction	Complementary base pairing between DNA strands and interaction between silicate nanodisks and DNA	Drug delivery
Nanosilicates and carbon nanotubes <sup>182</sup>	Synthetic	DNA	Noncovalent	Enzymatic cyclization	Rolling circle amplification of DNA functionalized on nanosilicates and carbon nanotubes	Drug delivery
Carbon nanotubes <sup>183</sup>	Natural (salmon sperm)	DNA and carbon nanotubes (polypyrrole was added to the hydrogel by chemical oxidative polymerization)	Noncovalent	$\pi$ -stacking	Condensation and coagulation by room temperature hydrophilic ionic liquid <sup>16,17</sup>	Bioactuator
Carbon dots <sup>20</sup>	Synthetic	DNA	Covalent	Phosphoramidate linkage	Conjugation between amine group on carbon dots and 5' phosphate of DNA	Drug delivery
Gold nanoparticles <sup>184</sup>	Synthetic	DNA	Covalent	Enzymatic crosslinking	Phosphodiester bond formation between DNA strands using DNA ligase	Drug delivery
Gold nanoparticles <sup>23</sup>	Synthetic	Thiol modified DNA	Covalent	Oxidation-reduction	Sulfide link between thiol group in DNA and gold nanoparticles	Cell free protein synthesis

**Table 3.** Overview of the applications of DNA-based hydrogels.

Application	Objective	Primary Materials Used	Mechanism of action
Environmental	To detect low concentrations of Pb <sup>2+</sup>	<ul style="list-style-type: none"> <li>DNA-polyacrylamide polymer is crosslinked with a Pb<sup>2+</sup>-specific DNAzyme</li> <li>Pre-trapped AuNPs</li> </ul>	<ul style="list-style-type: none"> <li>The enzymatic function of the DNAzyme is activated in the presence of Pb<sup>2+</sup>, inducing cleavage of the substrate sequence.</li> <li>Colourimetry and quantitative readout were used to detect Pb<sup>2+</sup> concentration.<sup>195</sup></li> </ul>
	To simultaneously detect and capture Hg <sup>2+</sup>	<ul style="list-style-type: none"> <li>T-rich DNA functionalized polyacrylamide hydrogel</li> <li>Dye binding DNA hairpin structure</li> </ul>	<ul style="list-style-type: none"> <li>Thymine-rich DNA can bind to Hg<sup>2+</sup> and form a hairpin loop between to T bases.</li> <li>Fluorimetry was used to detect the presence of Hg<sup>2+</sup>.<sup>190</sup></li> </ul>
	To detect low concentrations of Cu <sup>2+</sup>	<ul style="list-style-type: none"> <li>DNA-polyacrylamide polymer crosslinked with a Cu<sup>2+</sup>-specific DNAzyme</li> <li>Pre-trapped AuNPs</li> </ul>	<ul style="list-style-type: none"> <li>In the presence of Cu<sup>2+</sup>, the DNAzyme irreversibly cleaves the substrate.</li> <li>Colourimetry was used to detect Cu<sup>2+</sup> concentrations.<sup>193</sup></li> </ul>
Catalysis	To oxidize a chromogenic substrate for the detection H <sub>2</sub> O <sub>2</sub>	<ul style="list-style-type: none"> <li>DNA-polyacrylamide chains crosslinked by peroxidase-mimicking DNAzyme</li> </ul>	<ul style="list-style-type: none"> <li>The peroxidase-mimicking DNAzyme oxidizes the chromogenic substrate in the presence of H<sub>2</sub>O<sub>2</sub>.</li> <li>Colourimetry indicated the presence of H<sub>2</sub>O<sub>2</sub>.<sup>204</sup></li> </ul>
	To mimic horseradish peroxidase-like catalytic functions	<ul style="list-style-type: none"> <li>Complexes formed by G-rich sequences coordinated to hemin</li> <li>DNAzyme hydrogel</li> </ul>	<ul style="list-style-type: none"> <li>G-rich sequences coordinated to hemin have HRP-like catalytic abilities and catalyze oxidation reactions.</li> <li>Catalytic function was observed by a colour change and by absorbance.<sup>209</sup></li> </ul>
	To catalyze mediated electron transfer between oxidoreductase enzymes and the electrode	<ul style="list-style-type: none"> <li>DNA intercalated with redox probe with an aromatic structure and a dye</li> <li>Tertiary ammonium salt containing a redox center immobilized onto DNA</li> </ul>	<ul style="list-style-type: none"> <li>In the presence of an oxidoreductase enzyme, molecules are oxidized by the dye.</li> <li>Electrochemistry was used to observe oxidation reactions.<sup>198</sup></li> </ul>
Electroconductors and actuators	To link a bacteria's metabolism with redox process on electrodes	<ul style="list-style-type: none"> <li>Electrodes functionalized with DNA-coated carbon nanotubes or silica nanoparticles</li> <li><i>Shewanella oneidensis</i> (bacteria)</li> </ul>	<ul style="list-style-type: none"> <li>DNA-coated nanoparticles form gels aiding in extracellular electron transfer, allowing bacteria to proliferate.</li> <li>Electrochemistry was used to measure conductivity.<sup>28</sup></li> </ul>
	To synthesize a three-dimensional electron transporter	<ul style="list-style-type: none"> <li>DNA covalently conjugated to Indium-tin-oxide electrode</li> <li>Toluidine Blue O (phenothiazine dye)</li> </ul>	<ul style="list-style-type: none"> <li>Toluidine blue O intercalated within the DNA made the hydrogel electroconductive.<sup>212</sup></li> </ul>

	To synthesize an actuator that can be potentially applied to manufacture bio-artificial muscles	<ul style="list-style-type: none"> <li>• DNA</li> <li>• Carbon nanotubes</li> <li>• Polypyrrole</li> </ul>	<ul style="list-style-type: none"> <li>• Carbon nanotube and polypyrrole imparted electrochemical properties to the DNA-based hydrogel.</li> <li>• Application of cyclical voltage resulted in the contraction and expansion of the hydrogel.<sup>183</sup></li> </ul>
<b>Drug delivery</b>	To deliver Dexamethasone (water insoluble drug) to treat Allergic Conjunctivitis	<ul style="list-style-type: none"> <li>• DNA hydrogel</li> <li>• Dexamethasone encapsulated in PLGA nanospheres</li> </ul>	<ul style="list-style-type: none"> <li>• Increased cellular uptake, long retention time, and sustained release of dexamethasone.<sup>218</sup></li> </ul>
	To facilitate the capture and controlled release of multiple proteins	<ul style="list-style-type: none"> <li>• Allyl chitosan hydrogel</li> <li>• Aptamers specific to proteins and labelled with fluorescent dye</li> </ul>	<ul style="list-style-type: none"> <li>• Capture of proteins by binding to aptamers.</li> <li>• Release of proteins upon the presence of complimentary DNA.<sup>222</sup></li> </ul>
	To deliver tumor antigens, which recruit and activate antigen presenting cells, for cancer therapy	<ul style="list-style-type: none"> <li>• DNA hydrogel</li> <li>• Cytosine-phosphate-guanine DNA and P1 antigen (tumor antigens)</li> </ul>	<ul style="list-style-type: none"> <li>• Subcutaneous injection of hydrogel.</li> <li>• Tumor antigens recruit immune cells leading to antitumor effects.<sup>225</sup></li> </ul>
<b>Tissue engineering</b>	To synthesize aptamer functionalized hydrogel (mimicking the ECM) for cell specific adhesion	<ul style="list-style-type: none"> <li>• Polyethylene glycol</li> <li>• Aptamers (sgc8c) incorporated into hydrogel network by free radical polymerisation</li> </ul>	<ul style="list-style-type: none"> <li>• Biochemical cues (growth factors) and biophysical cues (binding sites) provided by aptamers (mimicking the ECM) recruit CCRF-CEM (lymphoblastoid) cells.<sup>230</sup></li> </ul>
	To synthesize anti-fibronectin aptamer functionalized hydrogel scaffold to improve cell adhesion	<ul style="list-style-type: none"> <li>• Polyethylene glycol diacrylate-thiolated hyaluronic acid hydrogel</li> <li>• Anti-fibronectin aptamers functionalized in the hydrogel by nucleophilic (Michael's) addition reaction</li> </ul>	<ul style="list-style-type: none"> <li>• Anti-fibronectin aptamers bind to fibronectin (serum protein), which improves cell attachment and colonization onto the scaffold.<sup>233</sup></li> </ul>
	To develop aptamer (Apt19s) functionalized scaffold to recruit resident mesenchymal stem cells (MSCs) and enhance cartilage regeneration	<ul style="list-style-type: none"> <li>• Silk fibroin polymer functionalized with Apt19s aptamer by EDC-NHS reaction</li> <li>• Hyaluronic acid-tyramine hydrogel enzymatically crosslinked to Silk fibroin-Apt19s aptamer</li> </ul>	<ul style="list-style-type: none"> <li>• Apt19s aptamers improve the homing of joint-resident mesenchymal stem cells to the scaffold, leading to improved cell recruitment and cartilage repair.<sup>237</sup></li> </ul>

<b>Biosensor</b>	To detect microRNA, miR-21 (biomarker for lung cancer)	<ul style="list-style-type: none"> <li>• Ferrocene tagged DNA probe complementary to target microRNA, miR-21</li> <li>• DNA hydrogel</li> </ul>	<ul style="list-style-type: none"> <li>• Probe present with DNA hydrogel was used to competitively bind with miR-21.</li> <li>• Electrochemistry was used to detect the presence of miR-21. <sup>256</sup></li> </ul>
	To detect tetracyclines (antibiotic whose accumulation is harmful)	<ul style="list-style-type: none"> <li>• Fluorescent labelled tetracycline-specific aptamer sequence as a recognition element</li> <li>• Graphene Oxide (GO) Sheets</li> </ul>	<ul style="list-style-type: none"> <li>• Aptamers present in DNA/graphene oxide hydrogel was used to form a tetracycline-aptamer complex.</li> <li>• Fluorimetry was used to detect the presence of tetracyclines. <sup>247</sup></li> </ul>
	To detect H5N1 influenza virus	<ul style="list-style-type: none"> <li>• Acrydite-aptamer with quencher that can bind to virus</li> <li>• Acrydite conjugated DNA</li> <li>• Quantum dot conjugated DNA</li> <li>• Polyacrylamide</li> </ul>	<ul style="list-style-type: none"> <li>• Quantum dot separated from quencher when aptamer bound to the virus.</li> <li>• The resulting fluorescence intensity indicated the presence of virus. <sup>260</sup></li> </ul>
<b>Biomolecule production</b>	To synthesize proteins outside living cells	<ul style="list-style-type: none"> <li>• X-DNA</li> <li>• Linear plasmids</li> </ul>	<ul style="list-style-type: none"> <li>• Hydrogel was incubated in cell lysate containing the necessary ingredients for protein synthesis.</li> <li>• Plasmids provided the genetic information for protein synthesis. <sup>263</sup></li> </ul>
	To synthesize proteins outside living cells cost-effectively	<ul style="list-style-type: none"> <li>• Polyethylene glycol diacrylate</li> <li>• Acrydite DNA</li> </ul>	<ul style="list-style-type: none"> <li>• Acrydite linked DNA contained gene for protein production, a promoter, a ribosome binding site, and a translation terminator.</li> <li>• Ammonium persulfate (radical initiator) and Tetramethylenediamine (catalyst) was used to form the hydrogel.</li> <li>• Resulting hydrogel was incubated with cell lysate to produce protein. <sup>265</sup></li> </ul>
	To synthesize small interfering RNA (siRNA)	<ul style="list-style-type: none"> <li>• X-DNA</li> <li>• Linearized plasmid</li> </ul>	<ul style="list-style-type: none"> <li>• Nanosized hydrogels were inserted into MDCK (epithelial) cells, which can produce green fluorescent protein.</li> <li>• siRNA synthesized by the hydrogel inhibited the production of green fluorescent protein by the MDCK cells. <sup>266</sup></li> </ul>

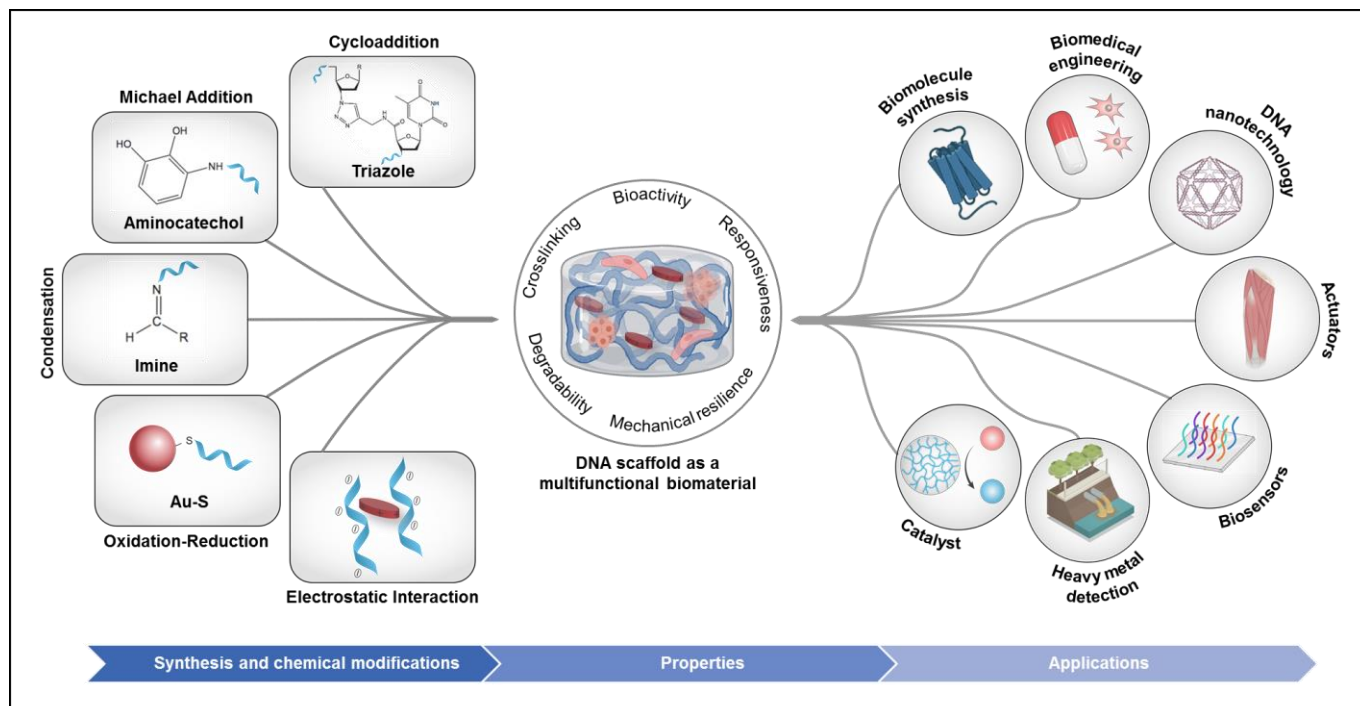


**Table of Contents Entry.** This review explores the chemical tools and strategies to synthesize DNA-based biomaterials. The focus is on the use of DNA as a generic polymer rather than a genetic material. Additionally, this review highlights the diverse applications of such bioactive, degradable, mechanically resilient polymeric materials in the fields of environment, electrochemistry, biologics delivery, and regenerative therapy.